الجمهورية الجزائرية الديمقراطية الشعبية

People's Democratic Republic of Algeria

وزارة التعـليـم العالي والـبـحـث الـعـلـمية

Ministry of Higher Education and Scientific Research

جامـعة الشهيد حمة لخضر الوادي

University of Echahid Hamma Lakhdar –El Oued

كلية علوم الطبيعة والحياة

Faculty of Natural and Life Sciences

قسم البيولوجيا الخلوية والجزيئية

Department of Cellular and Molecular Biology

END-OF-STUDIES MEMOIR

Submitted to obtain the academic master's degree

Specialty: Toxicology

THEME

Antioxidant Potential of Essential Oils from Selected Medicinal Plants: GC/MS Profiling, In Vitro Free Radical Scavenging, and In Silico Molecular Interaction

Presented by :

M^elle^ Acila Baraa **M^elle^ Chelalga Roumaissa**

M^elle^ Gadi Amani **M^elle^ Touahria Oula**

Jury Members:

President: ***Dr. Toumi Ikram*** **M.A.A, University of El *Oued***

Examinateur: ***Dr. Ghania Ahmed*** **M.A.A, University of El *Oued***

Supervisor: ***Dr.*** **Housseyn Chaoua** **M.A.B, University of El *Oued***

Co-supervisor: ***Dr. Lanez Elhafnaoui*** **M.C.A, University of El *Oued***

University Year: 2024/2025

Acknowledgments

We begin by expressing our deepest gratitude to **God** Almighty, whose guidance and blessings enabled us to carry out and complete this modest work. We sincerely hope it proves to be meaningful and beneficial.

We extend our sincere thanks and deep appreciation to the dean of the Faculty, **Dr.Abdelmalek Zaater**, for his continuous support and dedication to providing an outstanding academic environment.

we also express our hearfelt gratitude to the head of **the Department**, for his valuable guidance and constant encouragement throughout our academic journey.

Our heartfelt thanks go to **Dr.Lanez Elhafnaoui**, whose constant support and invaluable insights greatly contributed to the progression of this work. We are truly thankful for his availability and dedication, and we wish him continued health and prosperity-a lasting tribute to his wisdom and generosity.

We are eaually grateful to **Dr.Lanez Touhami**, Director of the VTRS Laboratory at the University of El-Oued, for his warm welcome and for providing us with the necessary tools and facilities to carry out our research. His willingness to support us has been truly appreciated.

We extend our appreciation to the respected members of the Committee for their time and contributions during the defense. Special thanks to **Dr.Ben Amor Mohammed Larbi**, whose dedication, efforts, and valuable input have had a significant impact on our orientation and progress.

Lastly, we extend our thanks to everyone who has supported and stood by us throughout this endeavor, whether near or far.

Dedication

Praise be to ***Allah***, by whose grace no effort is completed nor any pursuit fulfilled except with his favor. We only embark on beginnings through his ease, and we only reach endings through his guidance. We achieve our goals solely by his grace. So praise be to ***Allah*** with love, gratitude, and appreciation - praise be to ***Allah*** for the beginning and the end.

I dedicate this success first to ***my ambitious self*** - it began with a dream and ended with triumph. And then to everyone who supported me in completing this journey, may you forever remain a timeless source of strength in my life.

To the one who supported me without limits and gave without expecting anything in return, to the one who taught me that life is a struggle, and that its true weapons are knowledge and learning, to the one who planted in my soul the seeds of noble values, to the one whose name I carry with pride, my first supporter on this journey and my strength after god

« *My beloved Father* »

To the one beneath whose feet paradise lies, to the one whose prayers were the secret to my success, whose tenderness healed my wounds, my role model, my first teacher, and the friend of all my days « ***My gentle Mother*** **»**

To the loyal ***Friends***, and to everyone who was a support and a source of strength along this journey, I am deeply grateful to you all. I wouldn't have made it without your kindness, after the grace of god.

Baraa

Dedication

" وَآخِرُ دَعْوَاهُمْ أَنِ الحَمْدُ لله رَبِّ الْعَالَمِينَ "

Praise be to Allah when the starting and at the conclusion,
I dedicate the fruits of my humble effort to the sun that was absent, and the world is darkened, to the affectionate chest that has always rested my heart, to the only warmth in my life, to
'' My Beloved Mother''
To whoever paved the way of knowledge for me, to those who have enlightened my scientific paths with an indulge light, to my first teachers, to whom he has fulfilled his life for me,
To ***'' My Dear father"***
To whom I gathered the ceiling of one house ***'' My dear sisters''***, to a bond in life
'' My brothers'' '' NOUR EDDINE'' '' ABD ALLAH ''
To the joy of life ***''Sons of my sisters ''***
To ***Myself*** who bet on success, be patient and be patient, for there is no end…
To all my loved ones whose souls have suffered and embraced the dust
(My Dear Grandmother, Allah has mercy on you)…
To my companies on the journey ***'' My friends''***
To everyone who had a helping hand in writing this project, to all of them,
I dedicate this work. Allah grants me and you.

Roumaissa

Dedications

Before all things, I thank Almighty ***''Allah''*** for granting me the opportunity
To reach this stage of knowledge and for blessing me with the courage and patience to accomplish this work.
I dedicate this humble work to ***''My Dear Parents''***, with all gratitude and appreciation
For the sacrifices they have made for my education, support and encouragement throughout my life and academic journey.
To my elder sister **'' *IBTIHAJ''*,** who has always been a source of encouragement and support for me.
To *'' **My family** ''*, my dear ***''friends''*** and to everyone who contributed to the completion of this work.

Amani

Dedications

In the name of Allah, the Most Gracious, the Most Merciful,

All praise is due to Allah, praise abundant, pure, and blessed, as our Lord loves and is pleased with. And may the peace, blessings, and mercy of Allah be upon our Prophet Muhammad, the Seal of the Prophets and Messengers, and upon his family and companions.

To begin at this moment of crowning my efforts and reaping the fruits of years of perseverance and hard work, my heart overflows with gratitude and praise. I humbly hold my pen to dedicate these modest words to those most deserving:

To those whose prayers were my provision, whose satisfaction was my happiness, and whose efforts were my comfort, To my beloved father, who was my unwavering support at every step, a constant source of safety and reassurance, and to my dear mother, the fountain of tenderness, whose vast heart embraced me with patience and endless prayers,

I dedicate this humble achievement to you both, as a token of love and loyalty that words can never fully express. To myself, who endured when the path grew narrow, which rose after every stumble, and who persevered until reaching the goal, I dedicate this success to you a reminder that every hardship faced was a step toward greatness. And to my dear colleagues, Companions of the journey and partners in perseverance and late nights,

You were a beacon of hope during times of fatigue and a smile of support when the journey seemed long. To you, I offer all my gratitude and appreciation for your pure companionship and noble stances. I dedicate this work to everyone who taught me a letter, inspired me with an idea, or encouraged me to keep moving forward,

Asking Allah Almighty to make it sincerely for His sake, to benefit through it, and to grant us all success and guidance.

Oula

Abstract

The plant kingdom is a rich reservoir of bioactive compounds known for their antioxidant properties. This study aims to evaluate the antioxidant activity of the essential oil of *Cotula Cinerea* and that of *Origanum Majorana L*, using standardized laboratory techniques.

The essential oils were extracted from the plants using the hydrodistillation technique. The chemical composition of the oils was then analysed using Gas chromatography coupled with Mass Spectrometry (GC-MS). Upon identifying their constituents, *Cotula Cinerea* was found to contain 31 compounds, whereas *Origanum Majorana L* contained 42 compounds. The antioxidant activity was also evaluated using two methods: the DPPH free radical scavenging assay, Superoxide radical scavenging assay $O_2^{\cdot -}$. The results showed that both essential oils possess antioxidant activity, with a noticeable variation in efficacy between them. *Cotula Cinerea* exhibited higher antioxidant activity compared to *Origanum Majorana L* in both assays.

Molecular docking studies were performed to predict the interaction of key compounds in essential oils with antioxidant enzymes, and the results showed strong interactions that support the potential mechanisms of their antioxidant activity at the molecular level.

The study demonstrated that the essential oils of *Cotula Cinerea* and *Origanum Majorana L* contain natural compounds with antioxidant activity, supporting their potential use as natural supplements in the food or pharmaceutical industries. These findings also encourage further studies to evaluate their effectiveness in biological models.

Keywords: Essential Oil, antioxidant activity, *Cotula Cinerea*, *Origanum Majorana L*, Glutathione reductase, IC_{50}, DPPH, $O_2^{\cdot -}$.

Résumé

Le règne végétal constitue un réservoir riche en composés bioactifs reconnus pour leurs propriétés anti oxydantes. Cette étude vise à évaluer l'activité antioxydant de l'huile essentielle de *Cotula Cinerea* et de celle d' *Origanum Majorana L*, en utilisant des techniques de laboratoire standardisées.

Les huiles essentielles ont été extraites des plantes par la technique de l'hydro distillation. La composition chimique des huiles a ensuite été analysée par chromatographie en phase gazeuse couplée à la spectrométrie de masse (GC-MS). L'analyse a révélé que *Cotula Cinerea* contenait 31 composés, tandis qu'*Origanum Majorana L* en contenait 42. L'activité antioxydant a également été évaluée à l'aide de deux méthodes : le test de piégeage des radicaux libres DPPH et le test de réduction des radicaux anions superoxide. Les résultats ont montré que les deux huiles essentielles possèdent une activité antioxydant, avec une différence notable d'efficacité entre elles. *Cotula Cinerea* a montré une activité antioxydant plus élevée *qu'Origanum Majorana L* dans les deux tests.

Des études d'amarrage moléculaire ont été réalisées pour prédire l'interaction des composés clés des huiles essentielles avec les enzymes antioxydants, et les résultats ont montré de fortes interactions qui soutiennent les mécanismes potentiels de leur activité antioxydant au niveau moléculaire.

L'étude a démontré que les huiles essentielles de *Cotula Cinerea* et *Origanum Majorana L* contiennent des composés naturels ayant une activité antioxydant, ce qui soutient leur utilisation potentielle en tant que complément naturels dans les industries agroalimentaire ou pharmaceutique. Ces résultats encouragent également la réalisation d'études supplémentaires pour évaluer leur efficacité sur des modèles biologiques.

Mots-clés : Huile essentielle, activité antioxydant, *Cotula cinerea*, *Origanum Majorana L*, Glutathion reductase, IC_{50}, DPPH, $O_2^{\cdot -}$.

الملخص

تعد مملكة النباتات مصدرا فريدا للمركبات الحيوية التي تمتاز بخصائصها المضادة للأكسدة. تهدف هذه الدراسة إلى تقييم النشاط المضاد للأكسدة لكل من الزيت الأساسي لنبات الشّيحية والزيت الأساسي لنبات المردقوش وذلك بإستخدام تقنيات مخبرية معيارية.

حيث تم إستخلاص الزيوت الأساسية من النباتات بإستخدام تقنية التقطير المائي، ثمّ تمّ تحليل التركيب الكيميائي للزيوت بإستخدام تقنية الكروماتوغرافيا الغازية المقترنة بمطياف الكتلة للتعرف على مركباتهما فقد تميزت الشّيحية بإحتوائها على 31 مركبا أما المردقوش فقد إحتوى على 42 مركبا. تم كذلك تقييم نشاط مضاد للأكسدة باستخدام طريقتين إختبار إختزال الجذور الحرة، وإختبار قدرة إختزال جذور الأنيون الفائق، أظهرت النتائج أن كلا الزيتين يمتلكان نشاطا مضادا للأكسدة مع تفاوت ملحوظ في الفعالية بينهما. حيث سجّل زيت الشّيحية فعالية أعلى مقارنة بزيت المردقوش في كلا الإختبارين.

تم إجراء دراسات التحام جزيئي للتنبؤ بتفاعل المركبات الرئيسية في الزيوت العطرية مع إنزيمات مضادة للأكسدة، وقد أظهرت النتائج تفاعلات قوية تدعم الآليات المحتملة لنشاطها المضاد للأكسدة على المستوى الجزيئي.

أثبتت الدراسة أنّ الزيوت الأساسية لكل من الشّيحية والمردقوش تحتوي على مركبات طبيعية ذات فعالية مضادة للأكسدة، ممّا يدعم إمكانية إستخدامها كمكمّلات طبيعية في الصّناعات الغذائية أو الصيدلانية ويشجع كذلك على إجراء دراسات إضافية لتقييم فعاليتها في النّماذج الحيوية.

الكلمات المفتاحية: زيت أساسي ، نشاط مضاد للأكسدة، شيحية الإبل، المردقوش، اختزال الجليتاثيون ، 2,2- ثنائي فينيل-1-بيكريل هيدرازيل، جذر الأنيون الفائق.

List of figures

List of Tables

List of Abbreviations

ΔG: Binding free energy

Abs: Absorbance

ADMET: Absorption, Distribution, Metabolism, Excretion, and Toxicity

C: Concentration

CV: Cycle Voltammetry

DMSO: Dimethyl Sulfoxide

DPPH: 2, 2 -Diphenyl-1-picrylhydrazyl.

E: Energy

G: Gramm

GC/MS: Gas Chromatography-Mass Spectrometry

GR: Glutathione Reductase

IC_{50}: Concentration causing 50% inhibition of an activity

K: Binding Constant

Kg: Kilo Gramm

KJ: kilo joule

Mg : Milligramme

$O_2^{\cdot -}$: Superoxide Radical

PH : Hydrogen Potential

T°: Temperature

UV : Ultra-violet

Vis : Visible

α: Alpha

β: Beta

µl: Microlitre

SUMMARY

SECOND PART *:* EXPERIMENTAL

CHAPTER ONE: MATERIALS AND METHODS

CHAPTER TWO: RESULTS AND DISCUSSION

General Introduction

In recent years, there has been a growing global interest in medicinal plants, as they are considered an important natural source of treatment due to their content of biologically active compounds that exhibit various therapeutic properties, most notably antioxidant properties.

Antioxidant activity is one of the key features that contribute to the prevention of many chronic and serious diseases, such as heart disease, cancer, and neurological disorders, which result from the harmful effects of free radicals in the body.

As plants are considered a fundamental source for human health, interest in studying them has increased in the modern era due to their role in developing natural and safe therapeutic alternatives. Their ease of access and preparation may help reduce reliance on chemical compounds that often have side effects.

Many studies have shown that Algeria is rich in several important medicinal plants and a deeper understanding of the bioactive properties of local medicinal plants. Among these, we selected a plant from the Asteraceae family, *Cotula Cinerea*, and another from the Lamiaceae family, *Origanum Majorana L*, do the essential oils extracted from these plants exhibit significant antioxidant activity? and which specific chemical compounds are responsible for this antioxidant activity?

We therefore divided our research into two parts.

The first part

Chapter one: addresses the theoretical aspect of medicinal plants, including their classification, uses, as well as the description, classification, and uses of the studied plants.

Chapter two: discusses the concept of oxidation, free radicals, and their types.

The second part

Chapter one: represents the experimental section, in which we used essential oils extracted from *Cotula Cinerea* and *Origanum Majorana L*, and tested their antioxidant activity using various techniques.

Chapter two: we analysed and compared the obtained results.

Our study was not isolated from previous research, as many studies have demonstrated antioxidant activity in various plant oils, such as Rosmarinus officinal is (rosemary) oil and Thymus vulgaris (za'atar) oil. These findings motivated us to investigate other plants whose bioactive properties are still not well known, such as *Cotula Cinerea* and *Origanum Majorana L*., in an effort to uncover their potential and

future applications. Various analytical techniques have also been used in previous studies to investigate interactions. However, these methods often have drawbacks related to the cost of equipment, the complexity of analyses, and the availability of reagents. To address these limitations, UV-Visible spectroscopy and electrochemical methods have been employed due to their ability to provide direct monitoring, high sensitivity, and simplicity.

FIRST PART:

THEORETICAL

CHAPTER ONE : MEDICINAL PLANTS

I. Generalities about medicinal plants

1. Preface

There has been a notable rise in the interest surrounding the study and application of medicinal plants in disease treatment. This growing attention is largely due to the rich diversity of bioactive compounds found in plants, which offer substantial therapeutic potential. In fact, certain herbal treatments have been shown to be more effective than synthetic drugs in managing specific health conditions (Zulkipli et al., 2015).

2. Historical overview of medicinal plants

For thousands of years, humans have interacted with the natural world around them, experimenting with local plants initially in search of nourishment. Through this trial and error, they discovered that while some plants were harmful, others had healing properties and could ease pain. Interestingly, animals have been naturally guided by instinct to consume specific plants for nourishment or healing, without any teaching. This observation inspired early humans to follow and study animal behavior, hoping to uncover which plants could serve as remedies or sources of sustenance. In ancient China, around 2700 BC, the first recorded text on herbal medicine was written. This foundational work laid the groundwork for centuries of Chinese botanical knowledge, culminating in renowned texts such as the *Great Herbal* (Giannenas et al., 2020).

In ancient Babylon, knowledge of medicinal plants was documented on stone and clay tablets, listing more than 250 species, including well-known ones like cumin and turmeric. Similarly, in ancient Egypt, evidence of herbal medicine dates back to around 3000 BC, as seen in temple wall inscriptions, colorful illustrations, and herbal remnants found in tombs near mummified remains. Imhotep, recognized as the world's first physician, extensively used medicinal herbs such as myrrh, opium, aloe vera, and chaulmoogra to treat various ailments. For centuries, civilizations across the globe relied on these traditional Pharaonic healing methods, which remained dominant until the advent of the medical revolution in the early 19th century (Giannenas et al., 2020).

Prior to the advent of Islam, Arabs had limited knowledge in the fields of medicine and healing, often depending on the wisdom and experience of tribal elders for remedies. However, through their travels to regions like the Levant and Persia, they began to acquire medical knowledge from neighboring civilizations. In a similar vein, Algeria like many societies around the world has recently experienced a surge of interest in herbal medicine. The practice of using medicinal plants has become widespread across the population, cutting

across differences in gender, age, education, culture, and socio-economic status (Bahadur et al., 2007).

3. Definition

A medicinal plant is defined as any plant that contains one or more biologically active compounds in any of its parts whether root, stem, or leaf regardless of the chemical nature or concentration of these substances. These compounds have the ability to treat specific illnesses or alleviate their symptoms. Broadly, a medicinal plant refers to any botanical material used for therapeutic purposes and recognized for its healing effects. In scientific literature, medicinal plants are often referred to as "herbs," with the term encompassing any plant valued for its medicinal or biological properties. It's important to note that some medicinal plants are also highly toxic. These plants can act as effective treatments in small, controlled doses but may be dangerous or even fatal when consumed in large amounts. For this reason, careful attention must be given to dosage when using certain medicinal herbs (Azmir et al., 2013; Petrovska, 2012).

4. Basis of classification of medicinal plants

Medicinal and aromatic plants are categorized through five main classification systems, which often intersect across the fields of agriculture, medicine, and pharmacy. The following are the primary methods used for classification in this domain (Kan et al., 2017; Masarovičová et al., 2010).

4.1. Plant classification according to the effect of the active substance medically

A single plant can contain multiple active compounds, each with distinct therapeutic properties. Take camphor leaves, for example they are rich in essential oils that act as antiseptics and are commonly used to treat throat and nasal inflammations. Additionally, they play a key role in the formulation of widely used expectorant medications. Based on such characteristics, plants can be classified accordingly (Masarovičová et al., 2010; Vaou et al., 2022).

4.1.1. Plants that repel or kill worms

Examples include *Thymus vulgaris* (thyme), *Punica granatum* (pomegranate), and *Citrullus colocynthis* (bitter apple). The fruit of colocynth, in particular, is known for its ability to expel intestinal threadworms when boiled and consumed.

4.1.2. Plants used in cases of constipation and diarrhea

These plants possess an astringent compound called **tannin**, which is effective in treating diarrhea. For instance, *Punica granatum* (pomegranate) stimulates intestinal muscles to combat constipation, while *Tamarindus indica* (tamarind) and *Cassia acutifolia* (senna) support and promote bowel movements.

4.1.3. Plants with antiseptic and antimicrobial effects

Juniperus communis (juniper) produces an oil that was historically used by the ancient Egyptians in the embalming process due to its strong antimicrobial properties, helping preserve bodies for centuries.

4.1.4. Plants with a heart-stimulating effect

Plants rich in **glycosides**, such as *Polygonum fagopyrum* (buckwheat) and *Allium cepa* (onion), produce compounds in their leaves that are known to be helpful in managing certain heart conditions.

4.1.5. Plants with analgesic and narcotic effects

Plants that contain **alkaloids**, such as *Papaver somniferum* (opium poppy), are essential in the development of analgesic medications used to alleviate pain and soothe internal muscle spasms.

4.1.6. Plants with Hormonal Effects

Certain plants exhibit hormone-like properties, with some mimicking female hormones and others displaying effects similar to male hormones.

4.1.7. Plants with Effects on Kidney and Urinary Tract Treatment

These plants help facilitate the removal of stones from the urinary system, and their therapeutic properties can also be beneficial in other ways, such as *Ocimum basilicum* (basil), which can enhance production and improve the quality of livestock and poultry.

4.2. Chemical Classification of Plants

This method of classification relies on identifying the active chemical compounds found within the plant. Since a single plant can contain multiple active substances, the classification is typically determined by the concentration of the predominant compounds present, as outlined below (Tuyg'unovna, 2023).

4.2.1. Plants containing volatile aromatic oils

Such as *Cuminum cyminum* L. (commonly known as cumin) are characterized by their essential oil content, which contributes to their distinctive aroma and therapeutic properties.

4.2.2. Plants containing glycosides

Such as *Rheum officinale* (commonly known as rhubarb) are notable for these bioactive compounds, which play a significant role in their medicinal effects.

4.2.3. Plants containing tannins

Like *Lawsonia inermis* (commonly known as henna) are recognized for their astringent properties, which are attributed to their high tannin content.

4.2.4. Plants containing resins

Such as *Zingiber officinale* (commonly known as ginger) are valued for these compounds, which contribute to their medicinal and aromatic qualities.

4.2.5. Plants containing saponins

Like *Glycyrrhiza glabra* (commonly known as licorice) are known for their foaming properties and therapeutic effects linked to these active compounds.

4.2.6. Plants containing carbohydrates

Such as *Ceratonia siliqua* (carob) and *Althea officinalis* (marshmallow) are recognized for their carbohydrate-rich properties, which contribute to their nutritional and medicinal uses.

4.3. Classification based on the presence of the active ingredient in the plant

The active compound in a plant may be concentrated in a single organ or distributed across multiple organs, with the classification outlined as follows (Tsimogiannis & Oreopoulou, 2019):

4.3.1. Plants are used as a whole

The active compound is evenly distributed throughout the entire plant, without being concentrated in any specific part over the others, as seen in the case of *Pelargonium*.

4.3.2. Plants use their flowers or fruits

Plants that store their active compounds primarily in the petals of the flowers, like *Jasminum officinale* (jasmine), are examples of this type.

4.3.3. Plants use their roots or steorchismascula

Orchis mascula and *Glycyrrhiza glabra* tubers are examples of plants similar to salep.

4.3.4. Plants use their seeds

Examples include black seed and *Theobroma cacao* L. (cocoa).

4.3.5. Plants use their leaves

In some plants, the active compound is concentrated in the leaves, as seen in *Ocimum basilicum* (basil).

4.3.6. Plants use their fruits

Examples include the *Cuminum cyminum* L. (cumin) plant and *Vanilla planifolia* (vanilla).

4.4. Classification in Botany

In this classification system, plants are categorized based on their genetic attributes, complemented by morphological, anatomical, and physiological characteristics. This approach highlights the degree of relatedness among plant species and emphasizes specific distinguishing features. Notably, floral organs serve as a fundamental criterion for classifying and differentiating plants. The hierarchical units of this classification are illustrated in Figure 1 (Gledhill, 2008).

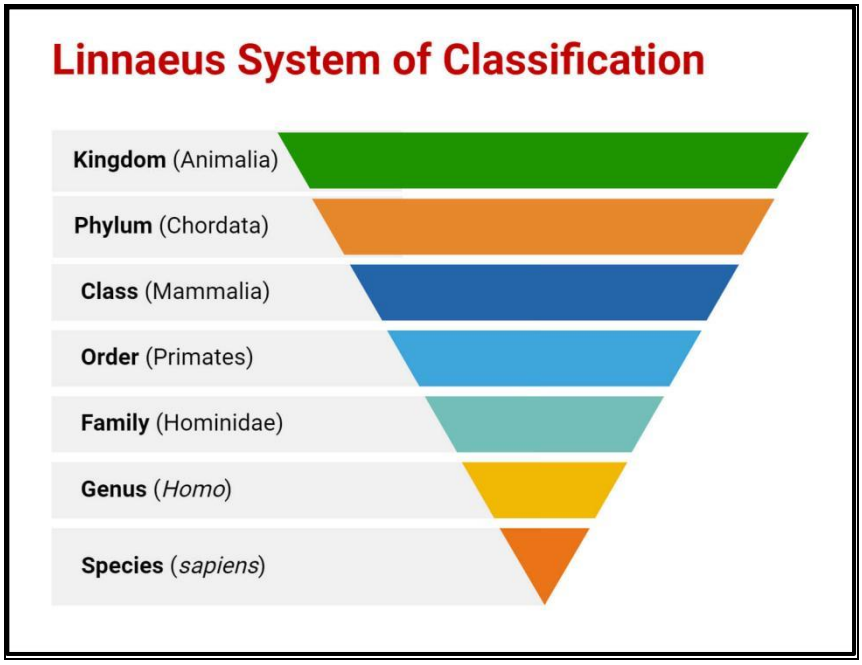

Figure 1: Classification Unit Dia gram in Plant Science (Microbe Notes.,2025)

5. Source of Medicinal Plants

Medicinal plants are sourced primarily through two methods. The first involves harvesting wild species that naturally thrive in environments such as valleys, plains, and forests. For certain plants, like the Yonka species found growing wild in Central African regions, this method can provide an adequate supply. The second method entails the deliberate cultivation of medicinal plants. In this approach, pharmaceutical companies andinvestment entities establish dedicated farms to grow specific plant varieties in quantities that meet the demands of local or global markets (Wink, 2012).

6. The most important uses of medicinal and aromatic plants

Medicinal and aromatic plants serve a variety of purposes, notably:

- Medicinal plants are utilized in the development of various pharmaceutical products, including analgesics for conditions like joint pain and rheumatoid arthritis, treatments for hypertension and arterial stiffness, as well as antiseptic agents (Bajaj, 2012).
- The production of fixed oils involves extracting oils from the seeds of certain plants, which are then used as ingredients in various medicinal formulations.

- Certain oils, such as sunflower seed oil, flaxseed oil, and castor oil, are used in the preparation of foods aimed at treating conditions like arteriosclerosis and angina.

- These oils are also used in the production of cosmetic powders, hair creams, and soaps.

- These oils are utilized in the creation of fragrances and perfumes, with plants like rose and jasmine being key ingredients (Bajaj, 2012).

- Insecticides are produced using toxic compounds derived from medicinal and aromatic plants, targeting both insects and fungi. Examples of such plants include henna and tobacco.

- They are utilized as spices, seasonings, beverages, flavor enhancers, or aromatic ingredients.

- They serve as sources for producing aromatic and medicinal oils (Ghorbanpour et al., 2017; Lubbe & Verpoorte, 2011).

II. Studied plants

1. Plant *Cotula cinerea*

1.1 Introducing the plant *Cotula cinerea*

Cotula cinerea, commonly referred to as "Shihia," is a perennial herbaceous plant distinguished by its strong, pleasant aroma reminiscent of musk. Typically reaching up to 30 cm in height, it features light green stems and leaves densely covered with fine white hairs, giving it a woolly appearance. The leaves are thick, velvety, and divided into two or three lobes at the upper part. The plant's branches culminate in composite yellow flowers that resemble small discs. *Cotula cinerea* thrives in spring, with its blooming period occurring at the end of this season (Djellouli *et al.*, 2015).

Cotula cinerea is native to the Arabian Peninsula and the Levant, where it appears sporadically. It thrives in elevated terrains and meadows adjacent to cultivated lands, often forming dense clusters in these environments. The species is predominantly found in the southern hemisphere and is especially prevalent in the desert regions of Arabia.

Cotula cinerea, commonly known as Shihia, is rich in bioactive constituents, particularly flavonoids, terpenes, and volatile oils. The volatile oils are responsible for the plant's distinctive and potent aroma. These compounds contribute significantly to the plant's diverse biological activities, including antioxidant, anti-inflammatory, and antimicrobial effects. Such properties underscore the therapeutic potential of *Cotula cinerea* in traditional and modern medicine.

1.2 Vegetable Classification of *Cotula cinerea*:

Scientific name: *Cotula cinerea Del*

Synonym: *Broccchia cinerea* (Del) vis

Common name: Grease, rupees, Scarlett.

Table1: Vegetable classification of *Cotula cinerea.*

Type	*Cinrea*
Sex	*Cotula*
Family	Starry
Community	Plague dialects
Division	Seed Cassettes

Kingdom	Plants

1.3 Vegetable Description of *Cotula cinerea*

A small herb that grows between 10 to 40 cm in height, known for its strong and distinct aroma. The plant's top is often pale and has a unique texture, with 3 to 5 branches extending from the base. Its tiny, disc-shaped flower heads measure 6 to 10 centimeters in diameter. The flowers are tubular and appear after the plant matures for about four years. The plant's stem is velvety with striped patterns, and it features a bud that initially forms a tight bud before opening into a golden hue. The fruit, though scarce, is small and photo-like in shape, as shown in the illustration (Dendougui *et al*., 2012).

Figure 2: Photograph of the *Cotula cinerea* (Mebarki L., 2016).

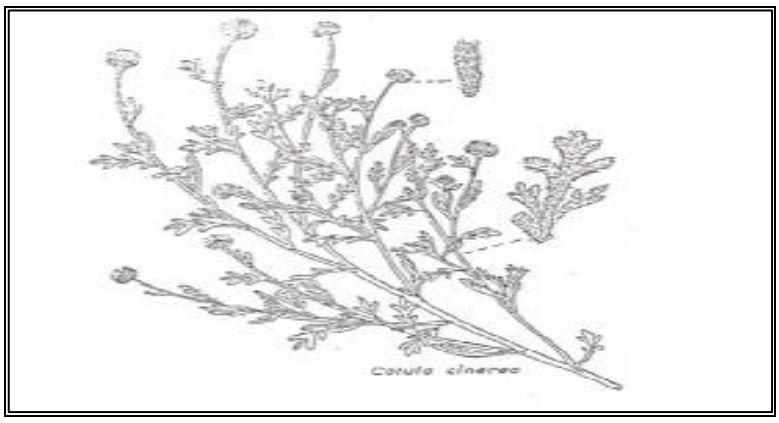

Figure 3: Schematic format for *Cotulacinerea* (Ozenda.,1967).

1.4. The geographical spread of *Cotula cinerea*

Cotula cinerea is widely found in the southern regions of the world, thriving in the Sahara, the Indian-Iranian deserts of Asia, and the deserts of the Arabian Peninsula. In Algeria, it grows primarily in desert and semi-arid zones, particularly in the southeastern parts of the country. The distribution of *Cotula cinerea* in Algeria is illustrated in Figure 4 (Franke, 2005).

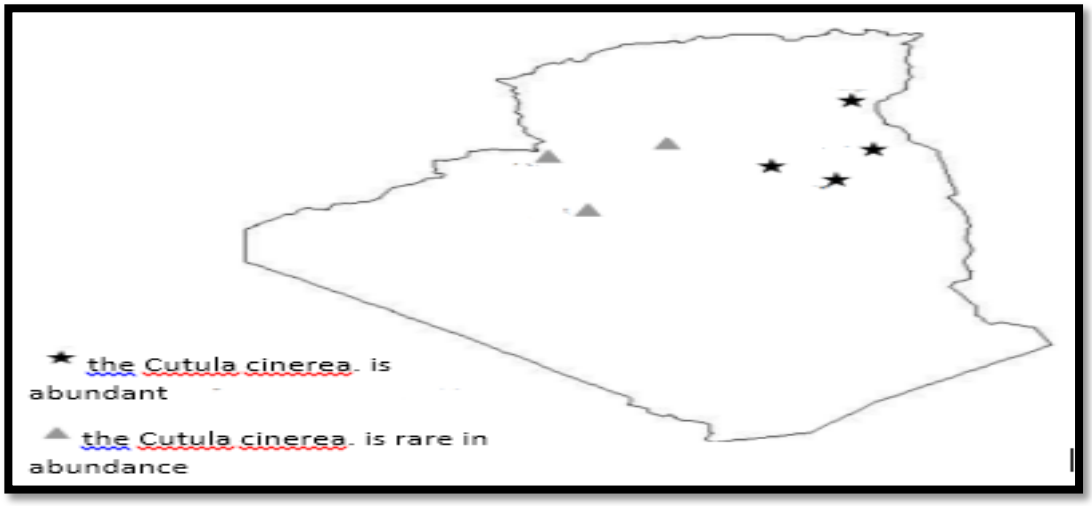

Figure 4: Prevalence of the *Cotula cinerea* plant in Algeria (Ben Amor M., 2011)

1.5 Economic and medical uses of *Cotula cinerea*

Cotula cinerea is utilized in various cultures, often as an ingredient in tea and coffee muffins. It is also commonly used in traditional medicine to alleviate abdominal pain, particularly as a digestive aid. Additionally, it is known for its properties in treating that the plant's extracts possess antifungal activity (Zahari *et al*., 2014).Respiratory infections, especially due to its ability to soothe coughing. Research has shown

Furthermore, it has been highlighted in studies (Arbain *et al*., 2022; Mekhadmi et al., 2023) for its medicinal benefits.

Flavonoid compounds extracted from *Cotula cinerea* are known to exhibit effects such as reducing inflammation, protecting against dehydration, and acting as a local remedy. In addition, in certain regions, this plant is used to treat stomach and abdominal discomfort (Buentzel et al., 2022).

2. A plant *Origanum Majorana L*

2.1. Definition of the *Origanum Majorana L* plant

The name "Onegaman" is derived from the Greek terms "oros," meaning mountains, and "gonos," meaning sunshine. It is thus associated with the stunning beauty and abundance of mountains found in the Mediterranean basin (Pezzani et al., 2017).

Origanum Majorana L., previously classified as Majorana hortensis Moench, is a herb with significant morphological and chemical diversity, exhibiting forty-nine distinct local varieties around the Mediterranean region (Vasudeva, 2015). Commonly known as sweet marjoram, it is native to Anatolia (Turkey) and Cyprus, and has been naturalized in various parts of the Mediterranean, particularly in Egypt. Historically, it was used as a medicinal agent, especially by pirate communities. Today, it is still recognized for its effectiveness in

treating respiratory issues, such as bronchial infections, coughs, and throat infections (Vasudeva, 2015).

2.2. Plant classification of *Origanum Majorana L*

Scientific name: *Origanum Majorana*

A synonym: Marjolaine

Common name: Mercenary.

Table2: Plant Classification of *Origanum Majorana L*.

Type	*Majorana L*
Sex	*Origanum*
Family	Oral
Level	No Mileage
Community	Plague dialects
Division	Flower Plants
Kingdom	Plants

2.3. Vegetation of *Origanum Majorana L*

It is a semi-woody plant that grows annually and is sensitive to cold. This aromatic shrub reaches a height of 30-60 cm, with square, reddish stems that branch out to form a dense structure. The stems are straight, fragile, and covered with fine hairs, with green, round leaves that have red spots (Paudel et al., 2022). The leaves are soft, simple, and aromatic, shaped from oval to oval-rectangular. They are pale green and arranged oppositely on square stems. The leaves are covered in fine hairs and are 0.5-1.5 cm long and 0.2-0.8 cm wide, with a pointed tip, smooth edges, and a straight base, exhibiting a network of prominent veins.

The plant produces small white or pale pink tubular flowers, which are accompanied by gray-green bracts. These bloom in clusters from mid to late summer, typically between June and September. Each flower is less than 0.3 cm long, and the flowers are predominantly female, producing small, dark oval seeds that turn brown as they mature, usually between August and September. The plant has a sub-cylindrical shape, and its roots are long with Occasional incisions. The outer diameter of the dark brown root is 0.6-0.2 mm, while the inner portion is light brown, with numerous long roots and visible root scars. The root cracks

are elongated, symbiotic, and fibrous, emitting a fragrant perfume-like scent (Hajlaoui et al., 2016).

Figure 5: Photograph of *Origanum Majorana L* (Amamra et al ,.2024).

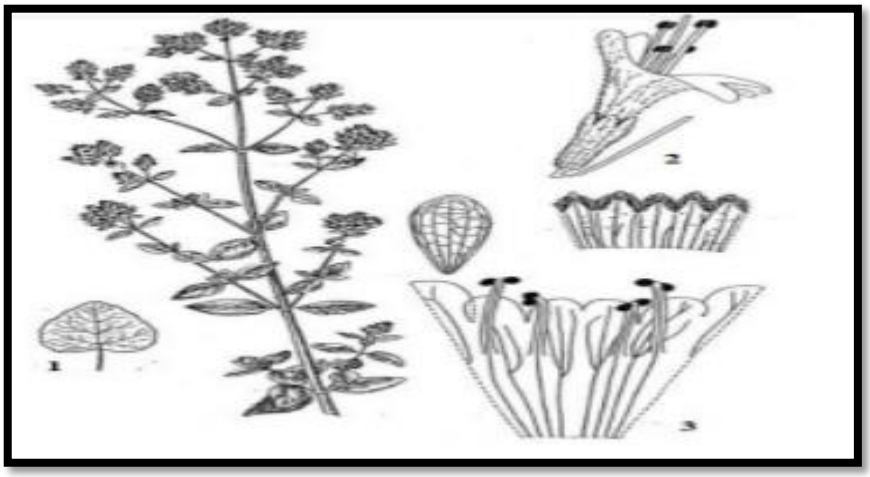

Figure 6: A schematic format for *Origanum Majorana L* *(Letswaart,J.H, 1980)*

2.4. Geographical spread of *Origanum Majorana L*

Native to Cyprus and Turkey, this plant has spread across various Mediterranean countries, including Lebanon, as well as to Iran, North America, the Arabian Peninsula, and India. It thrives in sunny areas such as meadows, fields, and rocky lands, particularly in dry climates. It is also extensively cultivated in the southern regions of Saudi Arabia (Tahmasebi et al., 2016).

The Figure (7) shows the spread of the *Origanum Majorana L* plant in Algeria.

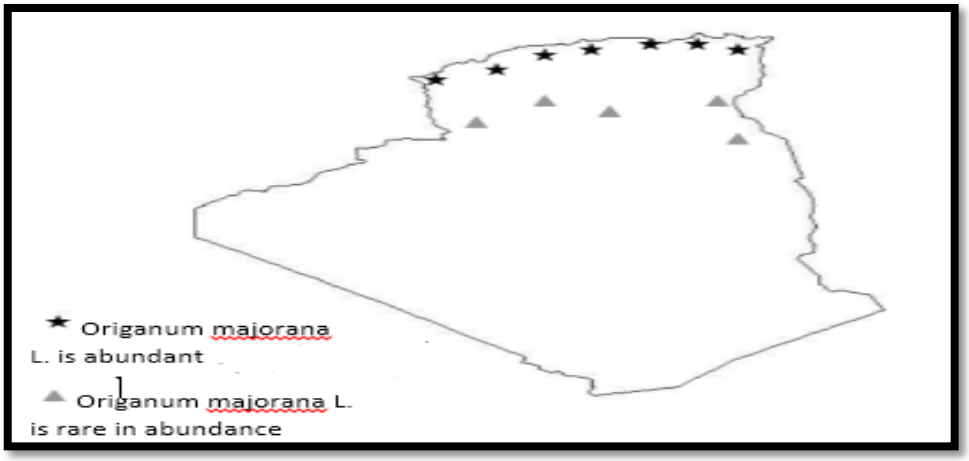

Figure 7: *Origanum Majorana L* in Algeria.

2.5. Economic and medical uses of *Origanum Majorana L*

It is considered an effective home remedy for a variety of conditions, including chest infections, coughs, throat infections, joint pain, neurological disorders, cardiovascular diseases, epilepsy, abdominal bloating, skin care, and digestive issues (Vasudeva, 2015).

This herb is commonly used in the food industry, especially in dishes with meat and vegetables. However, it is recommended to avoid its use during pregnancy due to its stimulating effect on the uterus. In traditional medicine, it is employed to treat conditions like diabetes, insomnia, asthma, and anxiety. Its essential oil is often added to enhance the flavor of various foods, including soups, gravies, meats, fish, and fried dishes, as well as beverages like wine and beer (Vasudeva, 2015).

III. General about essential oils

1. Definition of essential oils:

Essential oils are unique in that they can evaporate without undergoing decomposition, distinguishing them from fixed oils, which are non-volatile and tend to degrade when subjected to heat or evaporation (Gołębiowski et al., 2018).

These oils consist of intricate blends of aromatic and volatile substances produced by plants, originating from the secondary metabolism of aromatic plant species (Aqeel et al., 2023). Common extraction methods include steam distillation and cold pressing, particularly for citrus peels such as lemon. Depending on their chemical makeup, essential oils can range in texture from liquid to semi-liquid and may be either colorless or possess a noticeable hue.

Essential oils (les huiles essentielles) are valued for their pleasant aromas and are commonly used as attractants and flavor enhancers. These oils are found in various parts of

aromatic plants such as the leaves and stems, like in rosemary, or in the flowers, as seen in jasmine and narcissus. In some cases, they are also present in flower buds, like those of clove.

Essential oils are complex natural substances composed of various volatile compounds derived from plants. These substances are typically liquid at room temperature, colorless or lightly colored, and highly aromatic. Unlike fixed oils, essential oils do not have greasy or oily textures when touched (Hudaib et al., 2015; Rădulescu et al., 2010). They are highly volatile, flammable, and can degrade quickly upon exposure to air due to their sensitive composition.

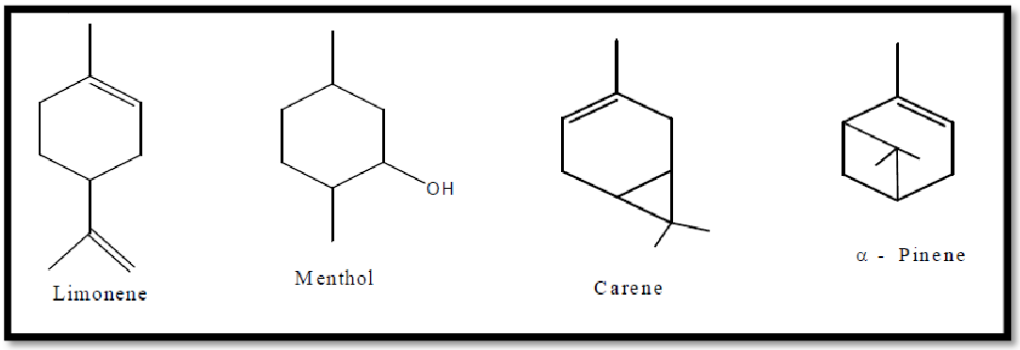

Figure 8: Structure of some essential oils (Sell, 2020).

2. Location of essential oils in vegetation

In plants, essential oils can be stored in a wide range of organs, including flowers, leaves, bark, wood, roots, rhizomes, fruits, and seeds (De Castro et al., 1999; Sharifi-Rad et al., 2017).

The production and accumulation of these oils are typically linked to specialized anatomical structures, as illustrated in Figure (9). Essential oils are synthesized within the cytoplasm of secretory cells and then gathered in glandular cells beneath a protective cuticle layer. The form and quantity of these secretory structures often referred to as secretory glands or trichomes can vary greatly between plant families, and even among species within the same family. In fact, multiple types of secretory structures may coexist within a single plant species (Morsy, 2017; Sell, 2020).

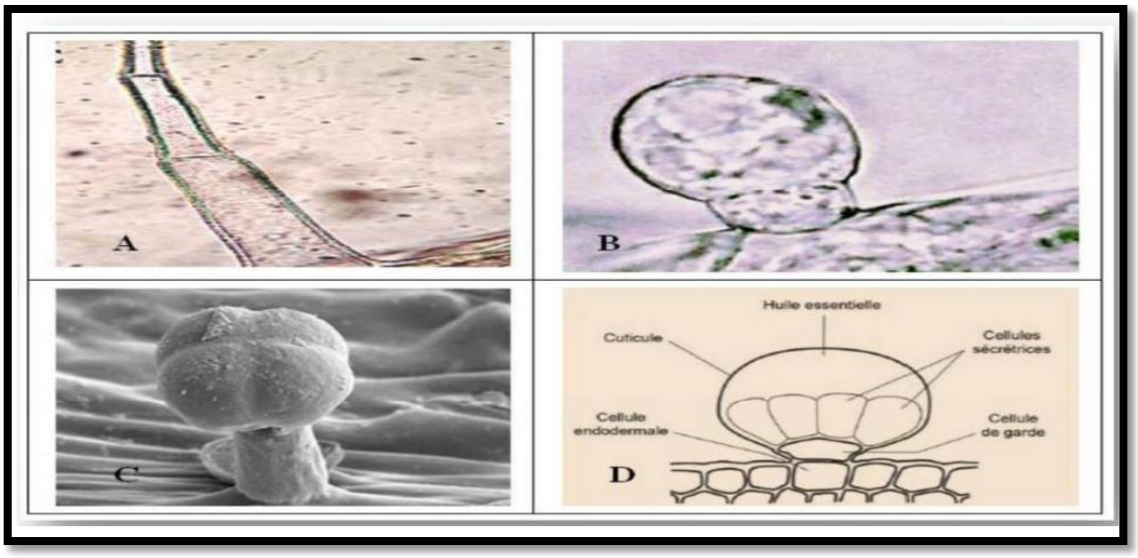

Figure9: Different types of infrastructure responsible for the formation of essential oils.

(A): Mentha pulegium-secretory hair.

(B): Mentha pulegium, mint-glandular trichome.

(C): Lippiascaberrima for glandular trichome.

(D): Thymus vulgaris - glandular trichome.

3. Installation of essential oils

Essential oils are complex blends composed of numerous chemical constituents. However, they primarily consist of two main categories: hydrocarbons, which form the core of the oil's fragrance, and oxygenated compounds. The latter group includes various organic substances such as acids, alcohols, esters, aldehydes, ketones, and ethers. In smaller amounts, essential oils may also contain compounds that include sulfur or nitrogen elements (Moghaddam & Mehdizadeh, 2017; Sadgrove et al., 2022).

3.1. Terpenes

Terpenes are natural compounds present in various parts of plants and make up a significant portion of the secondary metabolites responsible for the characteristic aromas of many plant species. The term "terpenes" originates from substances originally isolated from turpentine oil. Most terpenes are volatile and are commonly extracted from plants through essential oil isolation methods.

Terpenes play a vital role in daily life, with some, like vitamin A—a type of terpene being crucial for human health. A deficiency in vitamin A, for instance, can lead to impaired vision. In 1877, research by Owlach at the University of Göttingen in Germany revealed that the diversity of terpenes arises from variations in the number of isoprene units. Table (3) outlines the different categories of terpenes.

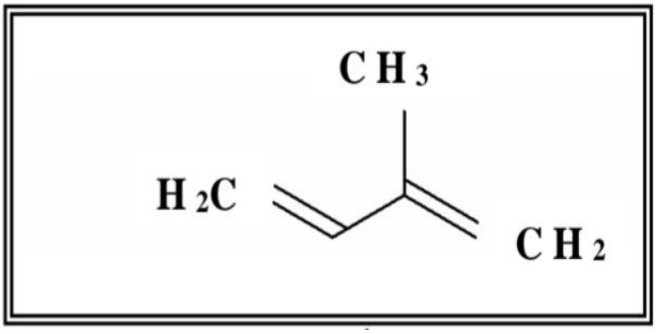

Figure10: Isoburn Unit (Agab roa, Slimani mohamed Djawad., 2024)

3.1.1. Monoterpenes

Monoterpenes are among the most widespread compounds in the plant kingdom, composed of two isoprene units. They are classified into monocyclic forms such as limonene and α-phyllandrene and bicyclic forms, with α-pinene and sabinene β-pinene being the most notable representatives (Vincken et al., 2007).

Bicyclic monoterpenes are produced in significant quantities and are further categorized into four groups based on their hydrocarbon carbon skeletons (Oyman, 2017).

✓Thujine Group
✓Karan Group Carene
✓Pinene Group
✓Kamphene Group

Togan and Karan derivatives are present in sandalwood oil, while the primary source of the pine family compounds is raw turpentine oil, which is typically extracted from the bark of pine trees.

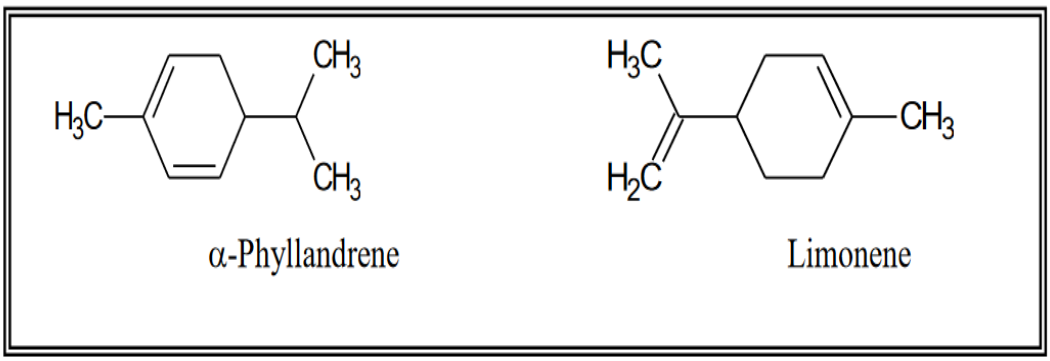

Figure 11: Monocyclic monoterpenes.

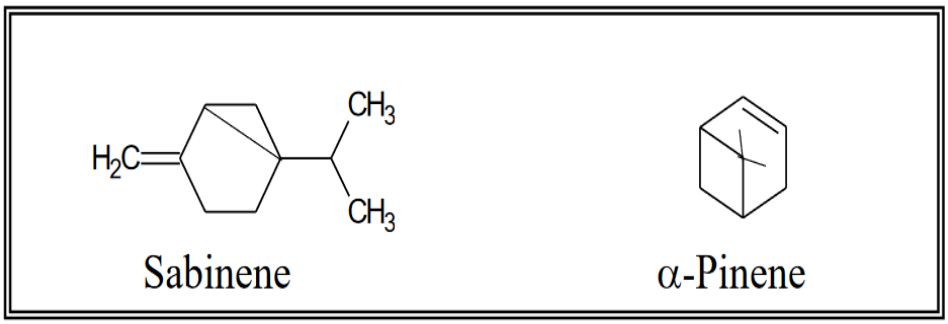

Figure 12: Monotrophine binary ring.

3.1.2. Diterpenes (digen)

These Terpenes are composed of 20 carbon atoms, equivalent to four isoprene units. Notable examples include phytol and vitamin A.

3.1.3. Sesquiterpenes

There are over 2,500 known molecules made up of three isoprene units, each containing 15 carbon atoms. These compounds are generally classified into two main types based on their carbon framework. One type is represented by Cadinene, a well-known Sesquiterpene, while the other type includes Selinene, which is commonly found in celery oil.

3.1.4. Triterpenes

A notable example is the compound known as esculine, which is regarded as a structural precursor or building block of cholesterol.

3.1.5. Tetraterpens

Each of these compounds is made up of eight isoprene units, commonly referred to as carotenoids. Three distinct carotenoids have been isolated, including α-carotene, δ-carotene, and β-carotene.

3.1.6. Polyterpenes

One of the most significant examples of this is natural rubber, which occurs naturally as a brown emulsion. It is extracted from rubber trees found in tropical regions, and its molecular structure consists of Cis forms that are linked through bilateral bonds (Sarkar & Bhowmick, 2018).

Table 3: Types of Terpenes.

Type of terpenes	Number of carbon atoms	Number of Isopren units
Monotheistic	10	2
Raising half a trio	15	3
Tuppering's a couple	20	4
Triple turbine	30	6
Tetra-turbation	40	8
Polytechnic	Over 40	More then 8

4. Aromatic oil extraction methods

There are several methods used to extract essential oils, with the most common being water distillation, steam distillation, cold pressing, and extraction using organic solvents (Stratakos & Koidis, 2016).

4.1. Distillation

In most plants, aromatic oils are extracted through this method, which involves heating the plant material to vaporize the essential oils. This allows the volatile components to be separated from the rest of the plant matter. The vapor is then cooled and condensed to obtain the oil. When carried out properly, this distillation process performed using one of two main techniques yields high-quality essential oils with desirable natural and chemical properties (Aziz et al., 2018; Directions).

4.1.1. Hydro distillation method

In this method, plant materials are immersed in water inside a container or metal vessel and then heated either directly over a flame or indirectly using a water bath to avoid burning the plant parts that come into contact with the container walls. This technique is particularly suitable for heat-tolerant and partially dried plants that have high essential oil content, such as seeds and peels (Aziz et al., 2018; Directions).

4.1.2. Steam distillation

In this method, plant materials are placed in perforated containers that allow steam to pass through them, facilitating the release and extraction of volatile oils. These vapors are then directed into condensation pipes, where the oil separates easily from the water. For optimal results, the plant matter is usually crushed or broken into smaller pieces to allow better

penetration of the steam and maximize oil yield. This technique is suitable for all plants that contain essential oils and can withstand high temperatures (Aziz et al., 2018; Directions).

5 .Basic oil uses

These natural substances play a crucial role in various industries, as highlighted by (Bolouri et al. 2022).

5.1 Pharmacist

It can be applied in the following ways:

It aids in reducing the oral medication dosage for an individual.

It supports her physiological effects.

5.2. In industry

5.2.1. Perfume and beauty industry

A large number of perfumes are derived from natural sources, with essential oils from flowers like rose and jasmine serving as key ingredients in many of them (de Sousa et al., 2023).

5.2.2. Nutrition

Essential oils, such as lemon oil and mint, are commonly used to enhance the flavor of foods like fruit juices and pastries (de Sousa et al., 2023).

CHAPTER TWO:

ANTIOXIDANT

ACTIVIY

I. Antioxidants

1. History

Initially, the term "antioxidants" referred to chemical substances that prevented the consumption of oxygen during the late 19th and early 20th centuries, research focused heavily on their applications in various industries, such as preventing metal corrosion, treating rubber, and reducing fuel reactions within combustion engines. As science progressed, the focus shifted to the biological role of these substances, especially in preventing the oxidation of unsaturated fats that leads to rancidity, at that time antioxidant activity was easily measured by observing oxygen consumption in sealed containers containing fats.

However, a major breakthrough came with the discovery of vitamins A, C, and E as antioxidants, which opened new horizons for understanding their vital role in living organisms. Scientists began to explore their mechanisms of action and found that substances with antioxidant properties are often those that are easily oxidized themselves, These compounds act as electron donors inhibiting oxidative reactions by scavenging free radicals before they can cause damage to cells (V. Lobo et al., 2010).

2 . Definition of antioxidants

Antioxidants are molecules capable of donating an electron to unstable free radicals, effectively neutralizing them and reducing their potential to cause cellular damage. Their main role is to delay or prevent cell damage through their free radical scavenging abilities. These low molecular weight antioxidants can safely interact with free radicals and halt the chain reaction before vital cellular components are harmed. Some antioxidants, such as glutathione, ubiquinol, and uric acid, are naturally produced in the body as part of normal metabolism. Others, typically lighter antioxidants, are obtained from the diet. While the body has enzymatic systems that help eliminate free radicals, the key antioxidant micronutrients vitamin E (alpha-tocopherol), vitamin C (ascorbic acid), and beta-carotene must be supplied through dietary sources, as the body cannot synthesize them (V. Lobo et al ., 2010).

3 .Types of Antioxidants

According to antioxidants can be classified into several types:

3.1 .Primary Oxidation Inhibitors

These antioxidants eliminate free radicals generated from oxygen and nitrogen after their formation, They do so by donating electrons to neutralize them, converting them into a stable form, or by preventing their formation altogether.

3.2 .Secondary Oxidation Inhibitors

These mechanisms act to halt the on-going oxidation of fats that begins due to interactions with oxygen or nitrogen radicals. This process is referred to as super-grease oxidation chains. These inhibitors are critically important, as their failure can lead to cell death or genetic mutations.

3.3. Tertiary Antioxidants

This group includes complex systems of various enzymes that repair the damage caused by free radicals when earlier defense mechanisms fail. Examples include enzymes involved in the repair of nucleic acids (Vijayshree Yadav et al., 2016).

4 .Classification of antioxidants

In recent years, there has been a significant increase in research on antioxidants compounds that play a crucial role in protecting the body from damage caused by free radicals, these antioxidants have been classified in various ways, but the most common classification relies on two main criteria (Stoia M, Oancea S., 2022):

4.1 .Mechanism of Action

Primary antioxidants: Also known as "chain breakers," they directly inhibit or stop oxidation reactions by interacting with free radicals and neutralizing them before they cause damage.

Secondary antioxidants: These do not react directly with free radicals but instead perform supportive roles, such as converting oxidizing substances into harmless compounds or stabilizing metals that accelerate oxidation reactions.

4.2 .Catalytic Properties

4.2.1. Enzymatic antioxidants

These are specialized proteins (e.g., SOD and glutathione peroxidase) that catalyse the breakdown of free radicals.

4.2.2. Non-enzymatic antioxidants

Include compounds like vitamins (e.g., C and E) and phenols, which work directly or indirectly to inhibit oxidation.

In addition, the terms "natural" and "synthetic" are frequently used when discussing antioxidants, Synthetic antioxidants are often viewed negatively due to fear of chemicals, although this perception is not always scientifically justified.

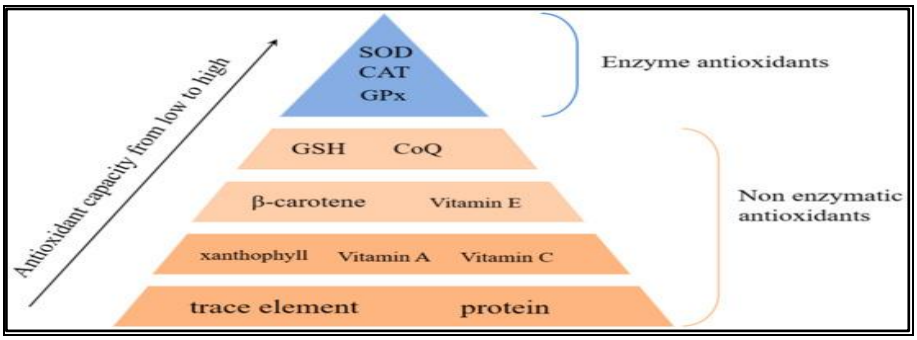

Figure13. A comparison the properties and roles of enzymatic and non-enzymatic antioxidant systems in cellular defense against oxidative stress(Guan G et al., 2024).

Enzymatic antioxidants, such as superoxide dismutase (SOD), catalase (CAT), and glutathione peroxidase (GPx), neutralize ROS in a stepwise manner. Non-enzymatic antioxidants, including glutathione (GSH), vitamins C and E, and plant derived antioxidants, directly scavenge free radicals and provide additional protection.

4.2.3. Natural antioxidants

Produced by living organisms such as bacteria, fungi, plants, and animals for self-protection.

4.2.4. Synthetic antioxidants:

Industrially manufactured by experts for human benefit, but they require safety testing before being approved for use. It's important to note that both types may carry some degree of toxicity. Recently, researchers have proposed a new classification system for antioxidants based on eight key criteria: mechanism of action, type of antioxidant reaction, molecular size, solubility, intended application, origin or natural presence, biological defensive role, and location within the biological system. Antioxidants can also be classified based on the types of molecules they protect, such as:

Lipids (e.g., tocopherols, carotenoids, ascorbic acid, phenols, glutathione peroxidase, lipoic acid)

Proteins (e.g., protective agents, tocopherols, phenols)

DNA (e.g., SOD, glutathione, cysteine, vitamins)

Antioxidants work together synergistically to protect cells from oxidative damage. Many of these compounds are small in size natural or synthetic, water or fat soluble and function by eliminating free radicals or preventing chain oxidation reactions. However, at high concentrations, they may act as pro-oxidants and become harmful.

Generally, synthetic antioxidants are purer and more stable than natural ones, offering consistent activity however they must pass regulatory safety assessments before being marketed.

Nature-identical antioxidants combine the benefits of both types: they are cost-effective, efficient, and stable like synthetic ones, while also being health-promoting like natural antioxidants.

Some antioxidants exhibit both biological and antioxidant activity known as bio-antioxidants, others may only show antioxidant effects without direct biological impact in some cases, their biological effects such as suppressing cytokine or IL-1β production or inhibiting cell proliferation are not directly related to their antioxidant function but may help enhance the effectiveness of therapeutic drugs (Guan G et al ., 2024).

II. Stress oxidative

1. Definition of stress oxidative

Oxidative stress is defined as a condition in which the body loses its ability to counteract reactive oxygen species (ROS) due to a disruption in the internal balance between these species and antioxidant agents (AO). This imbalance may lead to structural and functional damage within the body (Ayoub B., 2018).

1.1. Factors of the production of ROS (Reactive Oxygen Species)

can be rephrased as follows

- Intense physical activity leads to higher energy demands and increased oxygen consumption, which promotes the production of ROS.

Tissue ischemia, resulting from mitochondrial dysfunction, causes an increased release of ROS, leading to oxidative damage associated with inflammation.

In cases of arterial hypertension, the release of nitric oxide, a vasodilator, causes cerebral hypoperfusion. This situation stimulates ROS production and results in cerebral edema through the activation of neutrophilicpolymorphonuclear cells (Ayoub B., 2018).

1.2. Mechanisms of Reactive Oxygen Species (ROS) Generation

Reactive oxygen species (ROS) are produced through several mechanisms, the most notable being mitochondrial respiration. When electron transport is disrupted due to the uncoupling of oxidative phosphorylation, the redox potential becomes imbalanced, promoting the auto-oxidation of biomolecules and leading to increased ROS generation.

Additionally, the intensification of inflammatory responses and elevated levels of free iron and other transition metals significantly contribute to ROS production.

During biotransformation processes, free radicals are generated as a result of the activation of nitric oxide synthase enzymes (NOS I, II, III) and the stimulation of various oxidases such as NOX, MAO, and XO (Ayoub B., 2018).

2 .Definition of free radical

Free radicals are molecules that contain one or more atoms with an unpaired electron in their outer orbit, making them highly unstable and extremely reactive with other biological molecules inside the cell, such as proteins, nucleic acids (DNA/RNA), and lipids.

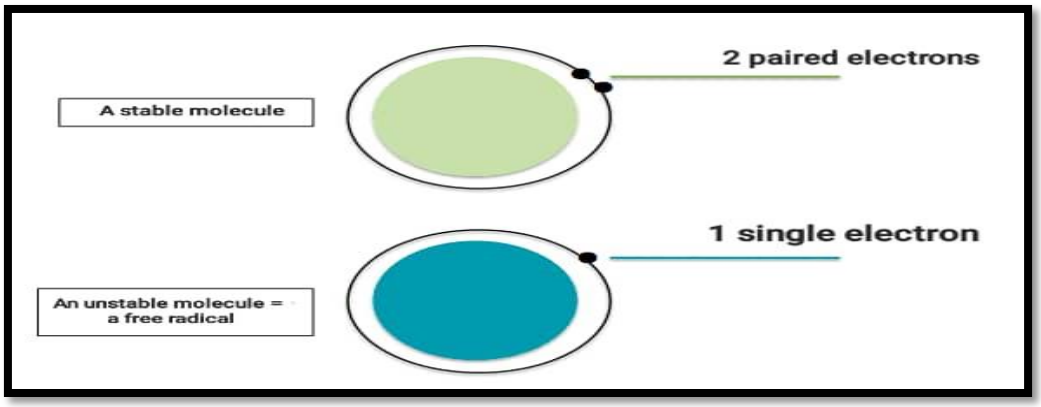

Figure 14: representation of a free radical (Durand K ,. 2018).

Free radicals belong to the group of reactive oxygen species (ROS), and examples include the superoxide radical $O_2^{\cdot -}$ The hydroxyl radical $OH^{\cdot}$, and singlet oxygen ($^1O_2$).

Free radicals vary in their chemical properties, such as their ability to diffuse within cells and their reactivity; some free radicals can play a positive role in the body at low concentrations, contributing to immune responses and cellular signaling pathways. However, when they accumulate excessively without adequate antioxidant defenses, they lead to a condition known as oxidative stress, This state causes damage to biological molecules and results in cellular aging, genetic mutations, cancer, and chronic diseases such as heart disease, diabetes, and neurological disorders.

Despite their small size, free radicals have a significant impact on cellular balance, and controlling them is essential for maintaining the health of cells and the entire organism (V. Lobo et al ., 2010).

3. Major types of free radicals

3.1. Reactive oxygen species

Reactive oxygen species (ROS) refer to a group of highly reactive oxygen-containing molecules, encompassing both radical and non-radical types. These species are involved in initiating and propagating chain reactions in biological and chemical systems. Free radicals, in particular, are a subset of ROS characterized by the presence of an unpaired electron, which makes them extremely reactive. Despite their short-lived nature, they can exist

independently for a brief moment and significantly influence chemical interactions (Shiv, 2011).

3.2. Reactive nitrogen species

Reactive nitrogen species (RNS) are highly reactive molecules capable of inflicting cellular damage by oxidizing and nitrating essential biomolecules. Among these species are nitric oxide (NO) and its derivative, peroxynitrite ($ONOO^-$). The formation of peroxynitrite typically occurs during inflammatory responses, and it has been associated with the progression of numerous diseases (Marina & Abraham, 2006).

SECOND PART:

EXPERIMENTAL

CHAPTER ONE: MATERIALS AND METHODS

1. Introduction

This study was conducted collaboratively between two specialized laboratories : the Valorisation and Technology of the Saharian Resources Laboratory (VTRS) at the Faculty of Exact Sciences, Department of Chemistry, University of El Oued, and the Centre de Recherche Scientifique et Technique en Analyses Physico-Chimique (CRAPC) in Ouargla, Algeria. The VTRS lab facilitated essential oil extraction, conducted *in vitro* and *in-silico* assays. Meanwhile, CRAPC handled the precise GC/MS analysis of the extracted oils. This collaborative effort ensured thorough and accurate experimentation, combining expertise and resources from both institutions.

2. Plant Material

2.1. *Cotula cinerea*

The *Cotula cinerea* plant was harvested at various time intervals ranging from December 2023 to January 2024 in a desert forest area in southeastern Algeria, specifically in Hassi Khalifa region in El Oued province. This region is characterized by the following specifications:

- Geographic Coordinates: Longitude 48°10' East, Latitude 23°09' North.
- Elevation above Sea Level: 44 meters.
- Distance from Sea Level: 290 kilometres.
- Bioclimatic Characterization : Desert.

2.2. *Origanum Majorana L*

The *Origanum Majorana L* plant was harvested at different time intervals extending from March 2023 to April 2023 in a desert forest area in southeastern Algeria, specifically in Akfadou region in El Oued province. This region is characterized by the following specifications:

- Geographic Coordinates: Longitude 67°6' East, Latitude 33° North.
- Elevation above Sea Level: 58 meters.
- Distance from Sea Level: 300 kilometres.
- Bioclimatic Characterization : Desert.

3. Chemicals and reagents

Dimethyl sulfoxide (DMSO) (HPLC-grade from Sigma-Aldrich) was utilized as a solvent in the experimental procedures. Additionally, 2,2-diphenyl-1-picrylhydrazyl (DPPH), a stable free radical commonly employed in antioxidant assays, served as the reagent for assessing antioxidant activity. Tetrabutylammonium tetrafluoroborate (Bu_4NBF_4) (electrochemical

grade, 99% purity, Sigma-Aldrich) was employed as the supporting electrolyte, maintaining a concentration of 0.1M, Molecular oxy-gen was provided from a cylinder (research grade (99.99%); Linde gaz Algérie), All other reagents utilized were of analytical grade.

4. Materials and Methods

4.1. Essential Oils Extraction

4.1.1. Apparatus

The essential oil extraction process required the use of specialized equipment to ensure accuracy and efficiency. In this study, the following apparatus was utilized:

- ✓ Adventurer – Pro AV53 sensitive balance
- ✓ Heating flask
- ✓ Refrigerant
- ✓ Clevenger apparatus
- ✓ Separating funnel
- ✓ Rotary evaporator

The Clevenger apparatus, a key component in the extraction process, is depicted in Figure 15

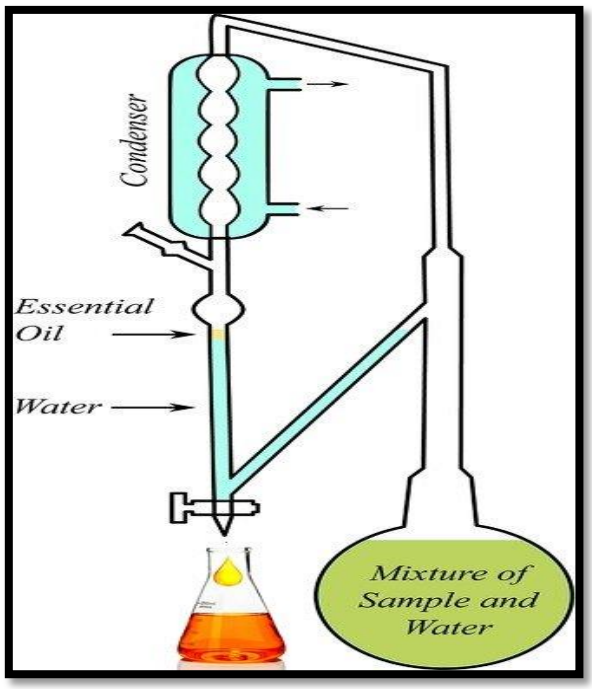

Figure 15. Schematic representation of the Clevenger apparatus used in the essential oil extraction process (Biswa *et al.*, 2023)

4.1.2. Procedure

The procedure for essential oil extraction involved a series of meticulous steps to ensure optimal results. The extraction process was conducted as follows:

- ✓ Cleaning of the plant sample to remove any impurities.
- ✓ Weighing the plant sample to a quantity of 100 g using a sensitive balance.
- ✓ Washing the plant sample with water to prevent burning, followed by placement in a heating flask.
- ✓ Addition of small pieces of boiling regulator to the flask.
- ✓ Direct heating of the mixture at a temperature of 100 degrees Celsius for three and a half hours.
- ✓ Conducting the steam distillation process and subsequent separation of oil and water phases using liquid-liquid separation with diethyl ether.
- ✓ Drying of the organic oily phase with anhydrous sodium sulphate.
- ✓ Filtration of the dried oil phase through filter paper to remove diethyl ether particles.
- ✓ Evaporation of the filtered oil phase using a rotary evaporator to remove any remaining organic solvent.
- ✓ Storage of the obtained essential oil in small brown bottles and refrigeration at a temperature of 5°C.

4.2. Yield of Essential Oil Extraction

Two distinct methodologies are commonly employed to ascertain the yield of essential oil extraction, each offering unique perspectives on the efficiency of the process.

4.2.1. Volumetric Yield - Mass-based (Naima *et al.*, 2019)

This approach involves evaluating the weight of the plant material used for essential oil extraction and comparing it to the volume of oil obtained. The extraction yield is subsequently determined using Equation 1:

$$R_{EO} = \frac{V_{EO}(ml)}{m_0(g)} \times 100 \qquad (1)$$

Where: R_{EO}: Essential oil yield, m_0: Mass of the utilized plant sample, V_{EO}: Volume of the extracted essential oil

4.2.2. Mass-based Yield - Mass-based (Larbi et al., 2018)

Another way to express the essential oil yield is as the ratio between the mass of the oil obtained and the mass of the plant material used in the extraction process. This ratio is determined using Equation 2:

$$R_{EO} = \frac{m_{EO}(g)}{m_0(g)} \times 100 \qquad (2)$$

Where: R_{EO}: Essential oil yield, m_0: Mass of the utilized plant sample, m_{EO}: Mass of the extracted essential oil.

These approaches have been consistently employed to calculate the essential oil yields from each of the analysed plant samples.

4.3. Characterization of Essential Oils

Essential oil characterization involves two key aspects: the assessment of physicochemical parameters and the analysis through Gas Chromatography-Mass Spectrometry (GC/MS).

4.3.1. Physicochemical Properties:

In this section, we explore the core physicochemical characteristics of essential oils, such as relative density, acid value, ester concentration, and refractive index. These parameters provide crucial information about the chemical structure and functional behavior of essential oils, shedding light on their composition and interactions within various environments (Atti-Santos et al., 2005).

Relate a temperature of 20°C, a 1 mL sample of the essential oil is precisely measured with a pipette, and its mass is recorded. The same steps are followed using distilled water. The density is then calculated based on Equation 3 (Valarezo et al., 2015).

- **Relative Density (AFNOR NF T75-111 Standard):**

$$d = \frac{m_{EO}}{m_{H_2O}} \qquad (3)$$

Where m_{EO}: Mass of the extracted essential oil, m_{H_2O}: Mass of the distilled water

- **Acidity Index (AFNOR NF T75-111 Standard)**

The acid value, which indicates the amount of free acids present in 1 gram of essential oil, is determined using a titration technique involving a potassium hydroxide (KOH) solution (Sahoo et al., 2007).

To begin, a small volume (0.5 mL) of the essential oil is combined with 2 to 3 drops of phenolphthalein indicator in a suitable container. This mixture is then titrated with a 0.5 N

KOH solution until a pale pink coloration emerges, signifying the complete neutralization of the free acids. The acid value is subsequently determined using Equation 4.

$$I_a = \frac{56.11 \times V \times C}{m} \qquad (4)$$

Where: V: the volume of the KOH solution, C: Concentration of KOH, m: the mass of the essential oil

➢ **Ester Index (AFNOR NF T75-111 Standard)**

The quantification of free acids produced through ester hydrolysis in the essential oil is carried out via titration using a 0.5 N potassium hydroxide (KOH) solution (Alajtal et al., 2018).

- Start by transferring 0.5 mL of the essential oil into a small container.
- Add 1 mL of 0.5 N potassium hydroxide (KOH) solution to initiate the titration.
- Place the mixture in a vacuum-sealed water bath for a designated period to promote the reaction.
- Once the mixture has cooled, add 0.5 mL of distilled water along with 3 drops of phenolphthalein indicator.
- Titrate the unreacted KOH with 0.5 N hydrochloric acid (HCl) until visible color shift signals neutralization.
- Record the volume of HCl used to neutralize the excess KOH.

Calculate the ester content using the following Equation 5:

$$I_e = \frac{2805}{m}(V_0 - V_1) - I_a \qquad (5)$$

Where: V_0 (ml): Volume of hydrochloric acid (HCl) without essential oil, V_1 (ml): Volume of hydrochloric acid (HCl) in the presence of essential oil, I_a: Acid value, I_e: Ester value and m: Mass of the essential oil sample.

➢ **Refractive Index (AFNOR NF T75-111 Standard)**

The refractive index of an essential oil is the ratio of the sine of the angle of incidence to the sine of the angle of refraction of a light ray, with a specific wavelength, as it passes from air into the essential oil, which is maintained at a constant temperature (Singh, 2002).

This refractive index is directly measured using a refractometer at a reference temperature of 20°C.

4.3.2. Gas Chromatography-Mass Spectrometry (GC/MS) analysis

The GC/MS coupling technique is widely regarded as the most commonly used method in essential oil analysis, allowing for the simultaneous separation, identification, and quantification of the different components found in the extracted oils.

➢ ***Principle:***

The method is based on the differing affinities of the compounds in the mixture for two phases: a stationary phase and a mobile phase. It depends on the distribution of the components between a stationary phase and a gaseous phase. The stationary phase consists of a silicone-based liquid embedded in an inert, granular solid material, which is contained within a typically coiled column made of steel or glass, ranging from 1 to 3 meters in length and 2 to 4 millimeters in diameter. The mobile phase is an inert carrier gas, such as nitrogen, helium, or argon.

The column is heated to a high temperature by a furnace, which causes the compounds to vaporize and become separable. The separation process is based on the differences in the partition coefficients of the volatile compounds between the stationary and gas phases. A detection system generates a signal as each molecule exits the column, which is recorded as peaks that represent each individual component.

When gas chromatography is coupled with a mass spectrometer (MS), the unknown peaks are identified through computerized comparison of their spectra with reference libraries, allowing for precise identification.

➢ **Apparatus**

The chemical constituents of the essential oils were identified using a gas chromatograph (HP 5890-SERIE II) fitted with an HP5 MS capillary column (30 meters long, 0.25 mm internal diameter, and 0.25 µm film thickness), coupled to a mass spectrometer (HP-MSD 5972).

Nitrogen (N2) was used as the carrier gas for analyzing the two essential oils. Spectra were recorded at emission energy of 70 eV, and the compounds were identified by comparing their spectra with reference data from the WILEY275 spectral libraries (Shamma, 1972; Kiryakov, 1968; Chiu et al., 1982; Guinaudeau et al., 1975).

➢ **Procedure**

The carrier gas (N2) is introduced at a flow rate of 1 mL/min, with 1 µL of essential oil being injected via a split injection method. The injector and detector temperatures are set at 250°C and 320°C, respectively. The oven temperature is initially set to 60°C, where it is held for 8 minutes, then gradually increased to 250°C at a rate of 2°C/min. Once it reaches 250°C, the temperature is held isothermally for 15 minutes before being raised to 300°C at a rate of 10°C/min.

4.4. *In Vitro* radicals inhibition assays

4.4.1. Cyclic Voltammetric Measurements

✓ **Apparatus**

The voltammetric measurements were performed using a Potentiostat/Galvanostat Model PGZ301 (Radiometer Analytical SAS), which was connected to a three-electrode electrochemical cell comprising:

- A glassy carbon electrode with a diameter of 5.2 mm².
- A mercury/mercurous chloride/saturated KCl reference electrode.
- A platinum auxiliary electrode with a diameter of 3 mm².

This setup was controlled by Pentium IV microcomputer (CPU 4.0 GHz and RAM 2 GB) running VoltaMaster4 software, version 7.08.

✓ **Reagents**

- Dimethyl sulfoxide (DMSO) solution
- Electrolyte support (Tetra-n-butylammonium tetrafluoroborate, 99%)
- Nitrogen (Gas)
- 2,2-diphenyl-1-picrylhydrazyl
- Superoxide anion $O_2^{\cdot-}$

✓ **Procedure**

The reaction between the essential oils and DPPH occurs within the electrochemical cell, where Dimethyl sulfoxide (DMSO) solution serves as the reaction medium.

Prior to each measurement, the working electrode is polished with p4000 abrasive paper. After polishing, the electrode is rinsed with ultra-pure water and dried using air, resulting in a mirror-like surface. The electrochemical cell is then assembled with the reference electrode, auxiliary electrode, and working electrode. The cell is filled with 10 mL of an DMSO solution containing the essential oils to be analyzed. Nitrogen gas is bubbled through the solution for 10 to 15 minutes to expel oxygen from the cell. A variable potential is applied at a constant scan rate, with the temperature maintained at 28 ± 2°C. The resulting voltammogram is analyzed to evaluate the interaction parameters between the essential oil and DPPH.

The ability of the test sample to scavenge the DPPH radicals (% Inhibition of DPPH) was calculated using Equation 6 (Lanez *et al.*, 2023; Lanez *et al.*, 2019),

$$\%\ radical\ scavenging\ activity = \frac{i_0 - i}{i_0} \times 100 \quad (6)$$

Where i_0 and i are the anodic peak current densities of the radical in the absence and presence of *Cotula cinerea* and *Origanum Majorana L* essential oils, respectively.

Following the same previous steps, the scavenging activity of superoxide anion radical ($O_2^{\bullet-}$) was evaluated using the same preparation, treatment and measurement conditions.

4.4.2. Spectroscopic Measurements

✓ **Apparatus**

UV-Vis measurements were conducted using a UV-Vis spectrometer (Shimadzu 1800) with a 5 mL quartz cell. Data collection was managed by a Pentium IV microcomputer (CPU 4.0 GHz, RAM 2 GB) running UV Probe software version 2.34 (Shimadzu). The collected data was processed with Origin Lab 9.0 software.

✓ **Reagents:**

- DMSO solution
- 2,2-diphenyl-1-picrylhydrazyl

✓ **Procedure:**

The electronic spectra of DPPH in DMSO solution were recorded both in the absence and in the presence of progressively higher concentrations of *Cotula cinerea* and *Origanum Majorana L* essential oils.

The capacity of the test sample to scavenge DPPH radicals (% inhibition of DPPH) was determined using Equation 7 (Filote et al., 2022).

$$\%\ radical\ scavenging\ activity = \frac{A_0 - A}{A_0} \times 100 \quad (7)$$

Where A_0 and A are the absorbances of the radical in the absence and presence of *Cotula cinerea* and *Origanum Majorana L* essential oils, respectively.

4.5. *In-Silico* analysis

4.5.1. Software

Computational simulations, such as Induced Fit Docking, molecular dynamics, and MM-GBSA calculations, were performed using the Glide, Induced Fit Docking, Prime, and Desmond modules within the Maestro version 11.7 interface of the Schrödinger suite (Small-Molecule Drug Discovery Suite 2021-4, Schrödinger, LLC, New York, NY, 2021) (Schrödinger, 2015). The simulations were carried out on a DELL system equipped with an Intel(R) Core(TM) i9-13900HX processor running at 2.20 GHz, 32.0 GB of RAM, and the 64-bit Linux Ubuntu 18.04.1 LTS operating system.

4.5.2. ADMET and drug-likeness evaluation

Drug candidates must exhibit favorable ADMET properties and ideally be non-toxic. Therefore, the main compounds identified from the essential oils extract were assessed for their ADME characteristics, including physicochemical properties, lipophilicity, water solubility, pharmacokinetics, drug-like qualities, medicinal chemistry, and various other parameters using the SwissADME module (Riyadi et al., 2021; Daina et al., 2017) available

on the SIB (Swiss Institute of Bioinformatics) webserver (https://www.sib.swiss). In addition, the toxicity potential of the compounds was predicted using the ProTox webserver (Banerjee et al., 2018) (https://comptox.charite.de/protox3/).

4.5.3. Docking setup

➢ Ligands preparation

The three-dimensional structures of the key compounds extracted from *Cotula cinerea* and *Origanum Majorana L* essential oils were retrieved from the National Library of Medicine (NCBI) database (Kim et al., 2016), available through the NCBI website (https://pubchem.ncbi.nlm.nih.gov/).

Ligand preparation involved energy optimization to determine the most energetically stable conformations for each compound. This optimization was carried out using the LigPrep module within the Schrödinger suite (Schrödinger, 2024), ensuring the compounds, including Montbretin A (a co-crystallized ligand), achieved their lowest energy configurations. The ionization states were determined at pH 7.0 ± 2.0, calculated using the Epik classic module, while maintaining the specified chirality and generating the relevant tautomeric forms. Additionally, partial atomic charges were calculated using the OPLS4 force field (Lu et al., 2021).

➢ Receptor preparation

The crystallographic data for human glutathione reductase (Table 04) (PDB ID: 1BWC) (Gallwitz et al., 1999) was obtained from the Protein Data Bank (http://www.rcsb.org) (Rose et al., 2017), with specific parameters including a resolution of 1.35 Å and a free R-value of 0.211. The protein structure was processed using the "protein preparation workflow" module in the Schrödinger suite (Madhavi Sastry et al., 2013), which involved several stages, including importing and processing the structure, reviewing and making necessary modifications, and refining the final model.

In the initial phase, the Prime tool was used to address missing residues and side chains while maintaining a pH of 7.0 ± 2.00, as set by PROPKA. The next steps involved optimizing and assigning hydrogen bonds and removing water molecules located beyond 8 Å from the protein structure. To achieve a stable, low-energy state, restraint minimization was carried out using the Optimized Potentials for Liquid Simulations (OPLS4) force field (Lu et al., 2021).

This stage of protein preparation focused on energy optimization, ensuring the protein was in its most energetically favorable form for further in-silico analyses.

The "Receptor grid generation" tool was then used to create a grid around the protein's active site, defined by the co-crystallized ligand Montbretin A. Default settings were applied, and the grid center was positioned at the coordinates X = -6.65, Y = 6.99, and Z = -20.65.

Table4. Target receptor information chosen for docking studies

Human glutathione reductase	**Detaille's**	
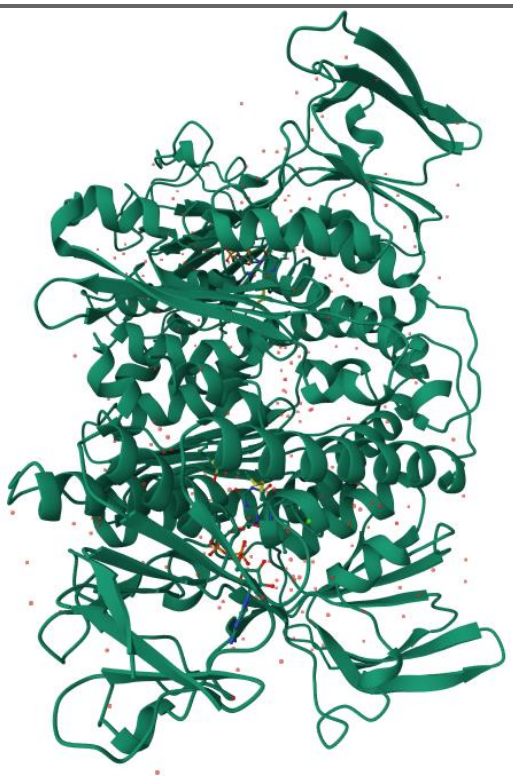	PDB ID	1BWC
	Mutation	No
	Resolution (Å)	2.10
	R-Value Free	0.230
	R-Value Work	0.180
	R-Value Observed	0.180
	Organism	Homo sapiens
	Expression System	Escherichia coli
	Space Groupe	C 2 2 2_1
	Sequence Length	478
Co-Crystallized Ligand	**Detaille's**	
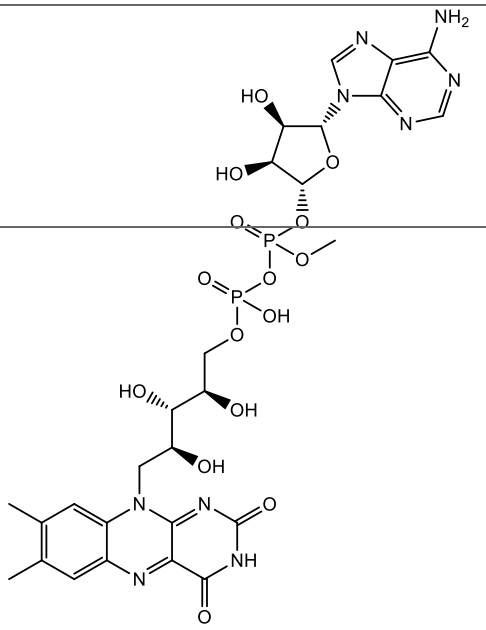	Name	FLAVIN-ADENINE DINUCLEOTIDE

	Formula	$C_{27}H_{33}N_9O_{15}P_2$

➢ **Molecular Docking**

Computational simulations, including Induced Fit Docking, molecular dynamics simulations, and MM-GBSA calculations, were performed using the Glide, Induced Fit Docking, Prime, and Desmond modules within the Maestro version 11.7 interface of the Schrödinger suite (Small-Molecule Drug Discovery Suite 2021-4, Schrödinger, LLC, New York, NY, 2021) (Schrödinger, 2015). These simulations were run on a DELL system with an Intel(R) Core(TM) i9-13900HX processor operating at 2.20 GHz, 32.0 GB of RAM, and a 64-bit Linux Ubuntu 18.04.1 LTS OS.

For all docking studies, the Glide module (Grid-based Ligand Docking with Energetics), part of the Schrödinger suite, was used as the molecular docking tool (Yang et al., 2021). The ligands, once prepared, were docked onto the target protein's binding site using the Glide module in Standard Precision (SP) mode (Friesner et al., 2006).

➢ **Induced Fit Docking (IFD)**

The Induced Fit Docking (IFD) module within the Maestro molecular modeling suite is recognized as a dependable and efficient method for considering flexibility in both ligands and the residues of the binding pocket in target receptors (Khelil et al., 2020). In the IFD process, Glide/SP (Standard Precision) docking was applied to each ligand, and the Prime refinement step focused on adjusting the side chains of residues within a 5 Å radius of the ligand. It is important to note that a maximum of 20 poses were retained for each ligand during the docking process.

➢ **Molecular Dynamics Simulation (MDS)**

The compound with the highest IFD docking score from each plant was selected for Molecular Dynamics Simulation (MDS). Considering the limitations of ligand docking in accurately reflecting biological systems in aqueous environments (Korb et al., 2012), a 100 ns MDS was conducted using the Desmond module of the Schrödinger suite (Bowers et al., 2006).

The MDS procedure consisted of three key stages: system setup, minimization, and the actual simulation. In the system setup phase, the protein-ligand complex was chosen and placed in a biological setting. The TIP3P solvent model, which includes transferable intermolecular potential with three points, was used to immerse the complex in an orthorhombic box with dimensions of 10 x 10 x 10 Å, ensuring that the boundary conditions were maintained throughout the simulation (Akbar et al., 2022). The OPLS-3e force field was consistently applied throughout the process (Roos et al., 2019). To neutralize the system, counter ions were added where necessary, and a concentration of 0.15 M NaCl was introduced to simulate physiological conditions.

Following system setup, the NPT ensemble was employed for energy minimization, maintaining constant pressure (1.0132 bar) and temperature (300 K). Once minimization was completed, the Molecular Dynamics Simulation (MDS) was carried out on the optimized protein-ligand complex (Halder et al., 2023).

- **Free Energy (MM-GBSA) Calculation**

After the completion of the dynamic simulation, the free binding energy between the protein and ligand was evaluated using the Prime MM-GBSA module within the Maestro molecular modeling suite (Wang et al., 2021). To calculate the ligand binding affinities, the Molecular Mechanics/Generalized Born Surface Area ΔG (MM-GBSA ΔG) method was applied to the optimized receptor-ligand complex. This calculation, carried out using the VSGB solvation model and the OPLS4 force field, provides a robust and methodologically sound approach for assessing molecular interactions and the strength of binding (Gorla et al., 2021).

CHAPTER TWO: RESULTS AND DISCUSSION

1. Introduction

This chapter presents the results of an investigation into the extraction yield, characterization, and detailed analysis of the antioxidant properties of essential oils derived from the aerial parts of *Cotula cinerea* and *Origanum Majorana L*. The primary objective of this study was to evaluate the antioxidant potential of these essential oils, positioning them as promising candidates for novel pharmaceutical applications.

The findings provide a thorough understanding of the chemical makeup of the essential oils, which was crucial for their inclusion in an in-silico study. Advanced computational methods, including Induced Fit Docking (IFD) and Molecular Dynamics Simulation (MDS), were employed to assess each compound's potential. These sophisticated techniques offer insights that are not attainable through conventional in vitro approaches.

2. Extraction Yield:

Figure 16 displays the essential oil yields extracted via hydrodistillation from the aerial parts of *Cotula cinerea* and the Eloued variety of *Origanum Majorana L*.

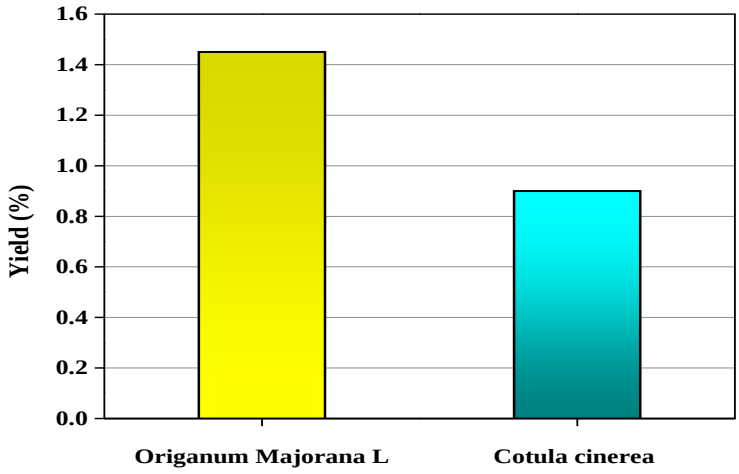

Figure16. The yields of extracted essential oils

It can be noted that *Origanum Majorana L* produces a higher yield of essential oil compared to *Cotula cinerea* (1.45% versus 0.90%). However, the disparity in yield between the two is statistically insignificant.

However, research by Alimi et al. (2022) shows that lower essential oil yields were obtained from *Origanum Majorana L* and *Cotula cinerea* when extracted by hydrodistillation at ambient temperature.

On the other hand, similar findings to ours were reported by Naima et al. (2019) for the essential oil extracted from the same variety using the same method. In contrast, Vera et al. (1999) achieved significantly higher yields when hydrodistilling *Origanum Majorana L* from the Indian variety.

These discrepancies in results can be attributed to various factors influencing essential oil yields, including plant-related factors (such as species, variety, and chemical composition) and experimental conditions (such as the extraction process and duration).

3. Chemical composition of essential oils

3.1. Organoleptic characteristics

Through the conducted work, it has been revealed that the essential oil extracted from the studied plants exhibits the following (Table 5) organoleptic properties:

Table 5. The organoleptic characteristics of essential oils

Plant	Smell	Aspect	Colour
Cotula cinerea	A distinctive aroma	liquid at room temperature	Dark-yellow
Origanum Majorana L	A pleasant fragrance	liquid at room temperature	Light-yellow

3.2. Physicochemical Properties

The physicochemical properties were carefully assessed following the guidelines set by the French Association for Standardization (AFNOR), utilizing standardized methods to determine relative density, refractive index, acidity index, and ester index, as presented in Table 6 below.

Table6. The physicochemical properties of essential oils

Plant	Relative Density	Refractive Index	Acidity Index	Ester Index
Cotula cinerea	0.958	1.4720	5.01	43.72
Origanum Majorana L	0.908	1.4512	4.39	41.23

When compared with findings reported by Naima et al. (2019) who recorded a density of 0.953, a refractive index of 1.474, an acidity index of 4.93, and an ester index of 45.96 and Alimi et al. (2022), who reported densities of 0.834 ± 0.02 and 0.835 ± 0.02, along with refractive indices at 25°C of 1.4596 ± 0.03 and 1.4622 ± 0.04, it is evident that our measurements, taken at 23°C, align well with the reference standards established by AFNOR (Afnor, 1982).

3.3. Gas Chromatography-Mass Spectrometry (GC/MS) analysis

The composition of essential oils derived from two distinct plant species was examined through gas chromatography coupled with mass spectrometry (GC/MS). The mass spectra corresponding to each detected peak were cross-referenced with both published data and the Weily electronic mass spectral library (Horai et al., 2010) to ensure accurate compound identification. Additionally, retention indices were calculated to support this identification process. The analysis employed a non-polar HP5 stationary phase within the gas chromatography column, ensuring consistency in both the number and sequence of eluted compounds.

The chromatographic profiles detailing the essential oil constituents of *Cotula cinerea* and *Origanum Majorana* L are presented in Figures 17 and 18, respectively.

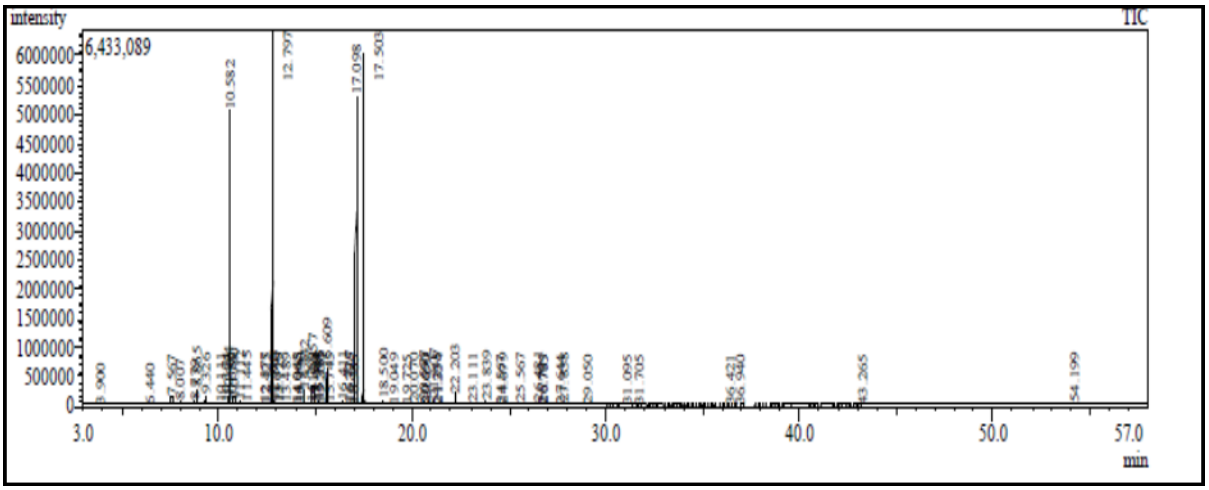

Figure 17. Chromatogram of the essential oil of *Cotula cinerea* plant obtained by GC/MS

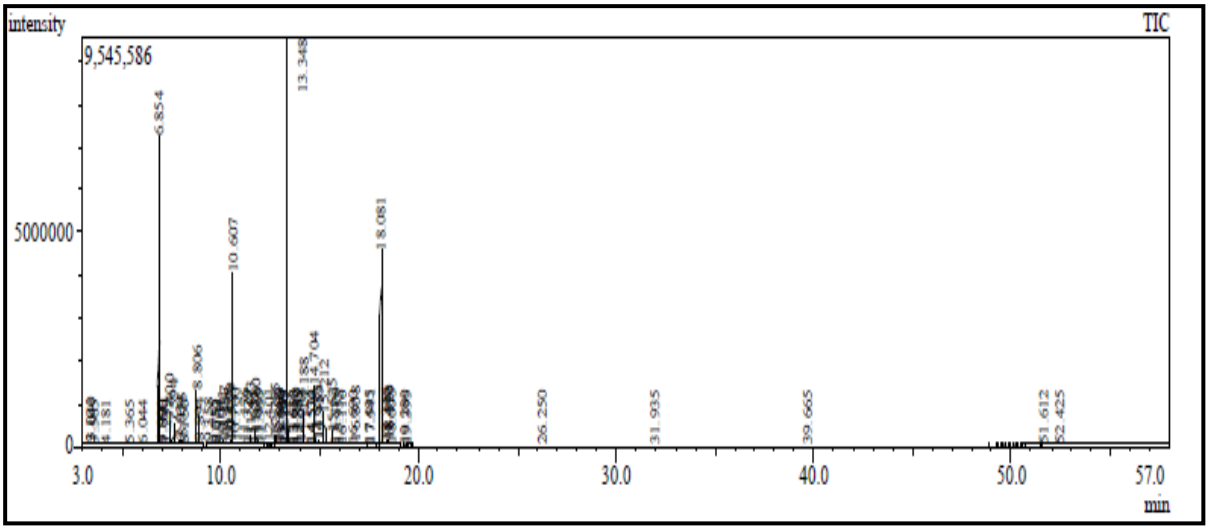

Figure 18. Chromatogram of the essential oil of *Origanum Majorana L* plant obtained by GC/MS

A close examination of the two chromatographic profiles reveals striking similarities, with clearly distinguishable peaks alongside several overlapping ones. Overall, the chromatograms can be broadly segmented into three distinct zones, each representing a specific range of compounds.

1. The first region, extending from 4 to 12.4 minutes, is characterized by several peaks corresponding to hydrocarbon monoterpenes.
2. The next section, ranging from 12.4 to 24 minutes, contains the most prominent peaks, which are primarily attributed to oxygenated monoterpenes key constituents of the essential oils.
3. The final interval, between 24 and 32.5 minutes, shows few peaks, indicating a limited presence of hydrocarbon sesquiterpenes in the essential oils.

The major compounds identified in the essential oils derived from *Cotula cinerea* and *Origanum majorana* L have been compiled and are presented below.

3.3.1. *Cotula cinerea*

Hydrodistillation of *Cotula cinerea* resulted in the extraction of a dark yellow essential oil, with a yield reaching 0.91%. Subsequent analysis using gas chromatography-mass spectrometry (GC/MS) revealed the presence of 31 distinct compounds, collectively representing 95.64% of the total oil content, as detailed in Table 7. The major fraction of this composition was made up of oxygenated monoterpenes, which constituted 68.16%.

Hydrocarbon monoterpenes followed with a proportion of 23.27%, while oxygenated sesquiterpenes were found in trace amounts, accounting for just 0.15%. The remaining 4.06% was composed of miscellaneous compounds.

Table 7. Essential oil constituents of *Cotula cinerea* identified by GC/MS

No	Compounds	IR_{Exp}	IR_{Ref}	(%)
01	**Santolina triene**	**908**	**914**	**10.6**
02	Alpha-thujene	931	935	0.88
03	**Alpha-pinene**	**939**	**943**	**2.02**
04	Camphene	953	956	0.85
05	**Sabinene**	**976**	**976**	**6.17**
06	Beta- pinene	980	981	0.58
07	Dehydro-1.8-cineole	991	988	0.64
08	Myrcene	991	993	0.07
09	Meta mentha-1(7)-8dien	999	997	0.06
10	Alpha-terpinene	1018	1017	0.83
11	Ortho cymene	1022	1020	0.43
12	Para cymene	1026	1029	0.6
13	**1.8-cineole**	**1033**	**1033**	**5.34**
14	**Delta-terpinene**	**1062**	**1057**	**1.57**
15	Cis sabinene hydrate	1068	1069	0.46
16	Terpinolene	1088	1088	0.36
17	Cis thujone	1102	1100	0.52
18	**Trans thujone**	**1114**	**1117**	**51.86**
19	**Camphor**	**1143**	**1140**	**2.63**
20	**Beta-terpineol**	**1163**	**1160**	**1.39**
21	**Terpin-4-ol**	**1177**	**1178**	**1.73**
22	Alpha-terpineol	1189	1190	0.58
23	Myrtenol	1194	1195	0.13
24	Neo iso dihydro carveol	1226	1224	0.53
25	Carvotanacetone	1246	1247	0.9
26	**Cis verbenyl acetate**	**1262**	**1264**	**5.07**
27	Iso pulegol acetate	1273	1274	0.06
28	Para cymen-7-ol	1287	1285	0.08
29	Neryl acetate	1365	1367	--

30	Cis jasmone	1394	1390	0.15
31	Germacrene D	1480	1481	0.06
Total		**95.64**		

The compositional analysis identified ten major constituents present in concentrations exceeding 1%, as listed in Table 7. Among these, trans-thujone was the most abundant, representing 51.86% of the essential oil. It was followed by santolina triene at 10.69% and sabinene at 6.17%. Additionally, 1, 8-cineole accounted for 5.34% of the total content. Other notable compounds, though present in smaller amounts, included α-pinene (2.02%), terpin-4-ol (1.73%), β-terpineol (1.39%), and camphor (2.63%).

Comparative analysis with previous research highlights certain similarities and differences. Notably, Ekhlil et al. (2016) reported a comparable percentage of santolina triene (11.67%), yet identified iso-thujanol as the dominant constituent at 47.38%, in contrast to our findings. In alignment with our results, El Bouzidi et al. (2011) reported similar proportions of trans-thujone (41.4%), 1,8-cineole (8.2%), and santolina triene (7.2%), though their reported camphor content was slightly higher at 5.5%. On the other hand, the study by Fournier et al. (1989) presented a markedly different profile, identifying camphor as the main component at 50%.

Figure 19 provides a detailed visual overview of the primary compounds (those exceeding 1%) identified in the *Cotula cinerea* essential oil, showcasing their chemical structures along with their corresponding IUPAC names.

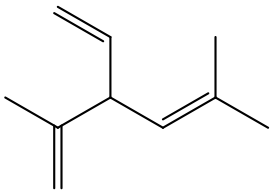

2,5-dimethyl-3-vinylhexa-1,4-diene
(Santolina triene)

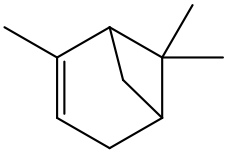

2,6,6-trimethylbicyclo[3.1.1]hept-2-ene
(Alpha-pinene)

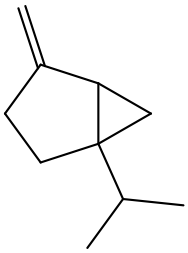

1-isopropyl-4-methylenebicyclo[3.1.0]hexane
(Sabinene)

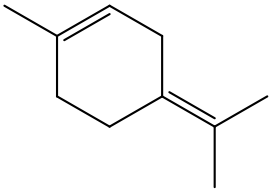

1-methyl-4-(propan-2-ylidene)cyclohex-1-ene
(Delta-terpinene)

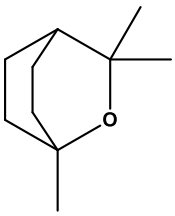

1,3,3-trimethyl-2-oxabicyclo[2.2.2]octane
(1.8-cineole)

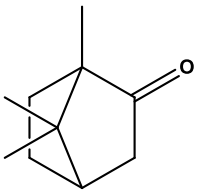

1,7,7-trimethylbicyclo[2.2.1]heptan-2-one
(Camphor)

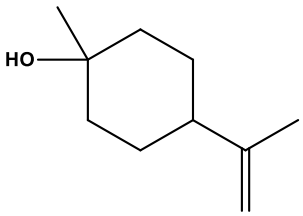

1-methyl-4-(prop-1-en-2-yl)cyclohexanol
(Beta-terpineol)

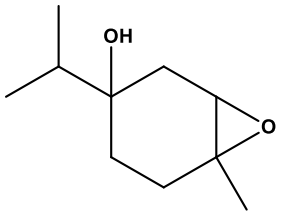

3-isopropyl-6-methyl-7-oxabicyclo[4.1.0]heptan-3-ol
(Terpin-4-ol)

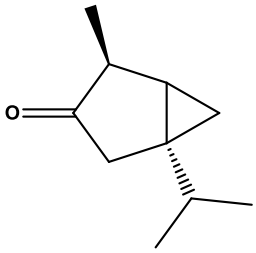

(1*S*,4*S*)-1-isopropyl-4-methylbicyclo[3.1.0]hexan-3-one
(Trans thujone)

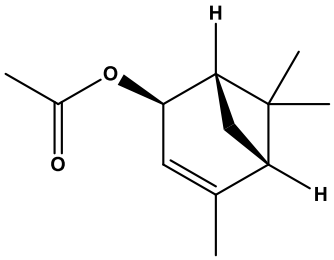

(1*S*,2*R*,5*S*)-4,6,6-trimethylbicyclo[3.1.1]hept-3-en-2-yl acetate
(Cis verbenyl acetate)

Figure19. Chemical structures and IUPAC names of the top major compounds identified in the essential oil of *Cotula cinerea*

3.3.2. Origanum Majorana L

The essential oil of *Origanum Majorana L.* was extracted using the hydrodistillation technique, resulting in a considerable yield of 1.5%. Subsequent analysis identified 42 distinct

constituents, accounting for 98.84% of the total oil composition (as shown in Table 8). The oil was predominantly composed of oxygenated monoterpenes, which made up more than 57% of the identified compounds, while hydrocarbon monoterpenes followed at 25.14%.

A particularly noteworthy aspect of this analysis is the high concentration of trans-Thujone, which accounted for 33.3% of the essential oil composition an element largely absent in most previously published studies. For example, in the research conducted by J. Chane et al. (Vera et al., 1999), Terpinen-4-ol was identified as the dominant compound at 38.4%, yet it was not detected at all in the current analysis. Likewise, Santolina triene was found to be the second most abundant constituent in our results at 16.40%, a finding not echoed in existing literature.

Despite these differences, some consistency with earlier studies was observed regarding the presence of Sabinene, which appeared at 3.12% in our investigation. This compares with 15% in the study by J. Chane et al. (Vera et al., 1999), 17% in K.H.C (Baser et al., 1993), and 2.14% as recorded by (Sellami et al., 2009). Other minor compounds detected included α-Thujene (1.44%), α-Pinene (1.19%), and β-Pinene oxide (4.42%).

In conclusion, the essential oil obtained from *Origanum Majorana L.* grown in the Eloued region demonstrates a unique chemical profile when compared to those sourced from other geographical areas. This distinction is primarily marked by the dominance of trans-Thujone and Santolina triene among its main constituents. Such variations are likely attributed to a combination of environmental and agronomic factors, including soil composition, climatic conditions, and the specific timing of plant harvesting. For a visual summary of the principal compounds identified, refer to Figure 20, which illustrates their molecular structures alongside their IUPAC names.

Table 8. Essential oil constituents of *Origanum Majorana L* identified by GC/MS

No	**Compounds**	**IR_{Exp}**	**IR_{Ref}**	**(%)**
01	Pentanol	759	762	0.12
02	Cis-2-Penten-1-ol	762	765	0.03
03	Hexanal	801	801	0.02
04	(Z)-Salvene	844	847	0.02
05	Isopentyl acetate	869	869	0.02
06	**Santolina triene**	**898**	**906**	**16.42**
07	Tricyclene	912	921	0.02
08	**Alpha-Thujene**	**918**	**924**	**1.44**
09	**Alpha-Pinene**	**925**	**932**	**1.19**
10	Camphene	941	946	0.43

11	**Sabinene**	**969**	**969**	**3.12**
12	Beta-Pinene	972	974	0.22
13	Beta-Myrcene	989	988	0.14
14	Alpha-Phellandrene	1003	1002	0.03
15	Propanoic acid, 2-methyl-, 3-methylbutyl ester	1012	1007	0.02
16	Alpha-Terpinene	1016	1014	0.36
17	Para cymene	1024	1020	0.20
18	Ortho Cymene	1026	1022	0.45
19	Sylvestrene	1028	1025	0.20
20	**1,8-Cineole**	**1031**	**1026**	**10.71**
21	Trans-decahydroNaphthalene	1054	1053	0.03
22	Terpinene	1059	1054	0.76
23	Cis Sabinene hydrate	1068	1065	0.89
24	Para-Mentha-2'4(8)-diene	1088	1085	0.11
25	Trans-Sabinene hydrate	1100	1198	0.86
26	Isopentyl-2-methylbutanoate	1104	1100	0.14
27	cis-Thujone	1107	1101	0.24
28	**trans-Thujone**	**1119**	**1112**	**33.30**
29	iso-3-Thujanol	1136	1134	0.04
30	**Camphor**	**1146**	**1141**	**2.85**
31	**Beta pinene oxide**	**1163**	**1154**	**4.42**
32	3-Thujanol	1168	1164	0.48
33	Alpha Terpineol	1192	1186	0.88
34	Dihydrocarveol	1197	1192	0.06
35	Safranal	1203	1197	0.01
36	Cis-3-Hexenyl 2-methyl butanoate	1233	1229	0.25
37	trans-Myrtanol	1257	1258	0.04
38	2-(1E)-propenyl Phenol	1258	1264	0.09
39	**cis Verbenyl acetate**	**1277**	**1280**	**15.05**
40	neoiso-3Thujanol acetate	1287	1281	0.09
41	Isobornyl acetate	1290	1283	0.21
42	Lavandulyl acetate	1293	1288	0.32
Total		**95.64**		

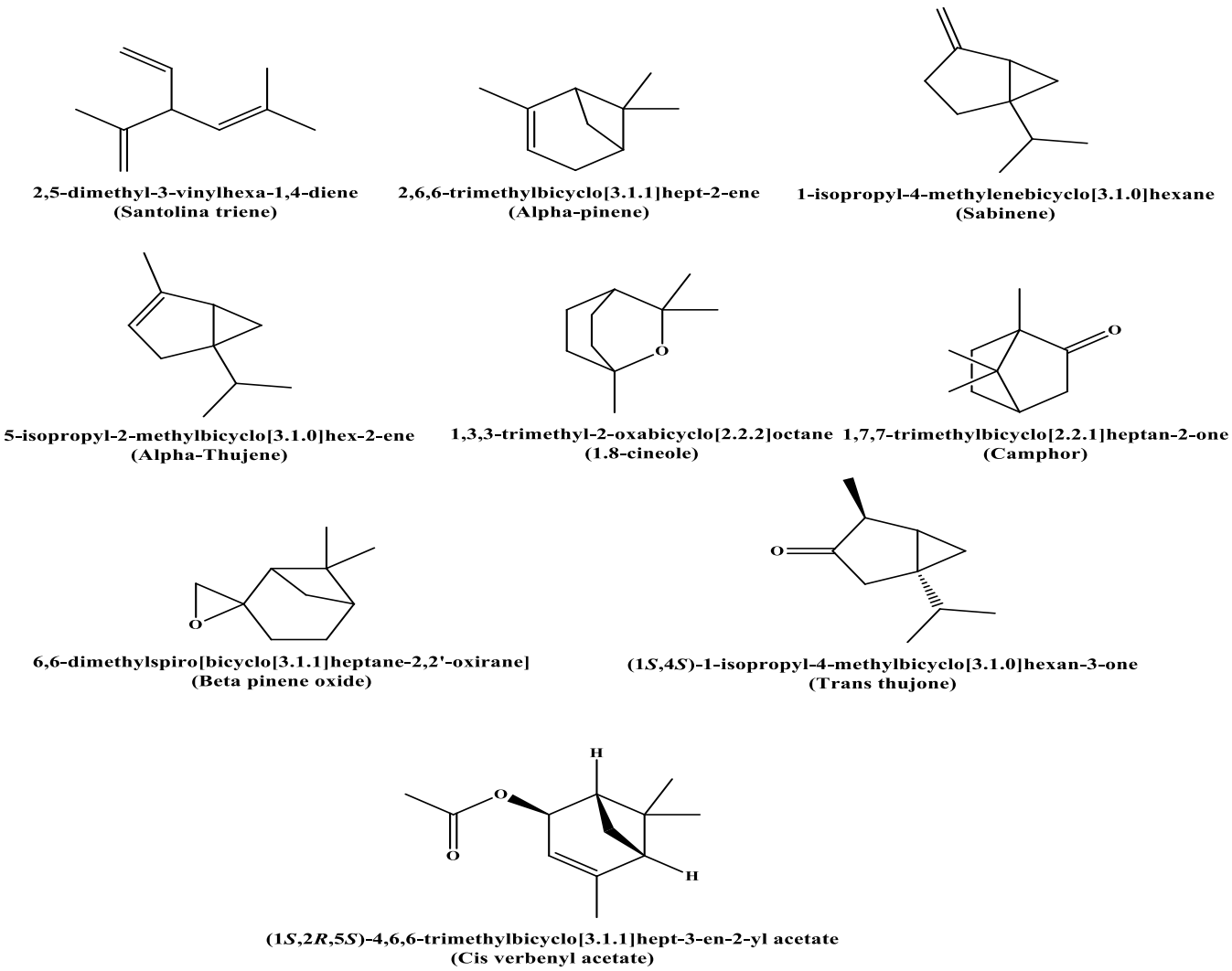

Figure20. Chemical structures and IUPAC names of the top major compounds identified in the essential oil of *Origanum Majorana L*

4. *In vitro* Antioxidant Activity

4.1. Using superoxide anion radical

In this study, the antioxidant properties of essential oils *from Cotula cinerea* and *Majorana Origanum L* were evaluated based on their ability to scavenge superoxide anion radicals $O_2^{\cdot-}$. Kinetic studies were conducted, and the half-maximal inhibitory concentration IC_{50} values were calculated to determine how effectively the compounds could neutralize $O_2^{\cdot-}$ radicals, as shown in Equation 08. The antioxidant potential of *Cotula cinerea and Majorana Origanum L* is represented by their IC_{50} values, indicating the concentration (mg/ml) needed to inhibit 50% of $O_2^{\cdot-}$ radical formation.

The percentage of $O_2^{\cdot-}$ radical scavenging activity is calculated using the formula (Kaoula *et al*., 2022):

$$\%\ O_2^{\cdot-}\ \text{radical scavenging activity} = \frac{ipa0 - ipa}{ipa0} = aC_{(mg/ml)} + b \quad (8)$$

Where i_{pa0} and i_{pa} are the anodic peak current densities of the superoxide anion radical in the absence and presence of *Cotula cinerea and Majorana Origanum L* respectively .

The linear equations obtained from the calibration plots within the tested concentration range for *Cotula cinerea, Majorana Origanum L*, and α-tocopherol are summarized in Table 09. In this table, 'y' corresponds to the anodic peak current density of the superoxide anion $O_2^{\cdot-}$, while 'x' indicates the sample concentrations in mg/ml.

According to the data in the table, both *Cotula cinerea and Majorana Origanum L* exhibited notable superoxide radical scavenging activity

Table 9. IC_{50} values (µg/ml) obtained using $O_2^{\cdot-}$ radicals scavenging activity

Compound	Equation	R^2	IC_{50}(µg/ml)
Cotula cinerea	y=3.423x+1.874	0.980	14.060
Majorana Origanum L	y=2.090x+20.445	0.965	14.141
α-tocopherol	y =141.113x+ 0.149	0,950	18.83

The classification of these compounds according to their antioxidant activity IC_{50}, is represented in the following curve: figure 21

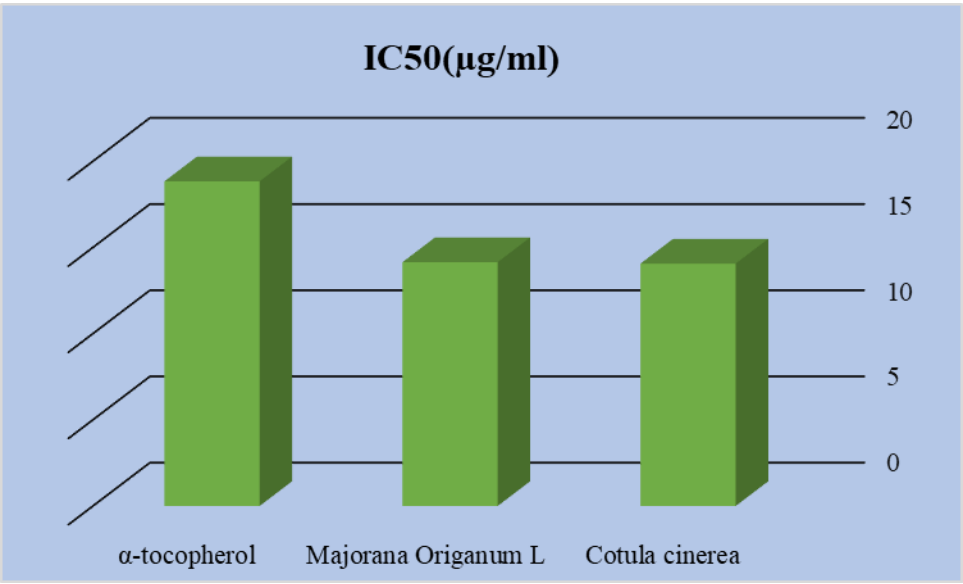

Figure 21: Classification of $O_2^{\cdot-}$ inhibition capacity according to IC_{50} values

The obtained results presented that *Cotula cinerea* and *Majorana origanum L* display the lowest IC_{50} values measured at (IC_{50} =14.060 µg/mL) and (IC_{50} =14.141 µg/mL) respectively,

which reflects a stronger antioxidant activity in comparison to α-tocopherol (IC_{50} = 18.83 µg/mL).

4.2. Electrochemical superoxide anion radical interaction study

The measurement of CV was performed using a glass carbon electrode in a potential window between 0.0 and -1.6 V to study the electrochemical behavior of the $O_2^{\cdot-}$ in DMSO in the absence and presence of varying concentrations of *Cotula cinerea* and *Majorana Origanum L* oils dissolved in the same solvent.

Figure 22 shows that redox pairs $O_2/O_2^{\cdot-}$ show a peak oxidation at -0.7 V and a reduction peak at -0.962 V. Furthermore, this figure shows how the addition of *Cotula cinerea and Majorana Origanum L* essential oils to DMSO solution affects the peak oxidation current density of the duo.

The observed reduction in anodic peak current density upon the addition of the tested compounds suggests to a chemical interaction between these compounds and the superoxide anion $O_2^{\cdot-}$ (Haji *et al* ., 2018) .The binding constant can be calculated using this reduction. The reaction pattern can be confirmed using the change in peak potential values.

When 1 mM amounts of essential oils of *Cotula cinerea and Majorana origanum L* were added, the density of the anodic peak current decreased significantly with a slight shift in peak potential ΔE ° towards the positive axis. The scavenging activity of the added compounds is responsible for this decrease, as show in Figure 22.

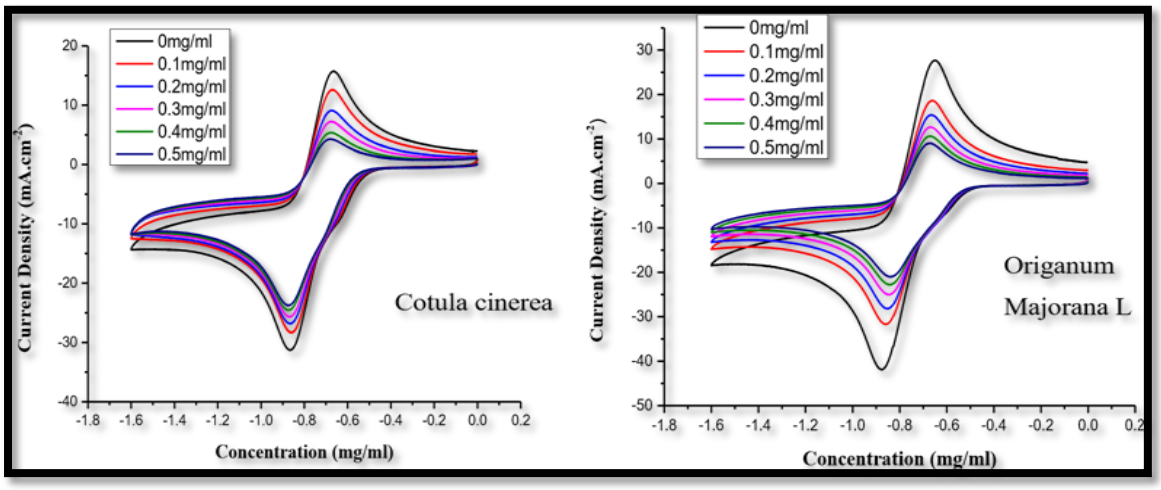

Figure 22. Cyclic voltammograms of oxygen-saturated DMSO on a GC electrode in the presence of a different concentration of *Cotula cinerea and Origanum Majorana L* essential oils.

Binding constant

The interaction between *Cotula cinerea and Origanum Majorana L* essential oils and the superoxide anion $O_2^{\cdot-}$ was studied by determining the association constant .

The addition of varying concentrations of these essential oils to a Dimethyl sulfoxide (DMSO) solution saturated with commercial oxygen resulted in a significant decrease in the peak current density, in Figure 22. This decrease is attributed to a decrease in free O_2 radical concentration resulting from the formation of $O_2^{\cdot-}$_*Origanum Majorana L,* $O_2^{\cdot-}$_ *Cotula cinerea* products.

The binding constant K_b values were determined from the intercepts of the linear fitting of the plots of log (1/C) versus log (i /i₀ − i), constructed according to equation 9 (Elhafnaoui *et al*., 2019):

$$\text{Log}\frac{1}{c} = \log kb + \log\frac{i}{i0-i} \qquad (9)$$

C: concentration of the compound tested (mol.l^{-1}) .

K_b: binding constant (l/mol) .

i and i_0: intensity of the anodic current in the presence and absence of the compound tested respectively.

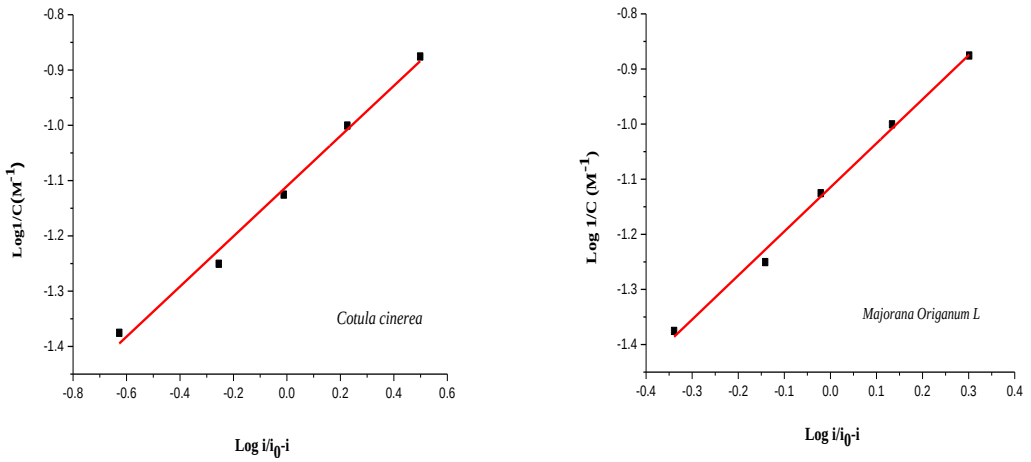

Figure 23. Plots of log (1/C) versus log (i/i_0-i) for $O_2^{\bullet-}$ with a variable concentration of essential oils of *Origanum Majorana and Cotula cinerea* in Dimethyl sulfoxide (DMSO), used to calculate the binding constants of products $O_2^{\bullet-}$ _ *Cotula cinerea*, $O_2^{\bullet-}$_ *Origanum Majorana L.*

Binding free energy: The binding free energy change was calculated using the following Equation 10:

$$\Delta G = -RT \ln K_b \qquad (10)$$

Where: ΔG is the binding free energy in KJ.mol^{-1}, R is the gas constant, 8.32 J.mol^{-1} K^{-1}, and T is the absolute temperature, 298K .

The binding constants were determined, and subsequently, the free binding energy was calculated by analysing the intercept obtained through linear curve fitting of the logarithmic transformation of the reciprocal of the concentration (log(1/C)) versus log/(i/i$_0$ − i) (Elhafnaoui et al .,2019). Table 10

Table10. Binding constants and values of binding free energies of products $O_2^{\cdot-}$_*Cotula cinerea,* $O_2^{\cdot-}$ _*Origanum Majorana L* at T= 298K.

Adduct	Equation	R^2	K (M^{-1})	ΔG(KJ.mol^{-1})
$O_2^{\cdot-}$ ***Cotula cinerea***	y=0.4538x-1.11005	0.98977	12.60	-28.06
$O_2^{\cdot-}$ ***Origanum Majorana L.***	y=0.79926x-1.11481	0.99393	13.03	-36.6

The calculated binding free energy ΔG reveals both the strength and nature of the interaction between the ligands and $O_2^{\cdot-}$. The magnitude of the binding free energy reflects the strength of the electrostatic interaction, while its sign indicates whether the binding process is spontaneous (Khennoufa .,2023).

4.2.1. Using 2,2-diphenyl-1-picrylhydrazyl (DPPH)

The DPPH radical (2,2-diphenyl-1-picrylhydrazyl) is widely recognized as a standard reagent for evaluating antioxidant activity. It stands out for its high sensitivity and allows for a quick, direct, and dependable measurement of antioxidant potential. Thanks to its chemical stability and ease of use, the method yields consistent and reproducible results. Moreover, DPPH is well-suited for analyzing a variety of sample types within a short timeframe. Its ability to detect even low concentrations of active compounds makes it an effective tool for preliminary screening of antioxidant properties (Brahmi , 2015).

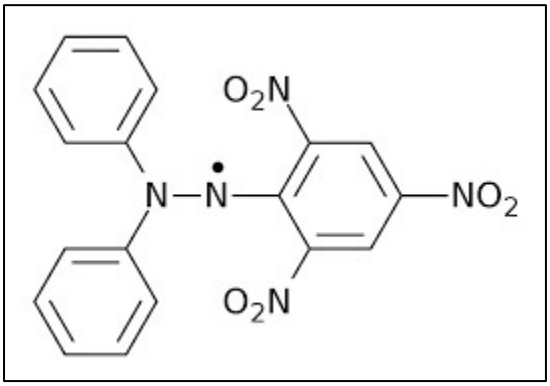

Figure 24. Chemical structure of the free radical DPPH (2,2-Diphenyl-1-picrylhydrazyl) (Ahmad Amri, Morteza Jabbari., 2024).

4.3. Electrochemical DPPH radical interaction study

4.3.1. Inhibitory concentration (IC_{50})

In this study, the antioxidant potential of *Origanum Majorana* L. and *Cotula cinerea* was evaluated based on their capacity to neutralize DPPH free radicals. To quantify this activity, kinetic curves were generated, and the half-maximal inhibitory concentration (IC_{50}) values were calculated, as represented in Equation 11. The antioxidant efficiency of the essential oil extracts from *Origanum Majorana* L. and *Cotula cinerea* is expressed in terms of IC_{50}, which corresponds to the sample concentration (mg/ml), required reducing DPPH radical levels by 50%.

$$\%\ \text{DPPH radical scavenging activity} = \frac{ipa0 - ipa}{ipa0} = aC\left(\frac{mg}{ml}\right) + b \qquad (11)$$

Here, ipa_0 and *ipa* refer to the anodic peak current densities of the DPPH radical measured in the absence and presence of *Origanum Majorana* L. and *Cotula cinerea*, respectively.

The linear calibration equations obtained across the tested concentration ranges for *Origanum Majorana* L., *Cotula cinerea*, and α-tocopherol are summarized in Table 11. In this table, 'y' corresponds to the anodic peak current density of the DPPH radical, while 'x' indicates the concentration of the samples, expressed in mg/ml.

Table 11. IC_{50} values (µg/ml) obtained using DPPH radical scavenging activity from electrochemical method

Compound	Equation	R^2	IC_{50} (µg/ml)
Origanum Majorana L	Y= 0.989x + 13.158	0.972	37.241
Cotula cinerea	Y= 1.575x + 38.118	0.995	7.544
α-Tocopherol	y = 1325,7x + 5,236	0.967	33.77± 3.21

According to the data shown in Table 11, *Origanum majorana* L., *Cotula cinerea*, and α-Tocopherol all exhibited notable effectiveness in scavenging free radicals.

Their antioxidant performance, assessed through IC_{50} values, is comparatively illustrated in the curve presented in Figure 25, which ranks the compounds based on their activity.

The antioxidant activity results show that *Cotula cinerea* has the highest potency with the lowest IC_{50} (7.544 µg/mL) and the best linear correlation (R^2 = 0.995), indicating strong free radical scavenging ability. α -Tocopherol, used as a standard, showed moderate activity (IC_{50} = 33.77 ± 3.21 µg/mL), while *Origanum majorana* exhibited the weakest effect (IC_{50} = 37.241 µg/mL). These findings suggest that *C. cinerea* is a promising natural antioxidant source.

The bar chart displays the IC_{50} values (in µg/mL) of three samples: α-Tocopherol, *Cotula cinerea,* and *Origanum Majorana L*, representing their antioxidant potency. The Y-axis shows IC_{50} values ranging from 0 to 40 µg/mL and the bars are colored in yellow with a 3D style against a blue background. *Cotula cinerea* shows the lowest IC_{50} value, indicating the highest antioxidant activity. α-Tocopherol has a moderate IC_{50} value. *Origanum majorana L* exhibits the highest IC_{50}, suggesting the lowest antioxidant activity among the three.

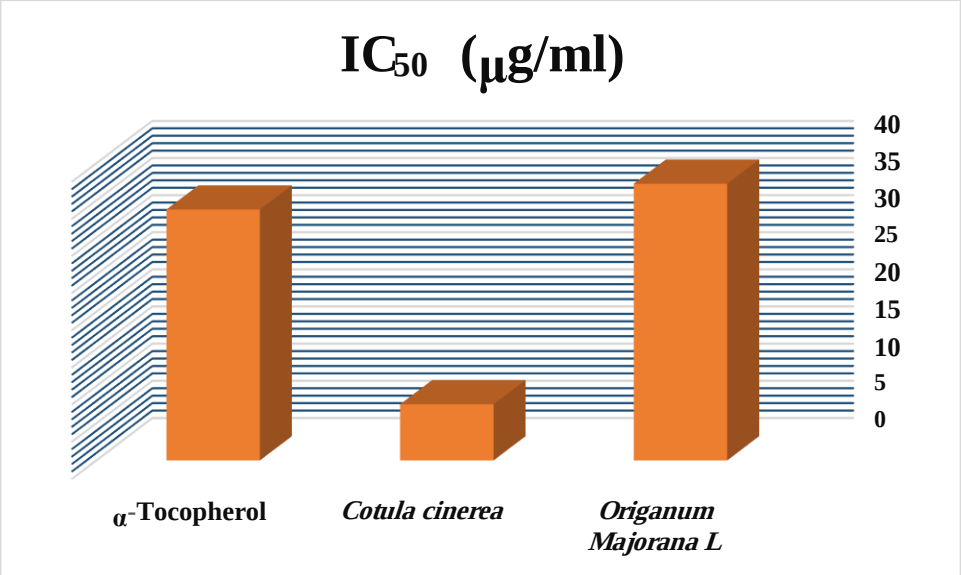

Figure 25. Classification of DPPH radical inhibition capacity according to IC_{50} values by electrochemical method

The bar chart clearly shows that *Cotula cinerea* possesses the strongest antioxidant activity, with an IC_{50} significantly lower than both α-Tocopherol and *Origanum majorana L*. This highlights its potential as a natural antioxidant source. Conversely, *O. majorana L* displayed the weakest activity, suggesting a comparatively lower efficacy in free radical scavenging (ZINEB .,2024).

Binding constant

The characteristic cyclic voltammetry (CV) response of dimethyl sulfoxide (DMSO) is recorded within the potential range of 0.0 to -1.6 V using a glassy carbon electrode, both in the absence and presence of various concentrations of test solutions. The tested concentrations for *Origanum majorana* L. were 7.508, 10.011, 13.348, 17.797, and 23.730 µg/ml, while the same concentration range was used for *Cotula cinerea*, all prepared in DMSO as the solvent.

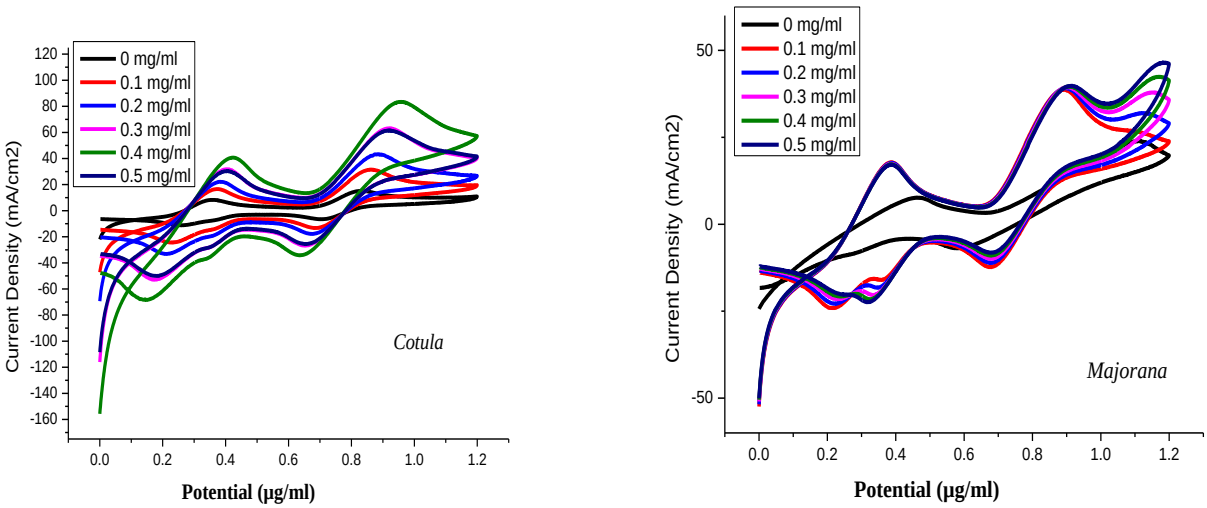

Figure26. Cyclic voltammograms of DPPH• in the presence of increasing concentrations of *Origanum Majorana L, Cotula cinerea* in acetonitrile at 298K.

Figure 26 displays the effect of introducing *Origanum majorana L.* and *Cotula cinerea* into a DPPH solution dissolved in DMSO on the oxidation peak current density of the redox system. The observed variation in anodic peak current density is attributed to the interaction

between DPPH and the plant extracts, leading to the formation of new reaction products. This interaction serves as the foundation for determining the binding constant (Ka) (Jesús F. Arteaga et al ., 2012)

Additionally, shifts in peak potential values offer insight into the underlying reaction mechanism.

The binding constants (Kb) are derived from plots of log(1/C) against log (i / (i - i_0)), based on Equation III.2, as illustrated in Figure 27(Ramaraj R Deepa et al ., 2018).

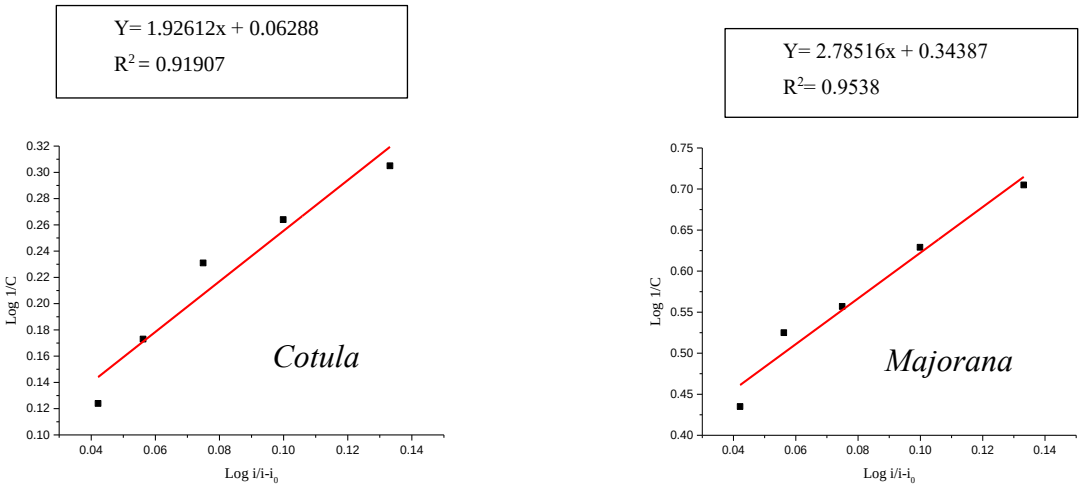

Figure27. Plots of log (1/ C) versus log (i/i-i_0) for DPPH with a variable concentration of *Origanum Majorana L, Cotula cinerea*, in Dimethyl sulfoxide (DMSO), used to calculate the binding constants of products *Origanum Majorana L, Cotula cinerea.*

Binding free energy

The change in binding free energy was determined using Equation III.3.

The binding constants, essential for this calculation, were obtained from the intercept of the linear regression plot of log (1/C) versus log(i / (i - i_0)), as described by Equation III.2. These constants were then used to compute the free energy of binding (Ramaraj R Deepa et al ., 2018), (Guzel Ziyatdinova and Alena Kalmykova .;2023).

Table12. Binding constants and values of binding free energies of products *Origanum Majorana L, Cotula cinerea* at T= 298 K

Adduct	Equation	R^2	K (M-1)	-ΔG (KJ.mol^{-1})
Origanum Majorana L	Y= 2.78516x +0.34387	0.9538	2.20 x 10^3	-19.05
Cotula cinerea	Y= 1.92612x +0.06288	0.91907	1.15 x 10^3	-17.44

The free binding energy values presented in the preceding table are quite close, implying a potential similarity in the binding modes *of Origanum majorana L.* and *Cotula cinerea.* The calculated -ΔG values range between -17.44 and -19.05 kJ/mol, where more negative values indicate stronger interactions with the DPPH radical.

A comparison of the two compounds reveals that *Origanum Majorana L.* demonstrates a stronger binding affinity, with a -ΔG of 19.05 kJ/mol, while *Cotula cinerea* shows a slightly weaker interaction at 17.44 kJ/mol. Since a higher negative free energy corresponds to greater

stability of the resulting complex, it can be concluded that *Origanum Majorana L.* forms the more stable complex, whereas *Cotula cinerea* results in a less stable one.

4.3. Electronic spectroscopy DPPH radical interaction study:

4.3.1. Inhibitory concentration (IC_{50})

In this specific analysis, we employed the DPPH radical scavenging method to assess the antioxidant activity of *Cotula cinerea* and *Origanum majorana*.

To determine their kinetic profiles and calculate IC_{50} values, we plotted the scavenging activity of the DPPH radical against different concentrations of these compounds, following Equation 12. The antioxidant effectiveness of *Cotula cinerea* and *Origanum majorana* L. is represented by their respective IC_{50} values.

$$\% \text{ DPPH scavenging activity} = \frac{A0-A}{A0} \times 100 = aC_{(mg/ml)} + b \quad (12)$$

In this case, A_o and A represent the absorbance of the DPPH radical in the absence and presence of *Origanum majorana* L. and *Cotula cinerea*, respectively.

The equations derived from the linear calibration curves within the tested concentration range for *Cotula cinerea, Origanum majorana* L., and α-tocopherol are summarized in Table 13. In these equations, 'y' corresponds to the anodic peak current density of DPPH•, while 'x' indicates the sample concentrations, expressed in mg/ml. (Ekowati., 2023)

Table 13: IC_{50} values (µg/ml) obtained using DPPH radicals scavenging activity from electronic spectroscopy method

Compound	Equation	R^2	IC_{50}(µg/ml)
Cotula cinerea	y = 0.415x + 20.375	0.95185	71.353
Origanium Majorana L	y = 0.48472x + 20.242	0.9223	61.390
α-tocopherol	y = 389.7x + 22,42	0.922	70.77

Table 13 presents the radical-scavenging activities of two oils, *Cotula cinerea* and *Origanum majorana* L.

Their antioxidant capacities, as indicated by IC_{50} values, are illustrated in the curve shown in Figure 28.

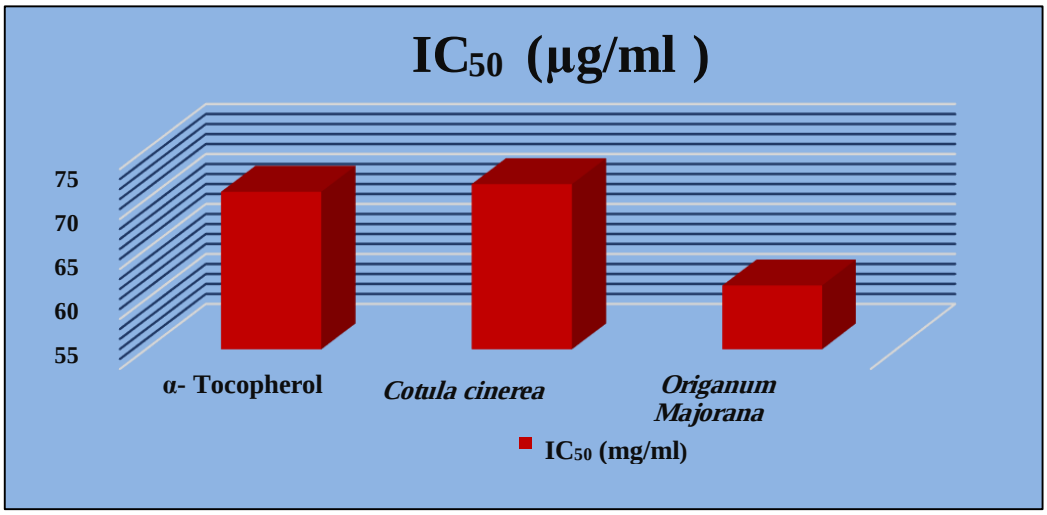

Figure 28: Classification of DPPH• inhibition capacity according to IC_{50} values from electronic spectroscopy method.

Origanum Majorana L. (IC_{50} = 61.39 µg/ml) is the most potent inhibitor, requiring lower concentrations for 50% inhibition. *Cotula cinerea* (IC_{50} = 71.35 µg/ml) and α-tocopherol (IC_{50} = 70.77 µg/ml) are less potent but still show good inhibitory activity. α-Tocopherol has a steeper slope (389.7), indicating a more significant change in activity with smaller concentration increases, whereas *Origanum Majorana L.* and *Cotula cinerea* have more moderate slopes. All compounds show strong linear relationships with high R^2 values, suggesting predictable dose-response behavior. (Lanez T, Henni M, 2016), (Djoko Agus Purwanto,et al., 2023).

5. In-Silico analysis:

5.1. ADMET and drug-likeness prediction:

Modern drug discovery involves evaluating the dynamic properties of molecules and their ability to reach target sites in an active form, a process that typically requires costly and risky cellular, animal, and human clinical trials (Ranjith D et al., 2019; Ranjith et al., 2019). Nowadays, computer-aided drug development has significantly advanced the prediction of absorption, distribution, metabolism, and excretion (ADME) properties. These computational tools provide rapid, predictive, and reliable data that complement experimental methods (Ranjith et al., 2019; Sliwoski et al., 2014). It has been shown that assessing ADME properties early in the drug discovery process greatly reduces the likelihood of pharmacokinetic failures during clinical trials (Ranjith et al., 2019; Hay et al., 2014).

In this study, we assessed the ADME properties of the major compounds (those constituting more than 10%) found in both essential oils using the SwissADME web tool. A total of four potent phytoconstituents were analyzed to evaluate various aspects, including general characteristics (Table 14), physicochemical properties (Table 15), lipophilicity and water solubility (Tables 16 & 17), pharmacokinetic parameters (Table 18), drug-likeness rules and bioavailability scores (Table 19), and medicinal chemistry properties (Table 20). The general characteristics of the compounds indicated that all of them have molecular weights under 500 Da, which is an ideal property for small molecules to be considered drug-like.

Table 14. General characteristics of the phytoconstituents of essential oils

SI. No	**Compounds**	**Molecular formula**	**Canonical SMILES**	**Molecular weight (g/mol)**
1	**Santolina triene**	$C_{10}H_{16}$	CC(=CC(C=C)C(=C)C)C	136.23
2	**trans-Thujone**	$C_{10}H_{16}O$	CC1C2CC2(CC1=O)C(C)C	152.53
3	**1,8-Cineole**	$C_{10}H_{18}O$	CC1(C2CCC(O1)(CC2)C)C	154.25
4	**cis-Verbenyl acetate**	$C_{12}H_{18}O_2$	CC1=CC(C2CC1C2(C)C)OC(=O)C	194.27

Table15. Physicochemical properties of the phytoconstituents of essential oils

Properties	Santolina triene	trans-Thujone	1,8-Cineole	cis-Verbenyl acetate
Num. heavy atoms	10	11	11	14
Num. arom. heavy atoms	0	0	0	0
Fraction Csp3	0.40	0.90	1.00	0.75
Num. rotatable bonds	3	1	0	2
Num. H-bond acceptors	0	1	1	2
Num. H-bond donors	0	0	0	0
Molar refractivity	48.76	45.90	47.12	56.12
TPSA (Å²)	0.00	17.07	9.23	26.30

Table16. Lipophilicity characteristics of the phytoconstituents of essential oils

Properties	Santolina triene	trans-Thujone	1,8-Cineole	cis-Verbenyl acetate
iLOGP	2.90	2.27	2.58	2.53
XLOGP3	4.22	2.27	2.74	3.73
WLOGP	3.33	2.26	2.74	2.54
MLOGP	3.56	2.30	2.45	2.65
SILICOS-IT	2.88	2.63	2.86	2.26
Consensus Log Po/w	3.38	2.35	2.67	2.74

Table17. Water Solubility characteristics of the phytoconstituents of essential oils

Small molecules	ESOL				Ali				SILICOS-IT			
	Log S (ESOL)	Solubility		Class	Log S (Ali)	Solubility		Class	Log S (SILICOS-IT)	Solubility		Class
		mg/ml	mol/L			mg/ml	mol/L			mg/ml	mol/L	
Santolina triene	-3.15	9.75e-2	7.16e-4	S	-3.93	1.60e-2	1.17e-4	S	-2.04	1.24e-0	9.10e-3	S
trans-Thujone	-2.15	1.08e-0	7.11e-3	S	-2.27	8.27e-1	5.43e-3	S	-2.15	1.08e-0	7.10e-3	S
1,8-Cineole	-2.52	4.63e-1	3.00e-3	S	-2.59	3.98e-1	2.58e-3	S	-2.45	5.45e-1	3.53e-3	S
cis-Verbenyl acetate	-3.26	1.06e-1	5.47e-4	S	-3.97	2.06e-2	1.06e-4	S	-2.11	1.51e-0	7.78e-3	S

Table18. Pharmacokinetics parameters of the phytoconstituents of essential oils

Proprieties	Santolina triene	trans-Thujone	1,8-Cineole	cis-Verbenyl acetate
GI absorption	Low	High	High	Low
BBB permeant	Yes	Yes	Yes	Yes
P-gp substrate	No	No	No	No
CYP1A2 inhibitor	No	No	No	No
CYP2C19 inhibitor	No	No	No	No
CYP2C9 inhibitor	No	No	No	Yes
CYP2D6 inhibitor	No	No	No	No
CYP3A4 inhibitor	No	No	No	No
Log Kp (Skin Permeation) (cm/s)	-4.13	-5.62	-5.30	-4.84

Table19. Druglikeness rule and bioavailability score of the phytoconstituents of essential oils

Proprieties	Santolina triene	trans-Thujone	1,8-Cineole	cis-Verbenyl acetate
Lipinski	Yes; 0 violations	Yes; 0 violations	Yes; 0 violations	Yes; 0 violations
Ghose	No; 1 violation: MW<160	No; 1 violation: MW<160	No; 1 violation: MW<160	Yes
Veber	Yes	Yes	Yes	Yes
Egan	Yes	Yes	Yes	Yes
Muegge	No; 2 violations: MW<200, XLOGP3>3.5	No; 2 violations: MW<200, Heteroatoms<2	No; 2 violations: MW<200, Heteroatoms<2	No; 1 violation: MW<200,
Bioavailability score	0.55	0.55	0.55	0.55

Table20. Medicinal Chemistry properties of the Phytoconstituents of essential oils

Proprieties	**Santolina triene**	**trans-Thujone**	**1,8-Cineole**	**cis-Verbenyl acetate**
PAINS	0 alert	0 alert	0 alert	0 alert
Brenk	1 alert: isolated_alkene	0 alert	0 alert	1 alert: isolated_alkene
Leadlikeness	No; 2 violations: MW<250, XLOGP3>3.5	No; 1 violation: MW<250	No; 1 violation: MW<250	No; 2 violations: MW<250, XLOGP3>3.5
Synthetic accessibility	3.22	2.79	3.65	4.50

Lipophilicity plays a crucial role in molecular discovery across various fields. It is quantitatively measured by the partition coefficient (P), which represents the distribution of a molecule between an n-octanol and water system (Daina et al., 2014). Due to its amphiphilic nature, n-octanol is often used as a surrogate for the phospholipid membrane in these studies (Liu et al., 2011). There are several algorithms available to compute the log P value, each based on distinct methodologies. The classic log P predictors are divided into two categories. The first includes molecular fragment-based approaches, such as KLOGP (Klopman et al., 1993), KOWWNIN (Meylan et al., 2000), or atomic approaches like ALOGP (Ghose et al., 1998; Wang et al., 1997), XLOGP (Moriguchi et al., 1994; Cheng et al., 2007). The second category involves topological methods, where a molecule's structure is related to its topology, using specific atomic counts or flags to represent groups or properties, such as in MLOGP (Moriguchi et al., 1992; Brenk et al., 2008), with predictions made using multiple linear regression on large molecular datasets. The SILICOS-IT is a hybrid model that combines both molecular fragments and topological descriptors, utilizing 27 fragments and 7 topological descriptors. It was trained on 23,455 molecules with experimentally determined n-octanol/water partition values (Daina et al., 2014). The third version of the XLOGP atomic model is based on 87 fragments and two correction factors, where differences between input structures and reference compounds are treated and the respective log P values are adjusted accordingly (Cheng et al., 2007). For this study, lipophilicity was calculated as the consensus log P (Mouada et al., 2019), which represents the average of all log P values obtained using different lipophilicity prediction criteria. Based on this, Santolina triene was identified as the most lipophilic compound, while trans-thujone exhibited the least lipophilicity. The water solubility of the small molecules ranged from highly soluble to soluble in water.

None of the small molecules were identified as inhibitors for the inactivation of CYP isoenzymes. The skin permeability coefficient (Log Kp), determined using multiple linear regression, indicates that the more negative the Log Kp (with Kp in cm/s), the lower the skin permeability of the molecule. Among the compounds, trans-Thujone (-5.62) exhibited the least skin permeability, while santolina triene (-4.13) demonstrated high permeability. The SwissADME tool also applies five different rule-based filters, each with specific property ranges within which a molecule is considered "drug-like." These filters include the Lipinski (Pfizer) rule of five, along with the Ghose (Amgen), Veber (GSK), Egan (Pharmacia), and Muegge (Bayer) methods. The use of multiple estimation methods allows for a consensus or selection based on the user's specific needs, such as chemical space or project requirements.

Any rule violations are clearly highlighted in the output. All four compounds adhered to the SwissADME filters, with only minimal violations observed.

The SwissADME analysis did not trigger any PAINS alerts for the four compounds under investigation. Brenk's approach, which expands beyond the traditional "Lipinski's rule of 5," focuses on compounds that are smaller and less hydrophobic, offering greater potential for lead optimization. This approach excludes compounds that might have mutagenic, reactive, or unfavorable groups such as nitro groups, sulfates, phosphates, 2-halopyridines, and thiols (Brenk et al., 2008). In the case of the compounds studied, all violated Brenk's criteria, with only a single alert being raised. Additionally, none of the compounds met the Lead-likeness criteria, primarily due to their molecular weight.

The in silico toxicity study is designed to optimize compounds by assessing their toxicity profiles. This approach significantly enhances the virtual screening process for identifying compounds with minimal or no toxicity, which could pave the way for selecting novel, non-toxic phytoconstituents from *Cotula cinerea* and *Origanum Majorana L* essential oils that exhibit strong antioxidant properties. The toxicity evaluation of the selected compounds was conducted using the ProTox-II web server (Drwal et al., 2014), which predicts various toxicity aspects, including hepatotoxicity (Dili), carcinogenicity (Carcino), immunotoxicity (Immuno), mutagenicity (Mutagen), cytotoxicity (Cyto), median lethal dose (LD50), and toxicity class (TC).

Based on the in silico toxicity profiles shown in Table 21, the toxicity class of all the phytoconstituents was determined to be 5, except for trans-Thujone, which was classified as 4. Santolina triene, trans-Thujone, 1,8-Cineole, and cis-Verbenyl acetate were predicted to be non-toxic, with the exception of cis-Verbenyl acetate, which showed a potential for immunotoxicity.

Table21. In silico toxicity profiles of the studied compounds

Molecule	Dili	Carcino	Immuno	Mutagen	Cyto	LD_{50} ($mg.Kg^{-1}$)	TC
Santolina triene	Inactive	Active	Inactive	Inactive	Inactive	2610	5
trans-Thujone	Inactive	Inactive	Inactive	Inactive	Inactive	500	4
1,8-Cineole	Inactive	Inactive	Inactive	Inactive	Inactive	2480	5
cis-Verbenyl acetate	Inactive	Inactive	Active	Inactive	Inactive	2600	5

5.2. Molecular Docking Study

In this study, the binding interactions between human glutathione reductase and the major compounds found in the essential oils of *Cotula cinerea* and *Origanum Majorana L*. were investigated through molecular docking. The compounds examined included trans-Thujone, alpha-Terpineol, beta-Terpineol, cis-Verbenyl acetate, Camphor, Sabinene, gamma-Terpinene, alpha-Pinene, 1,8-Cineole, Santolina triene, alpha-Thujene, and Beta-Pinene oxide each of which had a yield greater than 1%. The docking analysis was conducted using the Maestro version 11.7 user interfaces from the Schrödinger suite (Small-Molecule Drug Discovery Suite 2021-4, Schrödinger, LLC, New York, NY, 2021).

Each of the compounds was docked with human glutathione reductase (GR) to explore their interactions within the enzyme's active site. The binding affinities of the major compounds from *Cotula cinerea* and *Origanum Majorana L*. essential oils were found to be similar (Table 22). This suggests that the plant serves as a rich source of compounds that, whether individually or in combination, contribute to the inhibition of human glutathione reductase activity, as seen in the in vitro experimental analysis. Furthermore, the interactions were determined to be spontaneous, as indicated by the negative Gibb's free energy values (Avwioroko et al., 2020).

Research on the X-ray crystal structure and enzyme kinetics of glutathione reductase (GR) has revealed that its active site contains three key amino acid residues: HIS-467, GLU-472, and CYS-58. These residues are essential for the catalytic activity of the enzyme in the reduction of oxidized glutathione (GSSG) to reduced glutathione (GSH). Specifically, CYS-58 acts as the main nucleophilic agent in the reduction reaction, while GLU-472 helps regulate the proton state during the reaction, and HIS-467 plays a crucial role in stabilizing the transition state of the substrate within the active site 1(Savvas N. Savvides et al,2001),(Emil F. PaiS and Georg E. Schulz et al, 1982).

Table22. Docking score of the studied compounds

Compound	Rigid Docking Score (Kcal/mol)	IFD scores (Kcal/mol)
trans thujone	-5.34	-4.689
beta-Terpineol	-5.70	-5.392
cis Verbenyl acetate	-5.94	-5.479
Camphor	-4.67	-4.949
Sabinene	-4.88	-4.814

alpha-Pinene	-5.26	-4.730
1,8-Cineole	-5.23	-4.816
Santolina triene	-4.46	-4.523
alpha-Thujene	-4.90	-4.619
Beta Pinene oxide	-5.16	-5.827
Terpin-4-ol	-5.05	-5.188
Delta-terpinene	-5.35	-5.496

The results of the table 22 show that the tested compounds showed effective binding to the active site of glutathione reductase. Notably, these interactions were observed with the key catalytic residues of the enzyme (HIS-467, GLU-472, CYS-58).The compound Cis-Verbenyl acetate interacted with all three crucial amino acids involved in catalysis at the GR active site, whereas Beta-Terpineol engaged with two of the catalytic triad residues (HIS-467, GLU-472).Interestingly, interacted with only o Beta Pinene oxide ne of the key catalytic residues, despite having the secondhighest binding affinity to glutathione reductase among the compounds. This suggests that Beta Pinene oxide may exert its inhibitory effect through a non-competitive inhibition mechanism, while other compounds, including cis-Verbenyl acetate (which exhibited the best binding affinity), and likely operate via competitive inhibition. Overall, the in-silico analysis of the ligand-protein interactions between these compounds and the amino acid residues in the glutathione reductase active site (including TRP-58, TRP-59, TYR-62, GLN-63, ASP-197 ،GLU-233, and ASP-300) supported the reported inhibitory effects of these compounds .Moreover, the analysis confirmed the potential binding interactions between glutathione reductase and the phytochemicals present in the essential oils of *Cotula cinerea* and *Origanum Majorana L.*, as previously observed through spectroscopic methods. The best ligand-binding poses in the catalytic domain of GR, as well as the amino acid residues involved in these interactions, are depicted in Figure 29

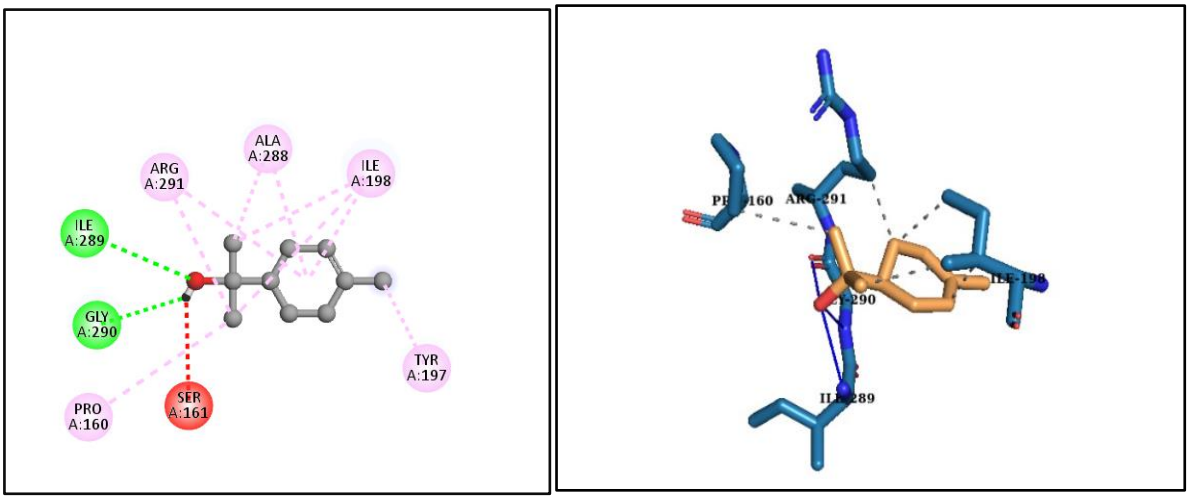

Docking complex and interaction plot for compound Beta-terpineol oxide with GR

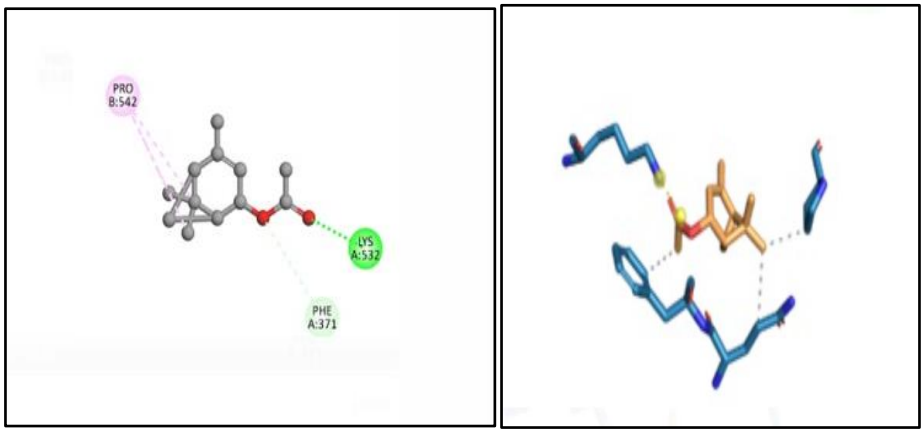

Docking complex and interaction plot for compound Cis- verbenyl acetate with GR

Figure 29. Molecular interactions of studied compounds.

5.3. Molecular Dynamics Simulation

Molecular Dynamics Simulations (MDS) were performed on the leading compound,Cis verbenyl acetate , which exhibited the best Induced Fit Docking (IFD) score, in complex with human glutathione reductase. The primary goal of these simulations was to evaluate the ligand-receptor complex under physiological conditions, which cannot be fully achieved through molecular docking alone (Dumitrică et al., 2007). During the MDS process, trajectory frames were generated at 100 picosecond intervals (Tu et al., 2008), resulting in a total of 1000 frames over a 100-nanosecond simulation period. The analysis focused on key parameters such as Root Mean Square Deviation (RMSD) and Root Mean Square Fluctuation (RMSF). RMSD values were calculated by aligning the protein and the ligand-protein complex frames with the reference frame. These metrics were used to assess the structural stability and dynamic variations of the complex throughout the simulation (Schreiner et al., 2012).

The Root Mean Square Deviation (RMSD) values for the ligand-receptor complex remained consistently within the acceptable range of 0 to 2 Å. Analysis of the complex showed no major conformational changes, although a slight deviation was observed between 8 and 20 nanoseconds, followed by a gradual drift from 45 to 55 nanoseconds. After these time frames, the complex displayed significant stability for the remainder of the simulation, with no further substantial conformational shifts (Figure 30).

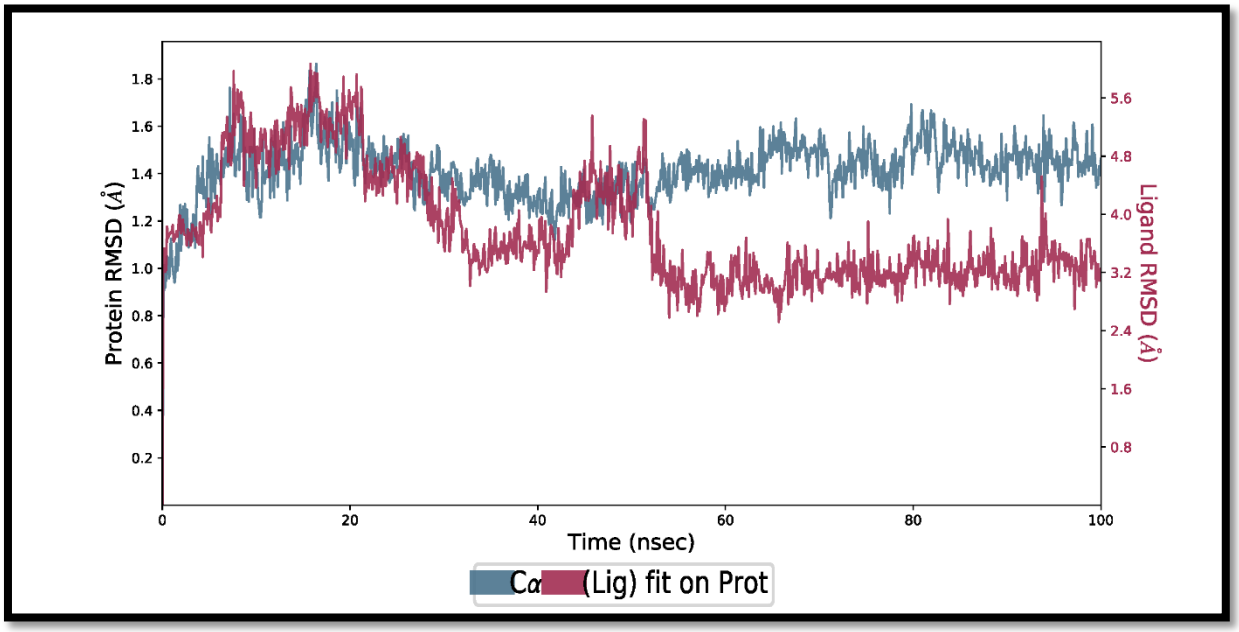

Figure30. RMSD plot of Cis verbenyl acetate and glutathione reductase complex

The Root Mean Square Fluctuation (RMSF) analysis offers valuable insights into the local variations along the protein chain, helping to identify residues that contribute to structural fluctuations within the complex (Dey et al., 2021). In this study, the fluctuations observed remained below 3 Å. Notable fluctuations, ranging from 2.20 to 2.63 Å and 1.81 to 2.96 Å, occurred in the C-terminal and loop regions (residues 223-225 and 363-366), which are located away from the glutathione reductase binding pocket. Apart from these loop regions, most residues exhibited RMSF values of less than 1.5 Å, suggesting a relatively stable conformation throughout the simulation. A graphical depiction of the RMSF plot, illustrating the specific interactions between the ligand and amino acid residues in the protein, is shown in Figure 31.

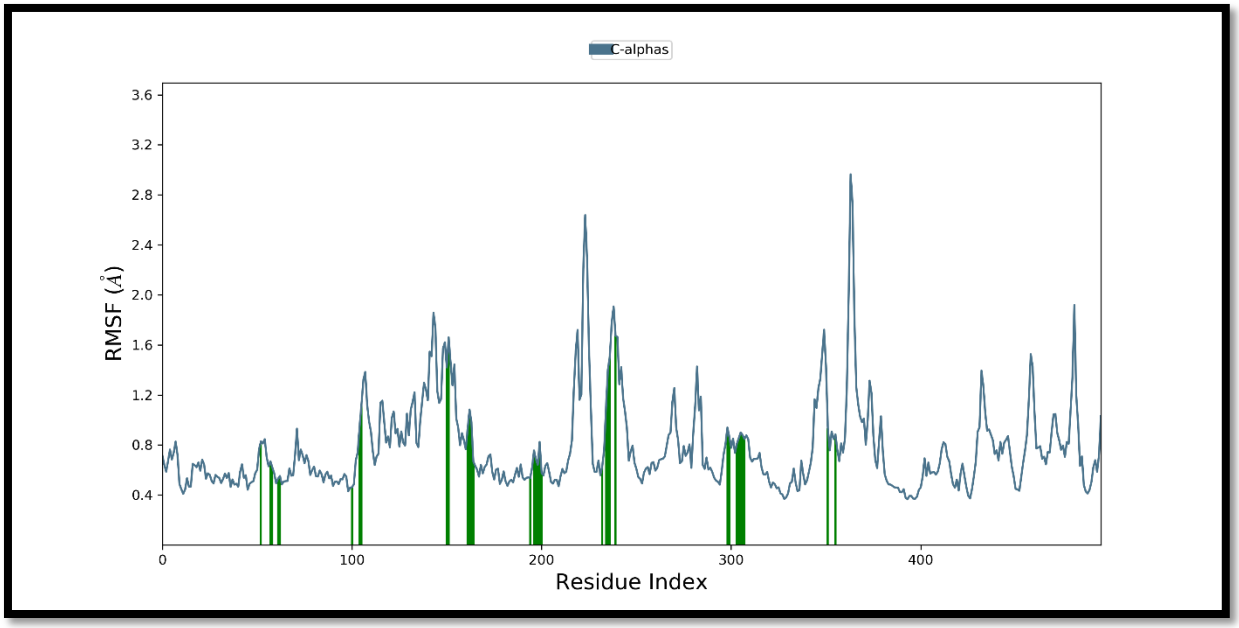

Figure31. RMSF plot of Cis verbenyl acetate and glutathione reductase complex

In the analyzed complex, significant hydrogen bonding interactions were identified with the residues HIS299, ASP197, and TRP58. Furthermore, water-mediated hydrogen bonds were also formed, involving these same residues. A visual representation of these interactions is shown in Figure 32.

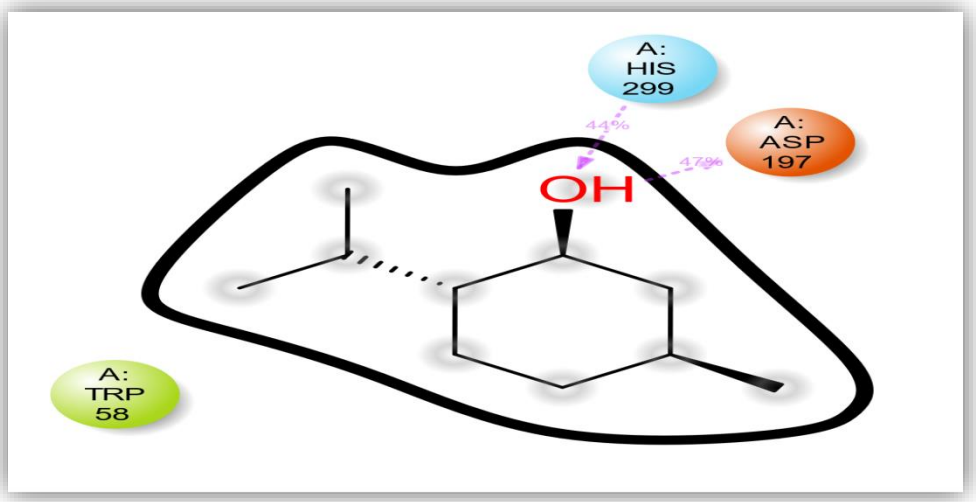

Figure32. Interaction diagram of protein-ligand after MDS

The analysis of protein-ligand interactions helps to understand the consistency of interactions between the ligand and protein residues over the course of the simulation. A numerical scale is used, where a value of 0.5 indicates that a specific interaction was

maintained for 50% of the simulation time. A value greater than 1 suggests that the protein residues formed multiple contacts of the same type with the ligand (Hatmal et al., 2017).

For the complex in question, the interaction values for residues GLU240, HIS201, ASP197, GLN63, GLU233, and THR163 are 1.25, 1, 1.75, 1, 0.60, and 1.5, respectively. These values represent different levels of sustained interaction between the ligand and the corresponding amino acids. Figure 33 provides a graphical representation of the protein-ligand contact histograms for better visualization.

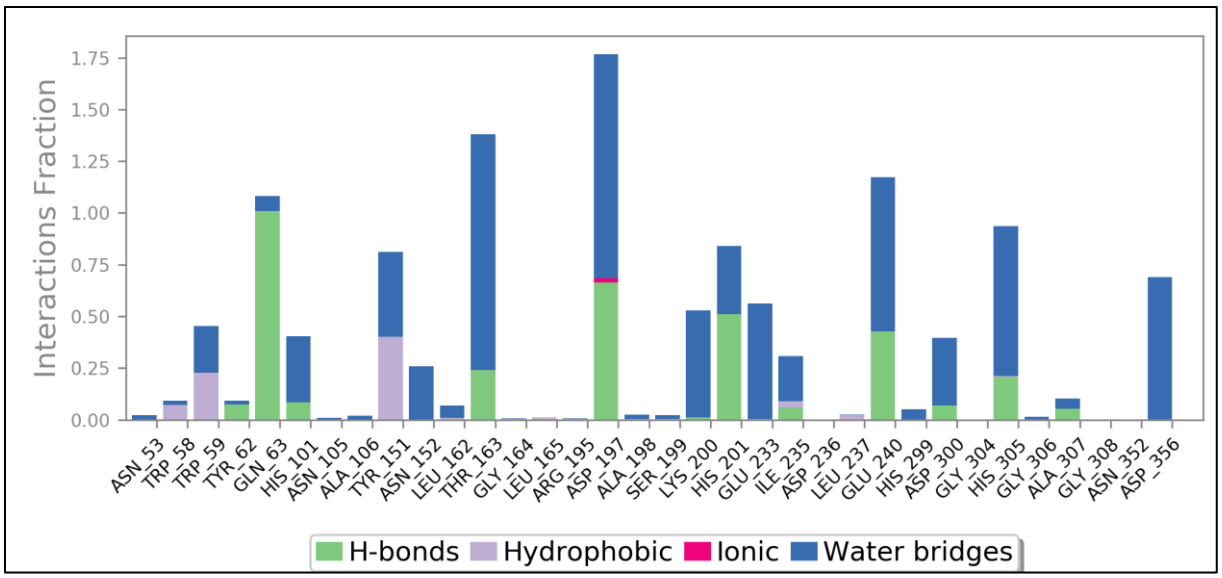

Figure33. Histogram of protein-ligand complex

To thoroughly examine the interactions between the ligand and human glutathione reductase receptor, two additional panels were introduced by Schrödinger following the Molecular Dynamics Simulation (MDS), as shown in Figure 34. The upper panel illustrates the total number of distinct contacts formed between the protein and ligand throughout the simulation. In contrast, the lower panel highlights the specific residues involved in interactions with the ligand at each frame of the trajectory.

Certain residues are observed to form multiple specific contacts with the ligand, which are depicted in various shades of orange on the plot, in accordance with the scale provided to the right. This detailed representation emphasizes the dynamic nature of the interactions and offers a comprehensive view of the residues that continuously participate in the ligand-receptor interaction. The inclusion of these additional panels improves the depth of our understanding of the molecular dynamics and specific contacts driving the ligand-receptor interaction throughout the simulation.

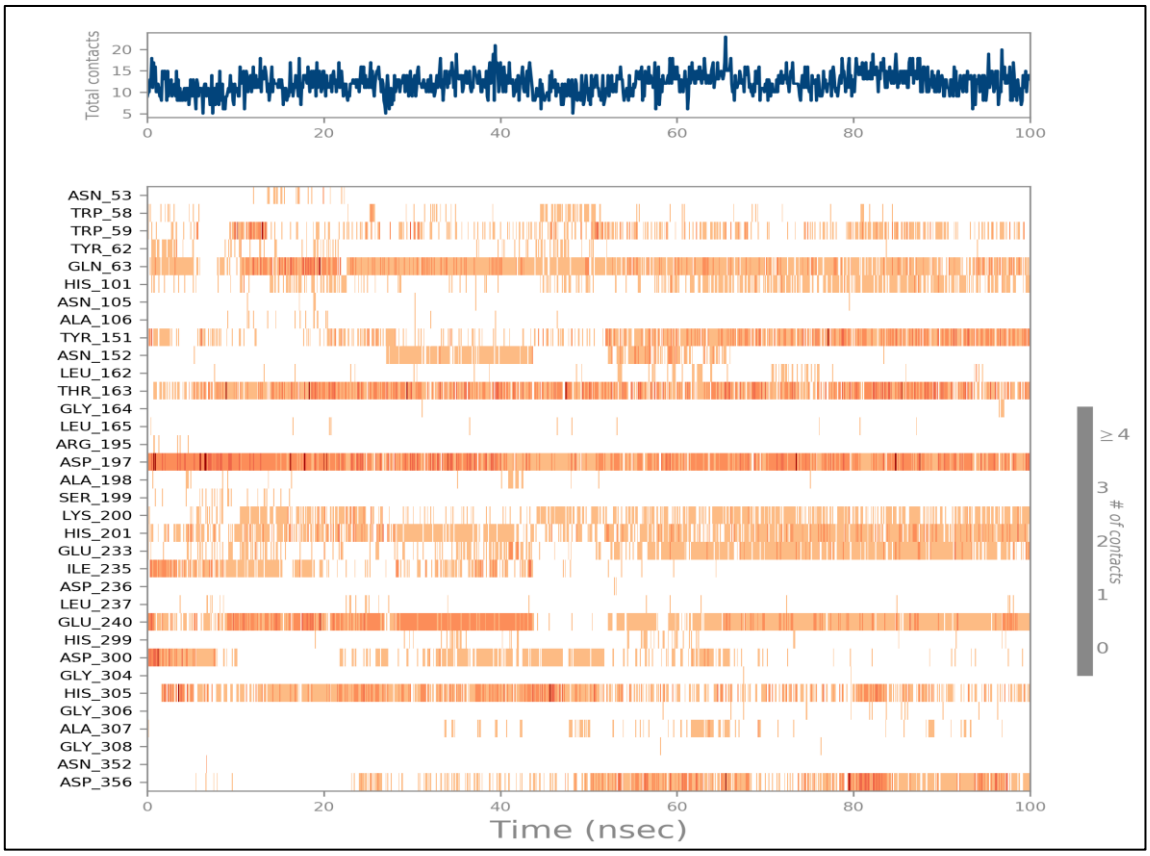

Figure34. Details of the protein ligand contact

5.4. Free Energy (MM-GBSA) Calculation

To assess the binding effectiveness of the leading compound,Cis verbenyl acetate, with the glutathione reductase protein, the Prime-MM-GBSA method was utilized to calculate the binding free energies. The formation of stable complexes is confirmed by favorable binding interactions between the compound and the protein. The calculation of binding free energy takes into account various energy components, including van der Waals (vdW), lipophilic (lipo), Generalized Born electrostatic solvation (Solv GB), Coulomb, and hydrogen-bonding (hbond) energies. The individual contributions of these energy components to the total binding free energy of the trans-thujone-glutathione reductase complex are outlined in Table 23.

Table23. Energy components of the studied complex

Component	Energy (kcal/mol)
ΔG Bind	-61.14
ΔG Bind Coulomb	-30.03
ΔG Bind Solv GB	48.10
ΔG Bind vdW	-54.91
ΔG Bind lipo	-20.51
ΔG Bind hbond	-3.79

The calculated ΔG Bind value of -61.14kcal/mol signifies a strong and favorable binding interaction. The individual energy contributions include a Coulombic energy of -30.03 kcal/mol, van der Waals interactions at -54.91 kcal/mol, lipophilic energy at -20.51kcal/mol, and hydrogen-bonding energy at -3.79kcal/mol. On the other hand, the solvation energy, as calculated using the Generalized Born model, contributed negatively with a value of 48.10 kcal/mol. The combination of these energy factors highlights the significant binding affinity within the complex.

Conclusion

In conclusion, we can only emphasize the great importance of medicinal plants in the present time, due to their rich content of various biologically active compounds that require thorough exploration and study to benefit from their biological properties, particularly their antioxidant potential.

In this study, we focused on the extraction of essential oils from *Cotula Cinerea* and *Origanum Majorana L,* using precise scientific techniaues. Our results showed that both oils possess antioxidant activity to varying degrees, with *Cotula Cinerea* oil demonstrating notably higher efficacy compared to *Origanum Majorana L* oil. These findings highlight the significant potential of these oils for use in various fields such as pharmaceuticals, cosmetics, and the food industry.

This scientific experiment was a valuable opportunity to refine our research, investigation, and laboratory analysis skills. It also allowed us to closely explore the precise scientific methodology used in studying the chemical properties of medicinal plants.

From this standpoint, we propose in the future:

- ✓ To expand the scope of research to include other local and global medicinal plants.
- ✓ To study the effect of different extraction methods on the quality and efficacy of the oils.
- ✓ To test the efficacy of these oils in vivo and not just in vitro, in order to enhance the credibility of the results and their real-world applications.

REFERENCES

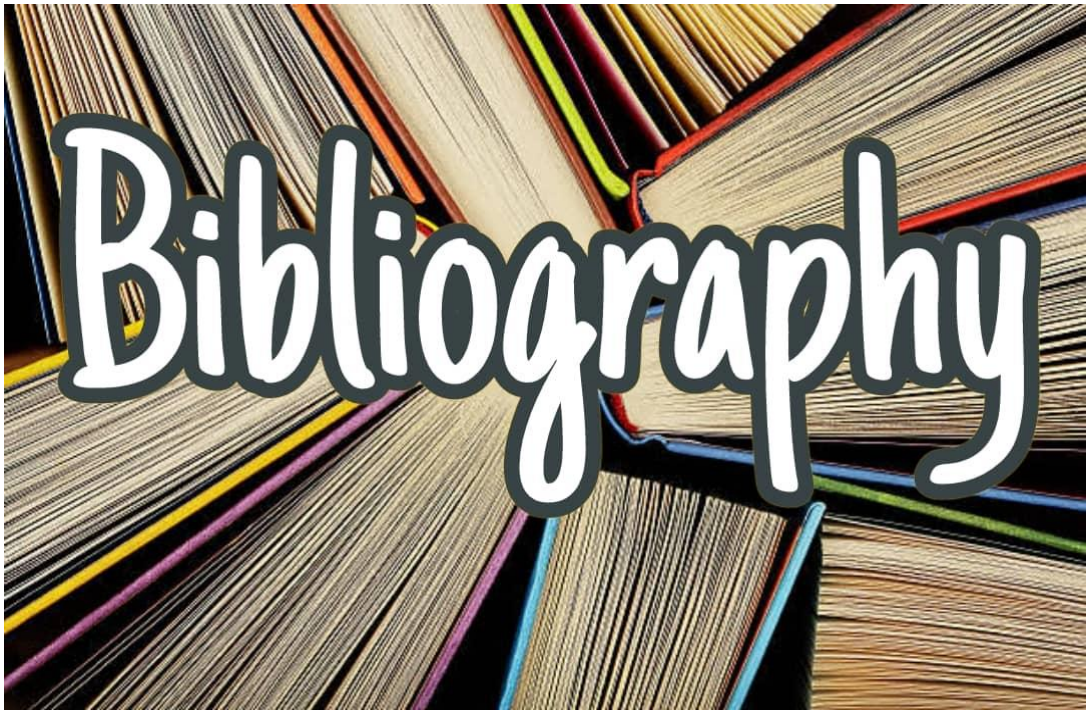

References

Afnor Ø (1982). Recueil de normes françaises des produits dérivés des fruits et légumes jus de fruits. AFNOR 325.

Agab Roa, Slimani Mohamed Djawad Eddine, (2024). Etude phytochimique et biologique d'une plante médicinale Algérienne du genre Senecio, Présenté poue l'obtention du diplôme Master, p11.

Ahmad Amri, Morteza Jabbari (2024). Exploring the DPPH radical scavenging capacity for activated carbon nanoparticles prepared from date seed by an electrochemical approach. Article in Journal of the Indian Chemical Society, DOI: 10.1016/j.jics.2024.101269.

Akbar S, Das S, Iqubal A, Ahmed B (2022). Synthesis, biological evaluation and molecular dynamics studies of oxadiazine derivatives as potential anti-hepatotoxic agents. Journal of Biomolecular Structure and Dynamics 40(20):9974-91. https://doi.org/10.1080/07391102.2021.1938233.

Alajtal AI, Sherami FE, Elbagermi MA (2018). Acid, peroxide, ester and saponification values for some vegetable oils before and after frying. AASCIT Journal of Materials 4(2):43-7.

Alimi D, Hajri A, Jallouli S, Sebai H (2022). Valorization of Volatile Oils and Some Crude Extracts from the Tunisian Plants Juniperus communis and Origanum majorana for the Control of Hyalomma scupense (Acari: Ixodidae). Waste and Biomass Valorization 13(10):4165-77.

Amamra Khouloud, Messaoudene Kaouther, (2024). Etude phytochimique et évaluation des activités antibactérienne, antioxydante, analgésique, antipyrétique, anti-ulcère, anti-inflammatoire, antidiabétique, et la toxicité des deux espèces Saussurea Lappa L, et Origanum majorana L. Présentée pour l'obtention du diplôme Master, p40.

Aqeel, U., Aftab, T., Khan, M., & Naeem, M. (2023). Regulation of essential oil in aromatic plants under changing environment. Journal of Applied Research on Medicinal and Aromatic Plants, 32, 100441.

Arbain, D., Sinaga, L. M. R., Taher, M., Susanti, D., Zakaria, Z. A., & Khotib, J. (2022). Traditional uses, phytochemistry and biological activities of Alocasia Species: A systematic review. *Frontiers in Pharmacology*, *13*, 849704.

Atti-Santos AC, Rossato M, Pauletti GF, Rota LD, Rech JC, Pansera MR, et al. (2005). Physico-chemical evaluation of Rosmarinus officinalis L. essential oils. Brazilian archives of biology and technology 48:1035-9.

Avwioroko OJ, Oyetunde TT, Atanu FO, Otuechere CA, Anigboro AA, Dairo OF, et al. (2020).Exploring the binding interactions of structurally diverse dichalcogenoimidodiphosphinate ligands with α-amylase: Spectroscopic approach coupled with molecular docking. Biochemistry and Biophysics Reports 24:100837. https://doi.org/10.1016/j.bbrep.2020.100837.

Ayoub Bensakhria, (2018). Toxicologie Générale - Le stress Oxydatif, Liverpool John Moores University https://www.researchgate.net/publication/326107870_Toxicologie_Generale.

Aziz, Z. A., Ahmad, A., Setapar, S. H. M., Karakucuk, A., Azim, M. M., Lokhat, D., . . . Ashraf ‹G. M. (2018). Essential oils: extraction techniques, pharmaceutical and therapeutic potential-a review. Current drug metabolism, 19(13), 1100-1110.

Azmir, J., Zaidul, I. S. M., Rahman, M. M., Sharif, K., Mohamed, A., Sahena, F., . . . Omar, A.(2013). Techniques for extraction of bioactive compounds from plant materials: A review.Journal of food engineering, 117(4), 426-436.

Bahadur, B., Reddy, K. J., & Rao, M. (2007). Medicinal plants: an overview. Adv Med plants Univ Press Hyderabad.

Bajaj, Y. P. S. (2012). *Medicinal and aromatic plants I* (Vol. 4). Springer Science & Business Media.

Banerjee P, Eckert AO, Schrey AK, Preissner R (2018). ProTox-II: A webserver for the prediction of toxicity of chemicals. Nucleic Acids Research 46(W1):W257-63. https://doi.org/10.1093/nar/gky318.

Baser KHC, Kirimer N, Tümen G (1993). Composition of the essential oil of *Origanum majorana L*. from Turkey. Journal of Essential Oil Research 5(5):577-9.

Ben Amor M, (2011). Valorisation des plants aromatiques et médicinales du sud Algérien extraction et analyse : Bricchiacinerea, Portulacaoleraceae L, Planta goalbicans L, Bassiamuricata L, Mathiolalivida. Mémoire de Magister, Ecole Normale Supérieure, Kouba, Alger, p20-46.

Biswa MS, Varsha T, Abhishek T, Bimal KB (2023). Green Chemistry using Essential Oils as Synthons. Journal of Indian Chemical Society Mar2023:1-24. https://doi.org/10.5281/zenodo.7841465.

Bolouri, P., Salami, R., Kouhi, S., Kordi, M., Asgari Lajayer, B., Hadian, J., & Astatkie, T . .(2022)Applications of essential oils and plant extracts in different industries. Molecules‹27(24), 8999.

Bouzidi L El, Abbad A, Fattarsi K, Hassani L, Leach D, Markouk M, et al. (2011). Chemical composition and anticandidal properties of the essential oil isolated from aerial

parts of Cotula cinerea: a rare and threatened medicinal plant in Morocco. Natural product communications 6(10):1934578X1100601021.

Bowers KJ, Chow E, Xu H, Dror RO, Eastwood MP, Gregersen BA, et al. (2006). Scalable algorithms for molecular dynamics simulations on commodity clusters. 2006 : p 84-es.

BRAHMI Fairouz,(2015), Évaluation de l'activité antioxydante et antimicrobienne d'Ammi visnaga L. durant trois périodes de croissance, Présenté pour l'obtention du diplôme

Brenk R, Schipani A, James D, Krasowski A, Gilbert IH, Frearson J, et al. (2008). Lessons learnt from assembling screening libraries for drug discovery for neglected diseases. ChemMedChem 3(3):435-44. https://doi.org/10.1002/cmdc.200700139.

Buentzel, S. K., Huebner, J., Buentzel, J., & Micke, O. (2022). Medicinal Plants Used for Abdominal Discomfort–Information from Cancer Patients and Medical Students. in vivo, *36*(5), 2422-2433.

Cheng T, Zhao Y, Li X, Lin F, Xu Y, Zhang X, et al. (2007). Computation of octanol-water partition coefficients by guiding an additive model with knowledge. Journal of Chemical Information and Modeling 47(6):2140-8. https://doi.org/10.1021/ci700257y.

Chiu SYC, Dobberstein RH, Fong HHS, Farnsworth NR (1982). Oxoaporphine alkaloids from Siparuna gilgiana. Journal of natural products 45(2):229-30.

Daina A, Michielin O, Zoete V (2014). ILOGP: A simple, robust, and efficient description of n-octanol/water partition coefficient for drug design using the GB/SA approach. Journal of Chemical Information and Modeling 54(12):3284-301. https://doi.org/10.1021/ci500467k.

Daina A, Michielin O, Zoete V (2017). SwissADME: A free web tool to evaluate pharmacokinetics, drug-likeness and medicinal chemistry friendliness of small molecules. Scientific Reports 7(1):1-13. https://doi.org/10.1038/srep42717.

De Castro, M. L., Jiménez-Carmona, M., & Fernandez-Perez, V. (1999). Towards more rational techniques for the isolation of valuable essential oils from plants. TrAC Trends in Analytical Chemistry, 18(11), 708-716.

Dendougui, H., Seghir, S., Jay, M., Benayache, F., & Benayache, S. (2012). Flavonoids from *Cotula cinerea* Del.

Dey D, Paul PK, Azad S Al, Mazid MF Al, Khan AM, Sharif MA, et al. (2021). Molecular optimization, docking, and dynamic simulation profiling of selective aromatic phytochemical ligands in blocking the SARS-CoV-2 S protein attachment to ACE2 receptor: an in silico approach of targeted drug designing. Journal of Advanced Veterinary and Animal Research 8(1):24-35. https://doi.org/10.5455/javar.2021.h481.

Djellouli, M., Benmehdi, H., Mammeri, S., Moussaoui, A., Ziane, L., & Hamidi, N. (2015).Chemical constituents in the essential oil of the endemic plant *Cotula cinerea* (Del.)

from the southwest of Algeria. Asian Pacific Journal of Tropical Biomedicine, *5*(10), 870-873.

Djellouli, M., Benmehdi, H., Mammeri, S., Moussaoui, A., Ziane, L., & Hamidi, N. (2015). Chemical constituents in the essential oil of the endemic plant Cotula cinerea (Del.) from the southwest of Algeria. Asian Pacific Journal of Tropical Biomedicine, *5*(10), 870-873.

Djoko Agus Purwanto , Betria Dwi Agustin, Juni Ekowati,10/10/2023 , A study ofthe stability of antioxidant activity of green tea extract powderwith vitamin C, Pharmacy Education23(4), Faculty of Pharmacy, Universitas Airlangga, Surabaya, Indonesia, page 159_163.

Drwal MN, Banerjee P, Dunkel M, Wettig MR, Preissner R (2014). ProTox: A web server for the in silico prediction of rodent oral toxicity. Nucleic Acids Research 42(W1):W53-8. https://doi.org/10.1093/nar/gku401.

Dumitrică T, James RD (2007). Objective molecular dynamics. Journal of the Mechanics and Physics of Solids 55(10):2206-36. https://doi.org/10.1016/j.jmps.2007.03.001.

Ekhlil B, Ghanmi M, Satrani B, Moulay A, Brahim S, Rhafouri R, et al. (2016). Chemical quality, antibacterial and antifungal activities of *Cotula cinerea* essential oil from South Morocco.

Elhafnaoui Lanez،Lazhar Bechki and Touhami Lanez,(2019),Antioxidant Activities, Binding Parameters, and Electrochemical Behavior of Superoxide Anion Radicals Twords 1-Ferrocenylmethylthymine and 1-Ferrocenylmethylcytosine,Current Physical Chemistry, 2020, 10, 10-22,DOI: 10.2174/1877946809666190424143752,p 14-16.

Emil F. PaiS and Georg E. Schulz, (1982). The Catalytic Mechanism of Glutathione Reductase as Derived from X-ray Diffraction Analyses of Reaction Intermediate. Article in Journal of Federal Republic of Germany, doi: 10.1111/j.1432-1033.1981.tb05718.x.

Filote C, Lanez E, Popa VI, Lanez T, Volf I (2022). Characterization and Bioactivity of Polysaccharides Separated through a (Sequential) Biorefinery Process from Fucus spiralis Brown Macroalgae. Polymers 14(19):4106. https://doi.org/10.3390/polym14194106.

Fournier G, Baghdadi H, Ahmed SS, Paris M (1989). Contribution to the study of Cotula cinerea essential oil. Planta medica 55(06):580.

Franke, R. (2005). Plant sources. Chamomile: Ind Profiles, *1*, 39-42.

Friesner RA, Murphy RB, Repasky MP, Frye LL, Greenwood JR, Halgren TA, et al. (2006). Extra precision glide: Docking and scoring incorporating a model of hydrophobic enclosure for protein− ligand complexes. Journal of medicinal chemistry 49(21):6177-96.

Gallwitz H, Bonse S, Martinez-Cruz A, Schlichting I, Schumacher K, Krauth-Siegel RL (1999). Ajoene Is an Inhibitor and Subversive Substrate of Human Glutathione Reductase and Trypanosoma cruzi Trypanothione Reductase: Crystallographic, Kinetic, and Spectroscopic Studies. Journal of Medicinal Chemistry 42(3):364-72. https://doi.org/10.1021/jm980471k.

Ghorbanpour, M., Hadian, J., Nikabadi, S., & Varma, A. (2017). Importance of medicinal and aromatic plants in human life. Medicinal plants and environmental challenges, 1-23

Ghose AK, Viswanadhan VN, Wendoloski JJ (1998). Prediction of hydrophobic (lipophilic) properties of small organic molecules using fragmental methods: An analysis of ALOGP and CLOGP methods. Journal of Physical Chemistry A 102(21):3762-72. https://doi.org/10.1021/jp980230o.

Giannenas, I., Sidiropoulou, E., Bonos, E., Christaki, E., & Florou-Paneri, P. (2020). The history of herbs, medicinal and aromatic plants, and their extracts: Past, current situation and future perspectives.In Feed additives (pp. 1-18). Elsevier.

Gledhill, D. (2008). *The names of plants*. Cambridge University Press.

Gołębiowski, W., Wolak, A., & Zając, G. (2018). Definition of oil change intervals based on the analysis of selected physicochemical properties of used engine oils. Combustion Engines‹57.

Gorla US, Gsn KR, Kulandaivelu U, Alavala RR, Das S, Joseph A (2021). Bioflavonoids as potential target inhibitors in covid-19: An in silico analysis. Journal of Research in Pharmacy 25(6):982-97. https://doi.org/10.29228/jrp.94.

Guinaudeau H, Leboeuf M, Cave A (1975). Aporphine alkaloids. 1975.

Guzel Ziyatdinova and Alena Kalmykova, (2023). Electrochemical Characterization of the Antioxidant Properties of Medicinal Plants and Products: A Review, Journal of Analytical Chemistry Department 28, 2308, https://doi.org/10.3390/molecules28052308.

Haji Muhammad ‹Muddasir Hanif ‹Iftikhar Ahmad Tahiri‹ Muhammad Ali Versiani, et al, (2018), Electrochemical behavior of superoxide anion radical towards quinones: a mechanistic approach, Research on Chemical Intermediates https://doi.org/10.1007/s11164-018-3496-8.

Hajlaoui, H., Mighri, H., Aouni, M., Gharsallah, N., & Kadri, A. (2016). Chemical composition and in vitro evaluation of antioxidant, antimicrobial, cytotoxicity and antiacetylcholinesterase properties of Tunisian Origanum majorana L. essential oil. Microbial pathogenesis, 95, 86-94.

Halder D, Das S, Joseph A, Jeyaprakash RS (2023). Molecular docking and dynamics approach to in silico drug repurposing for inflammatory bowels disease by targeting TNF

alpha. Journal of Biomolecular Structure and Dynamics 41(8):3462-75. https://doi.org/10.1080/07391102.2022.2050948.

Hatmal MM, Taha MO (2017). Simulated annealing molecular dynamics and ligand-receptor contacts analysis for pharmacophore modeling. Future Medicinal Chemistry 9(11):1141-59. https://doi.org/10.4155/fmc-2017-0061.

Hay M, Thomas DW, Craighead JL, Economides C, Rosenthal J (2014). Clinical development success rates for investigational drugs. Nature Biotechnology 32(1):40-51. https://doi.org/10.1038/nbt.2786.

Horai H, Arita M, Kanaya S, Nihei Y, Ikeda T, Suwa K, et al. (2010). MassBank: a public repository for sharing mass spectral data for life sciences. Journal of mass spectrometry 45(7):703-14.

Hudaib, M. M., Tawaha, K. A., Hudaib, H. S., & Battah, A. H. (2015). Chemical composition of volatile oil from the aerial parts of Rosmarinus officinalis L. grown in Jordan. Journal of Essential Oil Bearing Plants, 18(5), 1282-1286.

Jesús F. Arteaga, Mercedes Ruiz-Montoya, Alberto Palma, Gema Alonso-Garrido, Sara Pintado and JoséM. Rodríguez-Mellado, (2012). Comparison of the Simple Cyclic Voltammetry (CV) and DPPH Assays for the Determination of Antioxidant Capacity of Active Principles, Journal of Physical Chemistry and Organic Chemistry, 17, 5126-5138 ; https://doi.org/10.3390/molecules17055126.

Kan, H., Jin, L & ‹.Zhou, F. (2017), Classification of medicinal plant leaf image based on multi-feature extraction,Pattern recognition and image analysis, 27, 581-587.

Khaoula Douadi ‹Kaabi Ilhem, Tahar Douadi1,Mousa Al-Noaimi2 , Salah Chafaa,(2022),Superoxide Anion Radical Interaction With New Quinoline Compounds Measured By Cyclic Voltammetry ,Journal of Physical & Chemical Research.1(June) 32–39, p4.

Khelil CKM, Amrouche B, soufiane Benyoucef A, Kara K, Chouder A (2020). New Intelligent Fault Diagnosis (IFD) approach for grid-connected photovoltaic systems. Energy 211:118591.

Khennoufa Ali, (2023)‹Evaluation de l'activité antioxydante et étude in vitro et in silico de l'interaction de quelques N-(ferrocènylméthyl)anilines avec l'hémoglobine et l'albumine de sérum‹Présentée pour l'obtention du diplôme de DOCTORAT, p59 - 60.

Kim S, Thiessen PA, Bolton EE, Chen J, Fu G, Gindulyte A, et al. (2016). PubChem substance and compound databases. Nucleic Acids Research 44(D1):D1202-13. https://doi.org/10.1093/nar/gkv951.

Kiryakov HG (1968). Structure of dehydroglaucine: a new aporphine alkaloid. 1968:

Klopman G, Li JY, Wang S, Dimayuga M (1993). Computer automated log P calculations based on an extended group contribution approach. Journal of Chemical Information and Computer Sciences 33(4):752-81.

Korb O, Olsson TSG, Bowden SJ, Hall RJ, Verdonk ML, Liebeschuetz JW, et al. (2012). Potential and limitations of ensemble docking. Journal of chemical information and modeling 52(5):1262-74.

Lakhdar, M. (2018). Traditional uses, phytochemistry and biological activities of *Cotula cinerea* Del: A review. Tropical Journal of Pharmaceutical Research, *17*(2), 365-373.

Lanez E, Bechki L, Lanez T (2019). Antioxidant Activities, Binding Parameters, and Electrochemical Behavior of Superoxide Anion Radicals Twords 1-Ferrocenylmethylthymine and 1-Ferrocenylmethylcytosine. Current Physical Chemistry 10(1):10-22. https://doi.org/10.2174/1877946809666190424143752.

Lanez E, Saidi M, Lanez T (2023). Assessment of antioxidant and DPPH free radical scavenging activity of 1,2-dithiole-3-thione derivatives by using cyclic voltammetry, spectroscopic, and molecular docking studies. Journal of Sulfur Chemistry 44(5):542-58. https://doi.org/10.1080/17415993.2023.2200142.

Lanez T, Henni M, (2016),*SPECTROPHOTOMETRICAL STUDY OF ANTIOXIDANT STANDARDS INTERACTING WITH 2,2-DIPHENYL-1-PICRYLHYDRAZYL RADICAL,* Chemistry & Chemical Technology, Vol. 10, No. 3, 2016,P 256-257.

Larbi BAM, Naima B, Elsharkawy ER, Neghmouche NS (2018). Phytochemical characterization, in-vitro cytotoxic and antibacterial activity of Cotula cinerea (Delile) Vis essential oil. Journal of Natural Remedies 2018:107-12.

Letswaart,J.H, (1980). A taxonomic revision of the genus Origanum (Labiatae). Leiden Botanical Series, vol. 4. Leiden University. Press, the Hague.

Liu X, Testa B, Fahr A (2011). Lipophilicity and its relationship with passive drug permeation. Pharmaceutical Research 28(5):962-77. https://doi.org/10.1007/s11095-010-0303-7.

Lobo V, Patil A ،Phatak A, Chandra N (2010), Free radicals ،antioxidants and functional foods: Impact on human health, Pharmacognosy Reviews 4(8):118-126, https://doi.org/10.4103/0973-7847.70902.

Low-fat, plant-based diet in multiple sclerosis: A randomized controlled trial. Multiple Sclerosis and Related Disorders 9:80–90, https://doi.org/10.1016/j.msard.2016.07.001.

Low-molecular-weight synthetic antioxidants: Classification, pharmacological profile, effectiveness and trends. Antioxidants 11(4):638, https://doi.org/10.3390/antiox11040638.

Lu C, Wu C, Ghoreishi D, Chen W, Wang L, Damm W, et al. (2021). OPLS4: Improving force field accuracy on challenging regimes of chemical space. Journal of chemical theory and computation 17(7):4291-300.

Lubbe, A., & Verpoorte, R. (2011). Cultivation of medicinal and aromatic plants for specialty industrial materials. Industrial crops and products, *34*(1), 785-801.

Madhavi Sastry G, Adzhigirey M, Day T, Annabhimoju R, Sherman W (2013). Protein and ligand preparation: parameters, protocols, and influence on virtual screening enrichments. Journal of computer-aided molecular design 27:221-34.

Masarovičová, E., Kráľová, K., & Kummerová, M. (2010). Principles of classification of medicinal plants as hyperaccumulators or excluders. Acta physiologiae plantarum, 32, 823-829.

Mebarki L.(2016), Search of biological activity of plant molecules for controling Fusarium oxysporum f. sp. Albedinis. Phd thesis, USTOMB, Oran, Algeria, p191.

Mekhadmi, N. E., Mlik, R., Ramdani, M., Mouane, A., Lakhdari, W., Dehliz, A., . . . Figueredo,G. (2023). Chemical composition and biological properties of *Cotula cinerea* essential oil from Sahara of Algeria. Biocatalysis and Agricultural Biotechnology, *47*, 102613.

Meylan WM, Howard PH (2000). Estimating log P with atom/fragments and water solubility with log P. Perspectives in Drug Discovery and Design 19(1):67-84. https://doi.org/10.1023/A:1008715521862.

Microbe Note ,26/04/2025 at 09:50 https://microbenotes.com/plant-taxonomy/.

Moghaddam, M., & Mehdizadeh, L. (2017). Chemistry of essential oils and factors influencing their constituents. In Soft chemistry and food fermentation (pp. 379-419). Elsevier.

Moriguchi I, Hirano H, Nakagome I (1994). Comparison of Reliability of log P Values for Drugs Calculated by Several Methods. Chemical and Pharmaceutical Bulletin 42(4):976-8. https://doi.org/10.1248/cpb.42.976.

Moriguchi I, Hirono S, Liu Q, Nakagome Izum, Matsushita Y (1992). Simple Method of Calculating Octanol/Water Partition Coefficient. Chemical and Pharmaceutical Bulletin 40(1):127-30. https://doi.org/10.1248/cpb.40.127.

Morsy, N. F. S. (2017). Chemical structure, quality indices and bioactivity of essential oil constituents. Active ingredients from aromatic and medicinal plants, 175-206.

Mouada H, Lanez T, Lanez E (2019). Investigations of the binding parametres of the interaction of N'-ferrocenylmethyl-N'-phenylaceto-and propionohydrazide with DNA. Journal of Fundamental and Applied Sciences 11(2):875-82.

Naima B, Abdelkrim R, Ouarda B, Salah NN, Larbi BAM (2019). Chemical composition, antimicrobial, antioxidant and anticancer activities of essential oil from Ammodaucus leucotrichus Cosson & Durieu (Apiaceae) growing in South Algeria. Bulletin of the Chemical Society of Ethiopia 33(3):541-9.

Oyman, B. U. (2017). Essential oil analysis of some plant species and antimicrobial activities Sağlık Bilimleri Enstitüsü].

Ozenda P, (1967). Flore du Sahara. CNRS. Paris, p270.

Paudel, P. N., Satyal, P., Satyal, R., Setzer, W. N., & Gyawali, R. (2022). Chemical composition ،enantiomeric distribution, antimicrobial and antioxidant activities of *Origanum majorana L.* essential oil from Nepal. Molecules, 27(18), 6136.

Petrovska, B. B. (2012). Historical review of medicinal plants' usage. Pharmacognosy reviews,*6*(11), 1.

Pezzani, R., Vitalini, S., & Iriti, M. (2017). Bioactivities of *Origanum vulgare L.*: An update. Phytochemistry reviews, *16*, 1253-1268.

Radulescu, V., Popescu, M. L., & Ilies, D.-C. (2010). Chemical composition of the volatile oil from different plant parts of Anethum graveolens L.(Umbelliferae) cultivated in Romania. Farmacia, 58(5), 594-600.

Ramaraj R Deepa, Abraham A Daniel Arulraj, Abdul Kather A. Sheik Mideen, Rathinasamy R Gandhidasan, Vairathevar Sivasamy VS Vasantha1, (2018). Evaluation of Antioxidant Property of Quinones and Calculation of their Binding Constant Values with DNA by Electrochemical Technique, Journal of Natural product chemistry 10(5): 69-78.

Ranjith D, Ravikumar C (2019). SwissADME predictions of pharmacokinetics and drug-likeness properties of small molecules present in Ipomoea mauritiana Jacq. Journal of Pharmacognosy and Phytochemistry 8(5):2063-73.

Ranjith D, Viswanath S (2019). In silico antidiabetic activity of bioactive compounds in Ipomoea mauritiana Jacq. ~ 5 ~ The Pharma Innovation Journal 8(10):5-11.

Riyadi PH, Romadhon, Sari ID, Kurniasih RA, Agustini TW, Swastawati F, et al. (2021). SwissADME predictions of pharmacokinetics and drug-likeness properties of small molecules present in Spirulina platensis. IOP Conference Series: Earth and Environmental Science 890(1):2063-73. https://doi.org/10.1088/1755-1315/890/1/012021.

Roos K, Wu C, Damm W, Reboul M, Stevenson JM, Lu C, et al. (2019). OPLS3e: Extending Force Field Coverage for Drug-Like Small Molecules. Journal of Chemical Theory and Computation 15(3):1863-74. https://doi.org/10.1021/acs.jctc.8b01026.

Rose PW, Prlić A, Altunkaya A, Bi C, Bradley AR, Christie CH, et al. (2017). The RCSB protein data bank: Integrative view of protein, gene and 3D structural information. Nucleic Acids Research 45(D1):D271-81.

Sadgrove, N. J., Padilla-González, G. F., & Phumthum, M. (2022). Fundamental chemistry of essential oils and volatile organic compounds, methods of analysis and authentication . Plants, 11(6), 789.

Sahoo PK, Das LM, Babu MKG, Naik SN (2007). Biodiesel development from high acid value polanga seed oil and performance evaluation in a CI engine. Fuel 86(3):448-54.

Sarkar, P., & Bhowmick, A. K. (2018). Sustainable rubbers and rubber additives. Journal of Applied Polymer Science, 135(24), 45701.

Savvas N. Savvides,Michael Scheiwein, Catharina C. Bo¨hme, Gavin E. Arteel, P. Andrew Karplus, Katja Becker, and R. Heiner Schirmer,(2001). Crystal Structure of the Antioxidant Enzyme Glutathione Reductase Inactivated by Peroxynitrite. Article in Journal ofof Biochemistry and Biophysics, DOI 10.1074/jbc.M108190200.

Schreiner W, Karch R, Knapp B, Ilieva N (2012). Relaxation estimation of RMSD in molecular dynamics immunosimulations. Computational and Mathematical Methods in Medicine 2012 https://doi.org/10.1155/2012/173521.

Schrödinger (2015). Small-Molecule Drug Discovery Suite 2015-3: Schrödinger Suite 2015-3 Induced Fit Docking protocol; Glide version 6.8; Prime version 4.1. Glide version 6.

Schrödinger (2024). Schrödinger Release 2024-1: LigPrep, Schrödinger, LLC. 2024.

Sell, C. (2020). Chemistry of essential oils. In Handbook of essential oils (pp. 161-189). CRC Press.

Sellami IH, Maamouri E, Chahed T, Wannes WA, Kchouk ME, Marzouk B (2009). Effect of growth stage on the content and composition of the essential oil and phenolic fraction of sweet marjoram (Origanum majorana L.). Industrial Crops and Products 30(3):395-402.

Shamma M (1972). The Isoquinoline Alkaloids, New York and London. Academic Press 81:335-41.

Sharifi-Rad, J., Sureda, A., Tenore, G. C., Daglia, M., Sharifi-Rad, M., Valussi, M . . . ، Ademiluyi, A. O. (2017). Biological activities of essential oils: From plant chemoecology to traditional healing systems. Molecules, 22(1), 70.

Singh S (2002). Refractive index measurement and its applications. Physica Scripta 65(2):167.

Sliwoski G, Kothiwale S, Meiler J, Lowe EW (2014). Computational methods in drug discovery. Pharmacological reviews 66(1):334-95.

Stratakos, A. C., & Koidis, A. (2016). Methods for extracting essential oils. In Essential oils in food preservation, flavor and safety (pp. 31-38). Elsevier.

Tahmasebi, S., Majd, A., Mehrafarin, A., & Jonoubi, P. (2016). Comparative ontogenetic survey of the essential oil composition in Origanum vulgare L., and Origanum majorana L. Acta Biologica Szegediensis, 60(2), 105-111.

Tsimogiannis, D., & Oreopoulou, V. (2019). Classification of phenolic compounds in plants. In *Polyphenols in plants* (pp. 263-284). Elsevie.

Tu T, Rendleman CA, Borhani DW, Dror RO, Gullingsrud J, Jensen MO, et al. (2008). A scalable parallel framework for analyzing terascale molecular dynamics simulation trajectories. IEEE ; 2008 : p 1-12.

Tuyg'unovna, S. S. (2023). CHEMICAL COMPOSITION OF MEDICINAL PLANTS AND CLASSIFICATION. EUROPEAN JOURNAL OF MODERN MEDICINE AND PRACTICE, *3*(11), 33-35.

Valarezo E, Rosales J, Morocho V, Cartuche L, Guaya D, Ojeda-Riascos S, et al. (2015). Chemical composition and biological activity of the essential oil of Baccharis obtusifolia Kunth from Loja, Ecuador. Journal of essential oil research 27(3):212-6.

Vasudeva, N. (2015). Origanum majorana L.-Phyto-pharmacological review.

Vera RR, Chane-Ming J (1999). Chemical composition of the essential oil of marjoram (*Origanum majorana L.*) from Reunion Island. Food Chemistry 66(2):143-5.

Vincken, J.-P., Heng, L., de Groot, A., & Gruppen, H. (2007). Saponins, classification and occurrence in the plant kingdom. Phytochemistry, 68(3), 275-297.

Wang E, Fu W, Jiang D, Sun H, Wang J, Zhang X, et al. (2021). VAD-MM/GBSA: a variable atomic dielectric MM/GBSA model for improved accuracy in protein–ligand binding free energy calculations. Journal of Chemical Information and Modeling 61(6):2844-56.

Wang R, Fu Y, Lai L (1997). A new atom-additive method for calculating partition coefficients. Journal of chemical information and computer sciences 37(3):615-21.

Wink, M. (2012). Medicinal plants: a source of anti-parasitic secondary metabolites. Molecules, 17(11), 12771-12791.

Yadav V, Marracci G, Kim E, Tala, Spain R, Cameron M, Overs S, Riddehough A, Lid DKB, McDougall J, Lovera J, Murchison C, Bourdette D (2016).

Yang Y, Yao K, Repasky MP, Leswing K, Abel R, Shoichet BK, et al. (2021). Efficient exploration of chemical space with docking and deep learning. Journal of Chemical Theory and Computation 17(11):7106-19.

Zahari, R., Halimoon, N., Sajap, A. S., Ahmad, M. F., & Mohamed, M. R. (2014). Bioantifungal activity of selected medicinal plant extracts against root rot of fungal disease. Journal of Plant Sciences, *2*(1), 31-36.

Zineb Lakache ,Mohcene Sadallah , Hamza Aliboudhar , Hinda Hacib , Hassina Tounsi1 and Abdelkrim Kameli, (2024). In vivo wound healing and in vitro anti-oxidant Activity Evaluation of *Cotula Cinerea,* Journal of Laboratory of Ethnobotanyand Natural Substances, ENS-Kouba, Algiers *141 - 150.*

Zulkipli, I. N., David, S. R., Rajabalaya, R., & Idris, A. (2015). Medicinal plants: a potential source of compounds for targeting cell division.Drug target insights, 9, DTI. S24946.